AD-A148 716 ATMOSPHERIC PHOTOCHEMICAL MODELING OF TURBNNE ENGINE FUELS PHASE I EXPERI..(U) CALIFORNIA UNIV RIVERSIDE STATEWIDE AIR POLLUTION RESEARCH CE.. 1/2

UNCLASSIFIED W P CARTER ET AL. SEP 84 F/G 4/1 NL

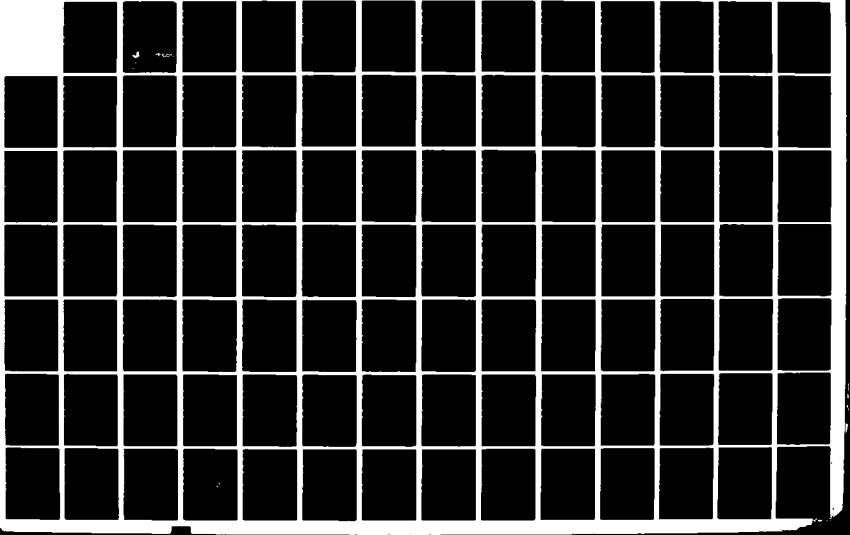

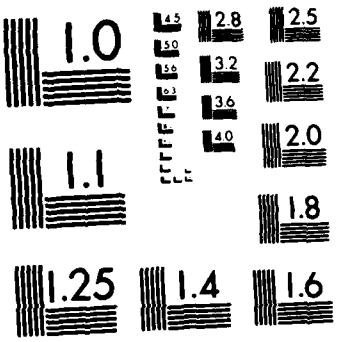

12

ESL-TR-84-32

Atmospheric Photochemical Modeling of Turbine Engine Fuels. Phase I. Experimental Studies Volume I of II Results and Disussion

W.P.L. CARTER, A.M. WINER, R. ATKINSON,
M.C. DODD, W.D. LONG, and S.M. ASCHMANN

STATEWIDE AIR POLLUTION RESEARCH CENTER
UNIVERSITY OF CALIFORNIA
RIVERSIDE, CA 92521

SEPTEMBER 1984

FINAL REPORT
JUNE 1983 - JUNE 1984

APPROVED FOR PUBLIC RELEASE: DISTRIBUTION UNLIMITED

AFESC

ENGINEERING & SERVICES LABORATORY
AIR FORCE ENGINEERING & SERVICES CENTER
TYNDALL AIR FORCE BASE, FLORIDA 32403

NOTICE

The commercial products Teflon®, Tenax®, Pyrex®, Purafil®, Carbowax®, Porapak®, Chromosorb®, and Superpax® are mentioned in this report. Because of the frequency of usage, the trademarks were not indicated. If it becomes necessary to reproduce any segment of this document containing these names, this notice must be included as part of that reproduction.

Mention of these products does not constitute their endorsement or rejection by the U. S. Air Force, and use of the information contained herein for advertising purposes without obtaining clearance according to the existing contractural agreements is prohibited.

NOTICE

PLEASE DO NOT REQUEST COPIES OF THIS REPORT FROM HQ AFESC/RD (ENGINEERING AND SERVICES LABORATORY). ADDITIONAL COPIES MAY BE PURCHASED FROM:

NATIONAL TECHNICAL INFORMATION SERVICE
5285 PORT ROYAL ROAD
SPRINGFIELD, VIRGINIA 22161

FEDERAL GOVERNMENT AGENCIES AND THEIR CONTRACTORS REGISTERED WITH DEFENSE TECHNICAL INFORMATION CENTER SHOULD DIRECT REQUESTS FOR COPIES OF THIS REPORT TO:

DEFENSE TECHNICAL INFORMATION CENTER
CAMERON STATION
ALEXANDRIA, VIRGINIA 22314

UNCLASSIFIED

SECURITY CLASSIFICATION OF THIS PAGE (When Data Entered)

REPORT DOCUMENTATION PAGE		READ INSTRUCTIONS BEFORE COMPLETING FORM
1 REPORT NUMBER ESL-TR-84-32	2 GOVT ACCESSION NO.	3 RECIPIENT'S CATALOG NUMBER
4 TITLE (and Subtitle) Atmospheric Photochemical Modeling of Turbine Engine Fuels. Phase I. Experimental Studies Volume I of II. Results and Discussion		5 TYPE OF REPORT & PERIOD COVERED Final Report: June 1983-June 1984 6 PERFORMING ORG. REPORT NUMBER
7 AUTHOR(s) William P. L. Carter, Arthur M. Winer, Roger Atkinson, Margaret C. Dodd, William D. Long, and Sara M. Aschmann		8 CONTRACT OR GRANT NUMBER(s) USAF-F08635-83-0278
9 PERFORMING ORGANIZATION NAME AND ADDRESS Statewide Air Pollution Research Center University of California Riverside, California 92521		10 PROGRAM ELEMENT, PROJECT, TASK AREA & WORK UNIT NUMBERS PE 62601F JON 19002040
11 CONTROLLING OFFICE NAME AND ADDRESS AIR FORCE ENGINEERING AND SERVICES CENTER TYNDALL Air Force Base, Florida 32403		12 REPORT DATE September 1984 13 NUMBER OF PAGES 149
14 MONITORING AGENCY NAME & ADDRESS(if different from Controlling Office)		15 SECURITY CLASS. (of this report) Unclassified 15a DECLASSIFICATION/DOWNGRADING SCHEDULE

16 DISTRIBUTION STATEMENT (of this Report)

Approved for public release; distribution unlimited.

17 DISTRIBUTION STATEMENT (of the abstract entered in Block 20, if different from Report)

18 SUPPLEMENTARY NOTES

Availability of this report is specified on reverse of front cover.

19 KEY WORDS (Continue on reverse side if necessary and identify by block number)

Ozone formation	Alkanes	Thiophene
Atmospheric reactivity	Aromatics	Pyrrole
Aviation fuels	Tetralin	
Environmental chambers	Naphthalene	
Photochemical models	Furan	

20 ABSTRACT (Continue on reverse side if necessary and identify by block number)

This report documents the results of the first phase of a two-part program aimed at developing for the U. S. Air Force experimentally tested computer models to predict worst-case potentials for air quality degradation resulting from use of current and potential future turbine engine (jet) fuels. The development and testing of such models requires an adequate data base derived from appropriate environmental chamber experiments and laboratory studies. In Phase I of this two-phase program, a total of 131 environmental

DD FORM 1 JAN 73 1473 EDITION OF 1 NOV 65 IS OBSOLETE

S/N 0102-LF-014-6601

UNCLASSIFIED

SECURITY CLASSIFICATION OF THIS PAGE (When Data Entered)

20. CONCLUDED

chamber experiments were carried out in a ~6400-liter, all Teflon indoor environmental chamber and several kinetic measurements were made in order to obtain data required for model development. The chamber experiments included 47 single component-NO_x-air irradiations of various representative fuel constituents and potential future fuel impurities, 15 fuel-NO_x-air irradiations employing one whole and six synthetic surrogate fuels, and 69 control or characterization runs.

The compounds studied in the single component-NO_x-air irradiations included the representative fuel constituents n-butane, n-octane, and methylcyclohexane; the representative aromatics benzene, toluene, m-xylene, mesitylene (1,3,5-trimethylbenzene), tetralin (1,2,3,4-tetrahydronaphthalene), naphthalene, and 2,3-dimethylnaphthalene; and the potential future impurities furan, thiophene, and pyrrole. Pyrrole, furan, and the methylbenzenes were found to be the most reactive in terms of rates of O_3 formation, with benzene, tetralin, the naphthalenes, and thiophene having intermediate reactivity, and the alkanes being by far the least reactive. The large differences in reactivity observed between these classes of compounds is primarily due to the differing effects their photo oxidations have on radical levels in NO_x-air irradiations, with the OH radical rate constant determining relative reactivities within a given class of compounds.

The fuel-NO_x-air runs showed that changes in the composition of these fuels can significantly affect their atmospheric reactivity. Increasing the total level of aromatics in the 15-component synthetic fuel resulted in increased rates of O_3 production, but also resulted in lower maximum O_3 yields. In contrast, increasing the ratio of alkylbenzenes to bicyclic aromatics (with the total aromatic concentrations unchanged) increased both the O_3 formation rates and the maximum O_3 yields. The addition of small amounts (1-2% on a mole carbon basis) of furan or pyrrole to the fuel resulted in dramatic increases in O_3 production rates and also suppressed O_3 yields, but the addition of comparable amounts of thiophene to the fuel had a relatively minor effect. The implications of these results for the photo oxidation mechanisms of these compounds are discussed.

In associated kinetic studies, OH radical rate constants were obtained for pyrrole, tetralin, 2-methylnaphthalene, 2,3-dimethylnapthalene, an O_3 reaction rate constant was determined for pyrrole, and NO_3 radical rate constants were determined for furan, thiophene, and pyrrole for the first time.

The results of this program provide an important and necessary data base required for the development of models for the atmospheric reactions of current and future turbine engine fuels. The development and testing of such models will be carried out in the second phase of this two-part program.

This technical report is divided into two volumes. Volume I contains a detailed summary of the experimental results and a discussion of their significance. Volume II contains a tabulation of the environmental chamber data gathered during the course of the experimental phase of this program. Volume II will only be available from Defense Technical Information Center or National Technical Information Services.

PREFACE

This report was prepared by the Statewide Air Pollution Research Center (SAPRC) of the University of California, Riverside, California 92521, under Contract No. F08635-80-C-0359, with the Air Force Engineering and Services Center, Air Force Engineering and Services Laboratory (AFESL/RDS), Tyndall Air Force Base, Florida 32403.

This report describes the first phase of a two-phase program aimed at developing experimentally tested models for the atmospheric reactions of turbine engine fuels. This phase consists of the experimental studies necessary for model development and testing. The second phase will consist of the necessary model and software development.

This technical report is divided into two volumes. Volume I describes the experimental results and discusses their significance. Volume II tabulates environmental chamber data gathered during the experimental studies phase of this program. For most purposes, Volume I is complete in itself but a few people may find it necessary to use Volume II in conjunction with Volume I. Initial distribution of Volume II was not made, but a copy was submitted to the Defense Technical Information Center. Those who need to use Volume II may obtain copies from the Defense Technical Information Center or from the National Technical Information Service (addresses are listed on inside of front cover).

This work was carried out between June 1983 and June 1984 under the direction of Dr. William P. L. Carter and Dr. Arthur M. Winer, Co-Principal Investigators, and Dr. Roger Atkinson, Program Manager. The principal research staff on this program were Ms. Margaret C. Dodd, Mr. William D. Long, and Ms. Sara M. Aschmann. Assistance in processing the data was provided by Ms. Lori A. Luisi and Ms. Minn P. Poe, and assistance in preparation of this report was provided by Ms. I. M. Minnich and Ms. Christy J. LaClaire.

Dr. Daniel A. Stone, AFESC/RDVS, was Project Officer for this contract.

This report has been reviewed by the Public Affairs Office (PA) and is releasable to the National Technical Information Service (NTIS). At NTIS it will be available to the general public, including foreign nationals.

This technical report has been reviewed and is approved for publication.

DANIEL A. STONE
Project Officer

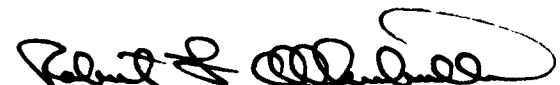

ROBERT F. OLFENBUTTEL, Lt Col, USAF, BSC
Chief, Environics Division

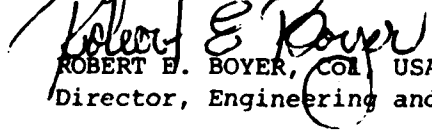

ROBERT E. BOYER, Col, USAF
Director, Engineering and Services Laboratory

(The reverse of this page is blank.)

TABLE OF CONTENTS

TABLE OF CONTENTS (CONCLUDED)

LIST OF FIGURES

LIST OF FIGURES (CONTINUED)

LIST OF FIGURES (CONCLUDED)

LIST OF TABLES

LIST OF TABLES (CONCLUDED)

(The reverse of this page is blank.)

SECTION I

INTRODUCTION

Normal operations of military aircraft within the United States involve the use of large quantities of turbine engine fuels, and some release of these fuels into the atmosphere is an inevitable consequence of their storage and handling. Further emissions of fuel vapor into the atmosphere occur through in-flight fuel jettisoning (Reference 1), where operational situations call for the aircraft's gross weight to be reduced to facilitate safe landing, and through the emission of unburned fuel components in jet exhaust (Reference 2). In the presence of oxides of nitrogen, which are emitted from aircraft engines and a variety of other anthropogenic sources, these vaporized fuel components can react in sunlight to form ozone and other photochemical oxidants and secondary pollutants, as well as aerosols. To comply with federal, state, and local air quality regulations, it is necessary to know the impacts of direct emissions of current jet fuels on air quality, and to be able to predict how future changes in fuel composition may affect air quality.

Significant changes in fuel composition may occur in the near future since it has become increasingly apparent that continued dependence on foreign oil as a source of these fuels is unacceptable from both a military and economic standpoint, and alternate domestic sources such as coal oil or shale oil are currently under active investigation. Such a change in derivation will almost certainly involve significantly broadened specifications for future fuels (Reference 3), which, in turn, may affect their atmospheric reactivity. In addition, fuels derived from coal or shale oil may also include sulfur-, oxygen-, or nitrogen-containing impurities at levels significantly higher than in present fuels, and this may also affect the extent to which release of the fuel affects air quality. However, the nature and magnitude of these effects are highly uncertain, and no reliable means yet exists by which they can be predicted.

Previous studies concerning atmospheric impacts of vaporized aircraft fuels are few, and have been highly limited in scope. Bouble et al. (Reference 4) and Scott (Reference 5) discussed fuel emissions from aircraft and Clewell (Reference 1) discussed fuel jettisoning, but none of these studies addressed the atmospheric reactions occurring after the fuel was emitted or released. More directly related to the problem of atmospheric reactions of vaporized fuels were two studies carried out in our laboratories, one in which a series of multiday outdoor chamber experiments were conducted where nine different military aircraft or commercial motor vehicle fuels were vaporized and irradiated in the presence of NO_x (Reference 6) and the other in which the effects of temperature and pressure on the NO_x-air irradiations of JP-4 and (to a lesser extent) JP-8 were studied in an indoor environmental chamber (Reference 7). The latter study was carried out to elucidate the effects of altitude on the atmospheric reactivity of these fuels. The reactivity of these fuels in terms of rates of NO oxidation and O_3 formation increased with altitude, with this effect apparently being primarily due to the effect of reduced pressure. In the former study, which concerned only ground-level effects, revealed that differences in fuel composition can significantly affect atmospheric reactivity, and data were obtained concerning the relative reactivities of the nine fuels studied.

However, in terms of being able to predict the effects of future changes in fuel composition on their atmospheric reactivities, it is apparent that the approach employed in our previous studies, i.e., to carry out chamber experiments under a variety of representative conditions for each of the many different present or potential future fuels or fuel types, is neither practical nor cost-effective. For example, to compare the reactivities of just nine different fuels, over 130 single- and multiday experiments were required, and experiments were carried out under a variety of temperatures and lighting conditions for only two of the fuels studied. A much more effective approach would be to develop reliable computer models for the atmospheric reactions for each of the major classes of fuel constituents and potential future impurities, and to use these models to predict the atmospheric reactivity of any present or

future fuel whose composition is known. This approach was employed in the study described in this report.

Developing reliable computer models for the atmospheric reactions of fuels involves a number of tasks, some of which have already been largely completed, others which were carried out as described in this report, and still others which remain to be completed. These tasks include the following: (1) identifying the major constituents of the fuels of interest and their potential future impurities which may be of significance; (2) reviewing the available data and chemical theories concerning the atmospheric reactions of members of the various major classes of fuel constituents and impurities, and using this information to develop chemically valid models for these processes; (3) carrying out environmental chamber experiments under carefully controlled conditions suitable for testing and refining these models; (4) using the results of these experiments to test the models and to allow values of uncertain mechanistic or kinetic parameters to be refined to be consistent with the data; and (5) incorporating this tested and refined model into computer software suitable for use by Air Force planners and others to predict effects of changes in fuel composition on air quality under various idealized scenarios. The status of these various tasks, as they relate to the studies described in this report is briefly discussed below.

The major constituents of turbine engine fuels have already been largely identified. As presently used, military jet fuels are multicomponent hydrocarbon mixtures, as exemplified by the petroleum- and shale-derived JP-4 and JP-8 fuels (Reference 6). The major individual components of these fuels are alkanes (straight chain, branched, and cycloalkanes) with lesser amounts of aromatics and very small amounts of alkenes (Reference 6). As an example, Table 1 shows a representative composition of JP-4, based on an analysis by the Air Force Aeropropulsion Laboratory (Reference 1). In addition, if future military aircraft fuels are derived from coal or from shale oil, they may also contain small (< 2 percent) amounts of sulfur-, oxygen-, and, less likely (Reference 4), nitrogen-containing organics. These heteroatom-containing organics are anticipated to include such compounds as thiophenes, furans, and pyrroles

TABLE 1. REPRESENTATIVE COMPOSITION OF JP-4 (FROM REFERENCE 1).

Component	Mass percentage
Isopentane	3.2
Isohexane	7.1
Cyclohexane	2.2
Benzene	0.3
3-Methylhexane	8.6
Methylcyclohexane	7.3
Toluene	0.8
4-Methylheptane	9.4
cis-1,4-Dimethylcyclohexane	7.7
m-Xylene	1.8
4-Methyloctane	8.7
Isopropylcyclohexane	4.6
1-Ethyl-2-methylbenzene	2.8
2,7-Dimethyloctane	7.0
p-Menthane (cis)	3.9
p-Cymene	2.1
Naphthalene	0.3
Undecane	4.7
3-Methylbutylcyclohexane	2.7
3-Methylenedecalin (trans)	4.0
1-Butyl-3-methylbenzene	1.2
1-Methylnaphthalene	0.3
Dodecane	2.8
3-Ethylbutylcyclohexane	1.3
1,3,5-Triethylbenzene (mesitylene)	0.6
2,3-Dimethylnaphthalene	0.3
Tridecane	1.1
3-Isopropylbutylcyclohexane	0.4
3,5-Diethyl-1-propylbenzene	0.1
Tetradecane	0.2
Pentadecane	0.1
Perhydrophenanthrene	2.2
Residual	0.2

(Reference 8), but further detailed analyses of these fuels are necessary to identify these components.

In addition to a knowledge of the composition of a given fuel, an adequate knowledge of the atmospheric chemistry of its major components is required before reliable models for its atmospheric reactions can be

developed. At the present time, many aspects of the kinetics and reaction mechanisms of O_3 and OH radicals with the simple organics are known or are becoming known from a combination of laboratory, environmental chamber, and computer modeling studies (References 9-18). In particular, the available kinetic data indicate that the major mode of initial reaction of the alkane and aromatic fuel constituents is reaction with the hydroxyl radical (Reference 18), and, based on our knowledge of the atmospheric chemistry of the simpler organics, some inferences concerning that for some of the major fuel constituents can be derived. However, significant gaps still remain in our understanding of the atmospheric chemistry of the aromatics and the larger alkanes (including the cycloalkanes), and even less is known about the atmospheric chemistry of the heteroatom-containing organics, the naphthalenes, and the other bicyclic aromatic hydrocarbons. These are precisely the classes of compounds whose atmospheric chemistry must be characterized before reliable, predictive models for air quality impacts of turbine engine fuels can be developed.

To improve its understanding of the atmospheric chemistry of these classes of compounds, and to develop reliable predictive models for the fuels, the Air Force Engineering and Services Laboratory contracted the Statewide Air Pollution Research Center (SAPRC) of the University of California at Riverside to carry out the remaining tasks required for model development. This program consists of two phases. The first phase involves conducting environmental chamber experiments to provide a data base suitable for testing and refining models for representative fuel components and representative surrogate and whole fuels (Task 3, above), and also involves a more limited study aimed at obtaining certain kinetic data required in developing these models. The second phase of this program involves using these and other available data to develop and test the models (Tasks 2 and 4) and to develop the necessary software so that the final chemical model can be used by the Air Force for planning purposes (Task 5). These two phases are being carried out sequentially, with the first experimental, model development phase now complete, and the second phase scheduled to begin (if funding is available) in October 1, 1984.

This report gives the results of the experimental phase of this program. By far the major effort of this program consisted of the environmental chamber experiments. In addition, experimental measurements of the rate constants for the reactions of (a) OH radicals with several bicyclic aromatic and alkane fuel constituents, (b) OH radicals and O_3 with pyrrole, and (c) NO_3 radicals with furan, thiophene, and pyrrole were carried out at no added cost to the Air Force. The methods employed and the results obtained are given in this report. These rate constants, which have not been previously determined, are required in any model for the atmospheric reactions of these potential fuel impurities.

The environmental chamber experiments were carried out, using the SAPRC ~6400-liter indoor Teflon chamber, and included a total of 62 NO_x-air irradiations of representative fuel components, various synthetic fuel formulations, and a preproduction batch of shale-derived JP-4 fuel. In addition, a total of 69 control and characterization runs were carried out. The number of experiments of the various types which were conducted in this program are summarized in Table 2.

NO_x-air irradiations of single representative fuel constituents are generally the most useful for testing models for the reactions of these individual compounds or classes of compounds. The single components studied consisted of benzene and the representative alkylbenzenes toluene, m-xylene, and mesitylene (1,3,5-trimethylbenzene), tetralin, naphthalene, and 2,3-dimethylnaphthalene, the representative alkanes n-octane, and methylcyclohexane, and the representative potential future heteratom-containing fuel impurities furan, pyrrole, and thiophene. These compounds constitute a reasonably good representation of the various classes of compounds present in current turbine engine fuels, or which are anticipated as possible impurities in future fuels.

NO_x-air irradiations of synthetic "surrogate" fuels, whose exact compositions are known, are useful for testing chemical models for the complete fuels without concern for effects of uncertainties in the exact fuel composition. The specific synthetic fuel mixtures studied in this program consisted of the following: (1) a "standard" 15-component

TABLE 2. SUMMARY OF EXPERIMENTS CARRIED OUT FOR TESTING MODELS FOR ATMOSPHERIC REACTIONS OF TURBINE ENGINE FUELS AND REPRESENTATIVE FUEL CONSTITUENTS.

Type of experiment	No. runs (total = 131)
Single Constituent	
Benzene	3
Toluene	2
m-Xylene	2
Mesitylene (1,3,5-Trimethylbenzene)	5
Tetralin	5
Naphthalene	5
2,3-Dimethylnaphthalene	4
n-Butane	1
n-Octane	4
Methylcyclohexane	4
Furan	4
Thiophene	4
Pyrrole	4
Synthetic Fuel	
Standard fuel	4
Standard fuel + furan	1
Standard fuel + pyrrole	1
Standard fuel + thiophene	1
Fuel #2 (high aromatics)	2
Fuel #3 (modified aromatics)	2
Whole Fuel	
Pre-production shale-derived JP-4	4
Control and Characterization	
NO_x-air irradiations	31[a]
NO_2 actinometry runs	25
Propene-NO_x irradiations	10
O_3 dark decays	2
Acetaldehyde Irradiations	1

[a]Not counting the 13 NO_x-air + alkane or aromatic experiments, which also give chamber characterization data.

synthetic fuel whose composition was specified by the Air Force before the beginning of this program, and was taken to represent military jet fuels currently in use; (2) a "high aromatics" fuel which had the same components as the "standard" fuel but in which the percentage of aromatics (on a mole carbon basis) was increased from 27 percent to 38 percent; (3) a "modified aromatics" fuel which had the same relative amounts of the alkanes and aromatics as did the standard fuel, but in which the ratio of the alkylbenzenes to the bicyclics tetralin, naphthalene, and 2,3-dimethylnaphthalene was increased by a factor of 2, relative to that in the other fuels; and (4) the "standard" fuel with 1-2 percent (on a mole carbon basis) of either furan, pyrrole, or thiophene added as an "impurity." These different formulations are useful for testing the effects of changing fuel composition on their atmospheric reactivity, and for testing models designed to predict these effects.

In addition to the above, it is also necessary to be able to test the predictions of the model using the results of experiments employing real fuels. Since environmental chamber data are already available concerning NO_x-air irradiations of various whole fuels from our previous USAF-funded programs (References 6 and 7), obtaining such data was not a major effort in this program. However, in order to further expand the available data base concerning whole fuels, a series of experiments employing a preproduction batch of JP-4 fuel was carried out.

In addition to the runs discussed above, a number of control and characterization runs were carried out in order that the conditions of the various experimental runs be sufficiently well-characterized so that they can be used for model testing. These include runs of the following type: (1) NO_2 actinometry experiments to monitor the light intensity, (2) organic tracer-NO_x-air irradiations to monitor the magnitude of the chamber radical source and contamination by reactive organics (Reference 19), (3) propene-NO_x-air control runs to condition the chamber (when required) and to test for overall chamber performance using a system whose chemistry is reasonably well understood (References 11, 15, and 17), and (4) O_3 dark decay rate determinations. The purpose and utility of these experiments are indicated in more detail when their results are discussed.

This report consists of two volumes, of which this is Volume I. This volume contains a full discussion of the experimental methods, results, and conclusions from this study, while Volume II contains the detailed data tabulations of all the environmental chamber experiments carried out. In this volume, the experimental facility, methodology, and analytical techniques of the environmental chamber studies are described in Section II, and the results of these chamber experiments are discussed in Section III. The rate-constant measurements carried out in this program are discussed in Section IV, and a chronological listing of the chamber experiments carried out is given in Appendix A. Although the major conclusions of this two-part program must await the completion of the model development phase, interim conclusions based on the results obtained are discussed in Section V.

SECTION II

ENVIRONMENTAL CHAMBER STUDIES: METHODS OF PROCEDURE

A. CHAMBER EMPLOYED

All experiments were carried out in the SAPRC ~6400-liter indoor Teflon chamber, shown schematically in Figure 1. The reaction chamber consisted of a replaceable 2-mil thick FEP Teflon bag constructed of Teflon sheets heat-sealed together using a double lap seam and externally reinforced with Mylar tape. During this program, three different reaction bags were used; these are indicated in the chronological data sets in Appendix A and in the detailed data tabulations in Volume II. The reactors were fitted inside an aluminum frame of dimensions of 6 feet by 8 feet by 4 feet. One edge was hinged to allow the bag to collapse to approximately one-third of its maximum volume. At the base of the aluminum frame was a motor attached to a Teflon-coated fan which was placed inside the reaction bag and used for mixing the contents of the chamber.

As shown in Figure 1, five Teflon ports were attached to each chamber. These consisted of a pure air fill port, an exhaust port, a continuous sampling port, a chromatographic sampling port, and an injection and formaldehyde sampling port. Pyrex tubes, of 0.5-inch outside diameter (o.d.), extended ~18 inches into the chamber at the various sampling ports, and sampling valves or lines were attached to these probes. The continuous sampling instruments drew their samples through a 0.25 inch o.d. FEP Teflon tube. Gas chromatographic (GC) samples were withdrawn through a 0.25-inch o.d. Pyrex tube with a Becton-Dickinson stainless steel lever-lok stopcock mainfold attached to the end.

Data from the continuous sampling instruments were collected every 15 minutes by an Apple II+ microcomputer data acquisition system. The signals from each instrument were collected and averaged over 20-second time intervals. These data were then printed and stored on a diskette for subsequent transfer to a central campus computer for processing.

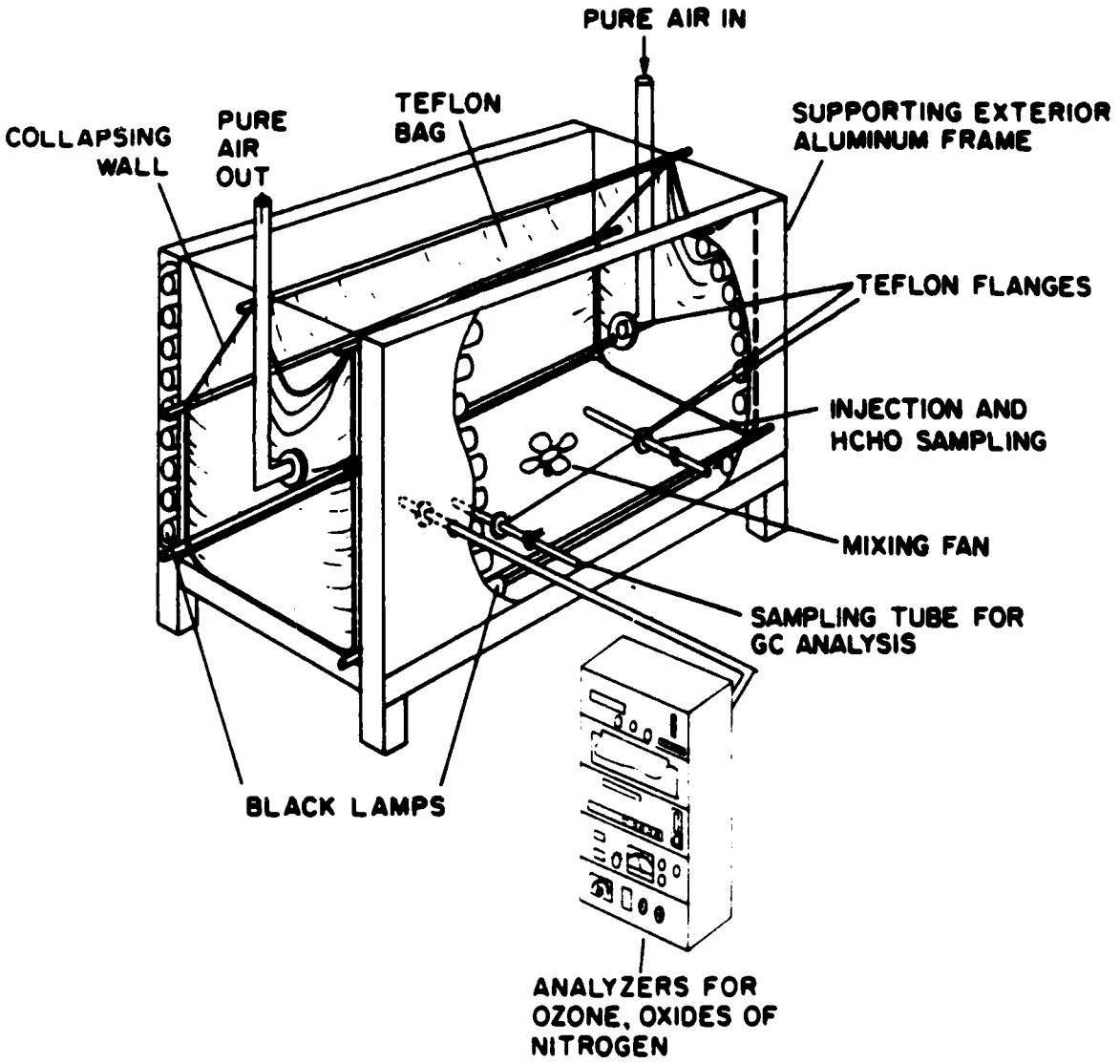

Figure 1. SAPRC All-Teflon Indoor Chamber with Associated Analytical Instruments.

The light source for this indoor Teflon chamber consisted of two diametrically opposed banks of 40 Sylvania 40-watt BL blacklamps backed by arrays of Alzak-coated reflectors. Although the light intensity could be controlled by switching sets of lights on or off, the light intensity was held constant at 70 percent of its maximum for all of the indoor runs reported here. The intensity and spectral characteristics of this light source are discussed in Section III-A-1.

Pure air for these experiments was provided by an air purification system which has been previously described (Reference 20). In this system, ambient air was drawn through Purafil beds (to remove NO_x), compressed by a liquid (water) ring compressor to 100 psig, and passed successively through a heatless dryer, a Hopcalite tower (to remove CO), and a second heatless dryer packed with activated coconut charcoal. The latter acts as a pressure-swing adsorption unit and routinely reduces the hydrocarbon levels (as measured in the chamber) to ~800 ppb methane, <5 ppb of C_2 hydrocarbons and propane and <1 ppb of all higher hydrocarbons. Finally, the air was humidified by passing it through a spray of distilled water and then into the chamber.

B. EXPERIMENTAL PROCEDURES

After the installation of a new reaction bag, the chamber was thoroughly flushed with purified air and was conditioned by irradiating a ~0.5-1 ppm propene and ~0.5 ppm NO_x mixture for at least 5 hours. Between each subsequent experiment, the chamber was flushed, using procedures which varied somewhat as the program progressed. Initially, the chamber was filled and emptied at least three times with purified air and with the last fill being air-humidified to ~50 percent relative humidity (RH). This procedure was subsequently modified so that the chamber was flushed continuously with humidified air for at least 1-5 hours prior to the experiments. After an experiment, the initial procedure was to empty and refill the chamber twice with dry purified air, but this was modified such that the chamber was flushed continuously with dry air for 2 hours, and modified again such that the dry flush was carried out for 2 hours with

the lights on, followed with a 2-hour flush with the lights off. These modifications to the flushing procedure were made as a result of relatively high NO oxidation rates being observed in tracer-NO_x-air irradiations following runs with fuels containing less volatile fuel constituents, suggesting some contamination by reactive organics (see Section III-A-2 for details). The modified procedures appeared to substantially reduce the magnitude of this problem.

After the chamber was filled or flushed and before injection of the reactants, samples were taken for analyses using all of the gas chromatographic instruments to determine background levels. The reactants were injected into the chamber, using several methods, depending on the reactant. In the case of NO, the calculated volume of gaseous NO was taken from a cylinder of Matheson, C.P. grade nitric oxide with a 5 ml gas-tight, all-glass syringe. This NO was then diluted to 100 ml with Liquid Carbonic Hi-Pure nitrogen in a 100 ml, gas-tight, all-glass gas syringe. The NO_2 injection was prepared in a similar manner, except that the NO was diluted with Liquid Carbonic Industrial grade oxygen to yield NO_2. Other gaseous compounds such as n-butane and propene were prepared by diluting the pure gas in Hi-Pure nitrogen. All of these compounds were introduced into the chamber through a Becton-Dickinson stainless steel lever-lok stopcock manifold attached to a 0.25-inch o.d. Pyrex tube. This Pyrex tube was connected to a 0.5-inch o.d. Pyrex tube that protruded ~18 inches into the chamber. Hi-Pure nitrogen was flushed through the injection system both before and after each gaseous injection, and at the same time the Teflon-coated fan was turned on to mix the chamber contents. The fan continued to run for ~5 minutes after the last injection.

Compounds or fuels that were liquid at room temperature and pressure included benzene, furan, methylcyclohexane, n-octane, pyrrole, tetralin, thiophene, toluene, 1,3,5-trimethylbenzene, m-xylene, JP-4, and the three synthetic fuels. These were injected, using a second technique. (Each of the synthetic fuels was previously prepared by mixing the desired volumes or weights of its components. A single 10 ml batch for each fuel was sufficient for all the chamber experiments employing them.

The composition of these fuels is discussed in Section III-C-1.) The injection method involved introducing, by microsyringe, the desired amount of liquid into a ~1-liter glass bulb which had previously been flushed with Hi-Pure nitrogen for ~5 minutes. The glass bulb had a port designed for introduction of the liquid, and also had Teflon stopcocks at each end that were kept closed while the bulb was being dosed. Once the bulb was dosed, it was attached to the injection port of the chamber and also to a nitrogen source. The stopcocks were then opened, and the vaporized contents of the bulb were flushed into the chamber with nitrogen for ~5-20 minutes. When injecting the fuels, the bulb was heated with a heat gun. The chamber mixing fan was running throughout this procedure.

Naphthalene and 2,3-dimethylnaphthalene, which are solids at room temperature, were injected, using a third procedure. For these organics, the desired compound was packed into a 0.25-inch o.d. Pyrex tube and held in place with glass wool, and naphthalene or 2,3-dimethylnaphthalene vapors were injected into the chamber by connecting the tube to the injection port and flushing N_2 through the tube and into the chamber at 2 liters min^{-1} for the required amount of time to achieve the desired concentration. The required time was calculated by assuming the vapor leaving the tube and entering the chamber was saturated with the compound in the tube; this assumption was verified by GC analyses of the chamber contents before the irradiations. Using this procedure, it took 2 hours to inject 2.7 ppm of naphthalene, and 15 hours to inject 0.5 ppm of 2,3-dimethylnaphthalene, these being the highest concentrations of these compounds which were employed. The 2,3-dimethylnaphthalene injections took place on the night before the experiment, under the control of timers. The chamber contents were mixed by the fan at the completion of this flush.

For ozone-conditioning experiments, an Ultraviolet Products Pen-Ray SOG-2 12-inch lamp was inserted into the chamber through the injection port and turned on until the desired concentration of ozone ~1.1 ppm had accumulated. The contents of the chamber were mixed by means of the fan during this procedure.

Gas chromatographic (GC) and formaldehyde samples were taken prior to the beginning of the irradiations, and were generally taken hourly thereafter during standard 6-hour irradiations. The procedures for various conditioning, characterization, and control runs were similar, except that they were generally carried out for shorter time periods and required either more frequent or fewer GC samples.

C. ANALYTICAL TECHNIQUES

In this section, the analytical procedures employed for each set of compounds or physical parameters monitored in this program are described and their calibration techniques and estimated accuracy and precision are discussed.

1. Gas Chromatographic Analyses

Organic reactants and products were monitored, using five different gas chromatographic (GC) systems, each suitable for a particular set of compounds. Except as otherwise noted, samples for chromatographic analyses were withdrawn from the chamber using 100 ml gas-tight, all-glass syringes. Each syringe was flushed at least three times with the sample gas before the sample for analysis was taken. A syringe was attached to the sample port of the chamber to withdraw a sample. Depending on the gas chromatographic analysis system, the contents of the syringe were either (1) flushed through ~2 ml stainless steel or ~10 ml heated glass loops and subsequently injected onto the column by turning a gas sample valve, or (2) condensed in a trap cooled with liquid argon, and then injected onto the column by simultaneously turning the gas sample valve and heating the loop with boiling water or ice water. The various gas chromatographic systems used, and the compounds they monitored, are briefly described below.

Oxygenates such as acetaldehyde, acetone, and 2-butanone, and aromatic hydrocarbons such as benzene toluene, and the xylenes were monitored using the "C-600" gas chromatograph. This system consisted of a

Varian 1400 GC with a flame ionization detector (FID) and a 10-foot by 0.125-inch stainless steel column packed with 10 percent Carbowax 600 on C-22 Firebrick (30-/60-mesh). The flow through this column was set at 50 ml/min and, as was the case with all the GC's, the carrier gas was nitrogen. The hydrogen flow was kept at 45 ml/min, and the oxygen flow, used in the place of air to enhance sensitivity, was set at 250 ml/min. The detector was heated to 200°C, and the column was maintained at 75°C. Samples of 100 ml were withdrawn from the chamber and trapped by pushing the gas sample through a 10-inch by 0.125-inch stainless steel tube packed with 80-mesh glass beads, immersed in liquid argon. The sample was carried onto the column by immersing the trap in boiling water and simultaneously actuating the gas-sampling valve. The gas-sampling valve was heated to 95°C to prevent any compounds from being adsorbed on the valve.

C_2-C_5 alkanes and alkenes were monitored using the "DMS" GC, which consisted of the electrometer and flame ionization detector from a Varian 1400 GC with a 34.5-foot by 0.125-inch stainless steel column packed with 10 percent 2,4-dimethylsulfolane on acid-washed 60-/80-mesh Firebrick. At the end of this column, before the detector, was a 2-foot by 0.125-inch stainless steel "soaker" column packed with 10 percent Carbowax 600 on Firebrick. The carrier nitrogen flow through these two columns was set at 50 ml/min, as was the hydrogen flow. The oxygen flow was 330 ml/min. The columns were maintained at 0°C by keeping them packed in ice. The detector was heated to 115°C. The 100 ml gas samples were trapped on a 10-inch by 0.125-inch stainless steel column packed with 10 percent 2,4-dimethylsulfolane on Firebrick, 60-/80-mesh, immersed in liquid argon. The sample was then introduced to the column by simultaneously thawing the trap in ice water and turning the gas-sampling valve.

Methane, ethane, ethene, and acetylene were monitored using the "PN" GC which consisted of a Varian 1400 GC with a flame ionization detector and a 5-foot by 0.125-inch stainless steel column packed with Porapak N, 80-/100-mesh. The nitrogen carrier flow was set at 80 ml/min, the hydrogen at 60 ml/min, and the oxygen at 400 ml/min. The column was maintained at 60°C, while the detector was heated to 130°C. When a sample was to be analyzed for methane, 100 ml of the sample was pushed through a

2 ml stainless steel loop. The sample in the loop was then transferred onto the column by actuating the gas sampling valve. Sampling for ethene, ethane, and acetylene was accomplished by trapping the sample in an 11 inch by 0.125 inch stainless steel column packed with 10 percent Carbowax 400 on Firebrick, 30-/60-mesh, immersed in liquid argon. The sample was thawed by immersing the trap in ice water and at the same time turning the valve so that the sample was transferred to the column.

C_{5+} alkanes and alkenes, and aromatic hydrocarbons were monitored by the "DB-5C" system, which consists of a Hewlett-Packard 5711A gas chromatograph with a flame ionization detector and a 30 m by 0.322 mm fused silica capillary column. This column, manufactured by J&W Scientific, Inc., had a film thickness of 1 μm composed of the bonded, liquid phase DB5. The nitrogen carrier flow was set at 0.6 ml/min and the makeup gas, also nitrogen, was set to 30 ml/min. The hydrogen and oxygen flows were maintained at 30 ml/min and 230 ml/min, respectively. Before a sample was taken, the column oven was cooled to -90°C using liquid nitrogen. Sampling was accomplished by flushing 100 ml of sample through a dichlorodimethylsilane-treated 10.2 ml glass loop. The GC gas-sampling valve, which was maintained at 145°C, was then actuated, and the sample was transferred onto the -90°C column over a period of 12 minutes. The column was then heated from -90° to -50°C over a 1.3 minute duration. The temperature program was then started with the column being heated from -50° to 200°C at a rate of 8°C/min.

Peroxyacetyl nitrate (PAN) was monitored using a GC with an electron capture detector (ECD) which consisted of an Aerograph gas chromatograph with an ECD. The detector was equipped with a standing current control, and since the response was directly influenced by the standing current, it was maintained to within ±2 percent of a constant value during all experiments and calibrations. The column was a 12-inch by 0.125-inch FEP Teflon column containing 5 percent Carbowax 400 on Chromosorb G (80-/100-mesh) operating at room temperature with a nitrogen carrier flow of 75 ml/min. Analyses were carried out by flushing a ~2 ml loop with the sample, and injecting the contents of the loop onto the column.

Furan, methylcyclohexane, n-octane, thiophene, and reference alkenes used in the kinetic studies were monitored using the "C-20M" GC, consisting of a Varian 1400 GC with a flame ionization detector and a 20 foot by 0.125 inch stainless steel column packed with 2.5 percent Carbowax 20M + 2.5 percent DC703 on acid washed dichlorodimethylsilane treated Chromosorb G, 100-/120-mesh. The nitrogen carrier flow was set at 50 ml/min, the hydrogen flow at 45 ml/min, and the oxygen at 340 ml/min. The column was maintained at 60°C, while the detector was kept at 220°C. Analyses were performed by flushing the 3 ml stainless steel sample loop with the contents of an 100 ml syringe. The sample in the loop was transferred onto the column by actuating the six-port gas sampling valve.

Naphthalene, 2-methylnaphthalene, 2,3-dimethylnaphthalene, tetralin, and n-tetradecane were monitored using the "SP C-II" GC, which consisted of a Varian 1400 GC with a flame ionization detector heated to 225°C and a 6-foot by 0.25-inch Pyrex column packed with Superpax II. Directly attached to the column, through the 245°C heated injector was a 5-inch by 0.25-inch Pyrex tube packed with Tenax GC (60-/80-mesh) through which the nitrogen carrier gas flowed at 30 ml/min. The hydrogen flow rate was 30 ml/min, and the oxygen flow was 260 ml/min. For analysis using this system, sampling via a syringe was not employed. Instead, the sample was obtained by attaching the Tenax-packed tube to a "T"-joint in the continuous sampling instruments line, and drawing 100 ml of sample gas through the Tenax tube with an 100 ml gas-tight syringe. Then the Tenax tube was reattached to the GC, and the carrier flow was restarted. Immediately thereafter, a heated desorber was attached to the Tenax tube. The desorber consisted of two burner blocks electrically heated to 255°C and cut-out to surround the 0.25-inch Tenax tube. The temperature program was started 2 minutes after the carrier flow was started. Two different temperature programs and two different columns were used during this program. The temperature program employed in this analysis consisted of keeping the column at 80°C for 2 minutes and then heating the column to 140°C at 8°C/min. After an analysis was completed, and before another analysis was begun, the column was cooled to the starting temperature, the

carrier flow was stopped, the desorber was removed, and the Tenax tube was removed from the GC and capped.

Pyrrole was monitored using the "SP C-20M" system, which employed the same GC instrument and sample injection procedure as described above for the "SP C-II" system, except that a 6-foot by 0.25-inch Pyrex column, packed with 4 percent Carbowax 20M + 0.8 percent KOH on Superpak II was utilized, and the temperature program consisted of keeping the column at 100°C for 2 minutes after injection and then heating the column at 10°C/min to 160°C.

Calibrations of all GCs were performed at approximately 2- to 3-month intervals, and, except for the ECD and the Tenax system, were accomplished in the same general manner. First, all gas flows were measured to verify that no changes had occurred that would indicate previous measurements were erroneous. After measuring these flow rates, a calibration mixture was made up, using one of two methods. The calibration mixture, composed of known quantities of various compounds, was then injected into the correct GC. The elution time and height of each peak was recorded. The height of each peak was multiplied by the attenuation and the response in millivolts was obtained.

For gaseous compounds, two 2000 ml flasks, whose exact volumes had been determined by measuring with water, were flushed with nitrogen for 20 minutes, and then 2 ml of the pure gas was injected into the first flask with a 5 ml syringe. This flask was allowed to mix 20 minutes, and then 2 ml from this flask was transferred into the second flask. The second flask was allowed to mix 20 minutes. This resulted in ~1 ppm of the gas in the second flask. Loop calibrations were performed by connecting this second flask directly to the loop and flushing the loop with the contents of the flask. Trap calibrations were accomplished by diluting a 5 ml sample from the second flask with nitrogen in a 100 ml syringe, and passing the contents of the syringe through the trap. For a flask containing 1 ppm of the compound, this was equivalent to sampling 100 ml of gas containing 50 ppb of the compound.

Calibration of compounds that were liquid at room temperature was carried out using an all-glass carboy, of volume 46.6 liters, which was

first cleaned by being heated from the inside with a heat gun, then allowed to cool to room temperature and flushed with nitrogen for 1 hour. The carboy was then dosed with 1 μl of each pure liquid to be calibrated using a 10 μl syringe. These were allowed to mix for 1 hour before any samples were taken. Trap and loop calibrations were both accomplished in the same way. A 1 ml sample was taken from the carboy with a 5 ml syringe and diluted with 99 ml of nitrogen. The samples were extracted in the manner described previously. The exact concentration of each compound was calculated knowing the amount of liquid injected and its density.

Calibration samples of PAN for the ECD were available in pressurized cylinders as described previously (Reference 21) and the PAN concentration was determined by infrared absorption of the 8.6 μ band (absorption cross-section = 13.9×10^{-4} ppm^{-1} [Reference 22]). The contents of the cylinder were diluted, using a flow manifold with calibrated rotometers to yield the appropriate PAN concentrations (5-50 ppb), and 100 ml samples were taken directly from that manifold using gas-tight, all-glass syringes.

Calibrations of compounds that were monitored on the Tenax GC were performed by diluting or dissolving a known amount of the desired compound in 5 ml of n-hexane. A microsyringe was used to inject 1 μl of this solution onto the Tenax tube, and then the standard analysis procedure followed. In the case of this GC, peak areas were used to determine concentrations instead of peak heights. The peak areas were determined by multiplying the peak height by the width at half-height and multiplying by the attenuation.

The expected accuracy and precision of concentration measurements of most of the compounds determined by the above systems were, with the exception of PAN and acetaldehyde, ~5 percent or better. Due to varying peak widths, acetaldehyde concentrations were precise and accurate to ~20 percent. Peroxyacetyl nitrate measurements were estimated to have ~10 percent precision and ~25 percent accuracy.

2. Formaldehyde

Formaldehyde was monitored, using the chromatropic acid technique. Samples for analysis by this technique were obtained by drawing 20 liters of air at 1 liter min^{-1} from the chamber through a single bubbler containing 10 ml of doubly distilled water. Samples were taken through the injection and formaldehyde sampling port. A metal bellows pump at the downstream end of the bubbler with a calibrated flow meter and needle valve was used to pull the sample through the bubbler. The samples were developed by adding 0.10 ml of chromatropic acid (4,5-dihydroxy-2,7-naphthalenedisulfonic acid disodium salt) to a 4.0 ml aliquot of the sample. The solution was acidified by diluting it to 10.0 ml with concentrated sulfuric acid. The chromatropic acid solution was prepared by dissolving 0.10 g of the salt in 10.0 ml of doubly distilled water. The developed solutions had a purple color and the absorbances were measured at 580 nm by a Beckman Model 35 spectrophotometer, after zeroing the instrument using a prepared blank. Instrumental drift was also periodically checked during the measurements using the same blank.

Periodic calibrations of the spectrophotometer and flowmeters were carried out. The spectrophotometer was calibrated by subjecting a known concentration of formaldehyde salt to the same procedure as outlined above.

The accuracy and precision of this formaldehyde analysis technique depended upon a number of factors, including the calibration of the spectrometer and the efficiency in the bubbler in collecting formaldehyde in the air passing through it. In the past, the accuracy and precision of this technique had been quite variable, ranging from the optimum accuracy and precision of ~30 percent to periods of anomalously low readings apparently due to problems with the bubbler to periods of anomolously high and highly variable readings apparently due to contamination (see, for example, Reference 23). Attempts to improve the reliability of this technique for routine use have met with limited success.

3. Continuous Monitoring Instruments

Ozone, nitrogen oxides, and temperature were monitored continuously, using the instruments described below. Except as noted, samples for analysis by these systems were taken directly from a probe inserted ~18 inches into the chamber, using Teflon or glass sampling lines.

Ozone was monitored using a Dasibi Model 1003AH UV absorption ozone monitor, or by a Monitor Labs 8410 chemiluminescence ozone monitor. The Dasibi was employed for most experiments, except for those carried out using tetralin or the naphthalenes. Since these organics were observed to yield positive interferences on the Dasibi O_3 analyzer, presumably due to UV absorption by those compounds, both instruments were used for the synthetic fuel runs. Calibrations were carried out every 2 months against a Dasibi Model 1003AH ozone monitor transfer standard, which, in turn, was routinely calibrated by the California Air Resources Board. The ozone source for calibrations was the Teflon reaction chamber, first filled with pure air, as a zero check, and then ozone was produced at various concentrations, as for the ozone-conditioning experiments. Both instruments were allowed to equilibrate before readings were recorded. Several different ozone concentrations were used to check the linearity of the analyzer. If the response was not linear, corrective action was taken. Finally, the analyzer being calibrated was again zeroed with pure air. The precision and accuracy were both better than 5 percent.

Nitric oxide and total oxides of nitrogen (NO_x + organic nitrates) were monitored using a Columbia Scientific Industries Series 1600 or a Thermo Electron Corporation (Teco) Model 14-B chemiluminescence oxides of nitrogen analyzer. Calibrations were performed bimonthly by diluting the output of a NBS cylinder containing 92.8 ppm NO in N_2 with Liquid Carbonic Company Zero Air. The analyzer was first zeroed using Zero Air, then calibrated for NO by diluting in Zero Air and measuring the flow of each gas with a bubble meter. The analyzer was allowed to equilibrate at each concentration for 30 minutes. The first concentration used was ~0.30 ppm. The potentiometers in the analyzer were adjusted, if necessary, to

match the NO output of the analyzer with the actual concentration. Two lower concentrations of NO were used to verify linearity of the analyzer. The converter efficiency was checked by setting a NO concentration of about 0.30 ppm, and then reacting this with a lesser concentration of ozone. If the converter was operating properly, the NO_2 reading equaled the difference in NO. The linearity of the converter was verified by using three different concentrations of ozone. After this procedure was completed, the analyzer was rezeroed with Zero Air. The accuracy and precision of this instrument in the absence of interfering nitrates (see below) was estimated to be better than 5 percent.

The analyses of NO_2 and NO_x was complicated by the fact that for such instruments the converters have been shown (Reference 24) to convert PAN, organic nitrates, and HNO_3 to NO, and thus such species yield a positive interference in the NO_2 analysis cycle. The NO data are unaffected. Conversion of PAN and organic nitrates has been shown to be essentially quantitative (Reference 24) for the molybdenum converter employed in the Teco analyzer, but this has been shown to not be the case for the converter employed in the Columbia Scientific Industries instrument, and preliminary data from our laboratories have indicated that the conversion of PAN was not quantitative. It should be noted that organic nitrates are expected to be formed from larger alkanes, though the nitrates expected to be formed from those compounds could not be monitored due to lack of authentic samples for calibration purposes (they are not available commercially). Therefore, no correction for this interference with the NO_2 data was attempted.

Temperature was monitored with an Analogic Model AN 2572 Digital thermocouple indicator using an iron-constantan thermocouple. The thermocouple was installed in a probe inserted into the center of the chamber. This instrument was calibrated periodically, using ice water as the source for $0^{\circ}C$, and boiling water as the source for $99.1^{\circ}C$ (at 735 torr total pressure). The accuracy was better than 5 percent, and the precision was better than 1 percent.

Relative humidity was determined only at the beginning of a run by exposing wet-bulb and dry-bulb thermometers to the chamber exhaust at the

completion of the final flush. Once the thermometers had equilibrated, the indicated temperatures were recorded and, from these data, the relative humidity was calculated. These thermometers were calibrated periodically using ice and boiling water as described above. The accuracy was better than 5 percent, and the precision was better than 1 percent.

4. Light Intensity

Since the light source of the chamber was constant, the light intensity was determined approximately once a month, using the quartz tube NO_2 photolysis rate technique of Zafonte et al. (Reference 25). In this technique, the reactor cell consisted of a 100 cm segment of 25 mm (nominal) quartz tubing with 0.25-inch o.d. extensions at each end. The i.d. of this tube was measured at both ends using calipers and had an average value of 21.44 mm. The nitrogen dioxide was obtained from a Scott-Marrin, Inc., tank mixture of 2.1 ppm, and was not diluted. The NO_2 flow entered the reactor cell via 0.25 inch blackened FEP Teflon tubing, attached with a 0.25 inch stainless steel Cajon ultra-torr union. The exhaust from the cell was connected to the sampling line of the NO_x analyzer, and the excess was vented to the atmosphere via a "T." These sample lines were also blackened. The sample lines were inserted 5 cm into the cell. This allowed for secondary oxygen atom reactions to be completed before the gas reached the sampling line. Under typical conditions, the gas flow was set to 37 ml s^{-1}. With an exposed cell volume of 262 cm^3, a NO_2 residence time of 9.1 seconds was established within the cell. This allowed a sufficient buildup of NO which could then be accurately measured.

During photolysis, NO concentrations generally ranged from 100-150 ppb. NO and NO_2 were measured using either the Columbia or the Teco chemiluminescence NO_x detector described above. NO and NO_2 were alternately measured on a 30 second cycle.

The precision of these NO_2 actinometry measurements was generally ~5-10 percent. The accuracy of the NO_2 actinometry measurements were determined by a number of factors, including the accuracy of the NO_x analyzer, the extent to which plug flow conditions in the tube had been

established, and whether the tube was placed in a location in which the light intensity and spectral distribution accurately reflected that in the chamber. The results of these measurements are discussed in more detail in Section III-A-1.

SECTION III

CHAMBER EXPERIMENTS: RESULTS AND DISCUSSION

As indicated in Section I, a total of 131 environmental chamber experiments were carried out in this program, including 47 single component-NO_x-air experiments on 13 different representative fuel constituents and model compounds, 15 fuel-NO_x-air experiments on one whole fuel and six synthetic fuels, and 69 control or characterization runs. A chronological listing of all these runs is given in Appendix A, together with a brief summary of the description, purpose, experimental conditions, and major results of each experiment.

Detailed tabulations of the data from these runs are given in Volume II of this report. In addition to giving results of the experimental measurements made during each run, these computer-generated tabulations indicate which instrument was used for each set of measurements, and give overall averages for the major physical parameters measured during the runs. Comments taken from the laboratory notebooks describing the experimental operations, general weather conditions, and any relevant observations, problems, or special situations which occurred during the run are also included on these tabulations.

In the following sections, the results obtained in these experiments are summarized and discussed. The light intensity and chamber characterization data are discussed in Section III-A, followed by a discussion of the results of the single-component experiments in Section III-B. The experiments employing the whole or synthetic fuels are discussed in Section III-C. A detailed interpretation and modeling study of these experiments is reserved for Phase 2 of this program, but the major experimental observations in these experiments are summarized, and various reactivity characteristics of the individual fuel components, model compounds, and fuels studied in this program are discussed.

A. LIGHT SOURCE AND CHAMBER CHARACTERIZATION

1. Light Intensity and Spectral Distribution

If the results of these runs are to be useful for model testing purposes, both the intensity and the spectral distribution of the photolyzing light must be known. The absolute light intensity was determined by periodically measuring the rate of photolysis of NO_2

$$NO_2 + h\nu \rightarrow NO + O(^3P) \qquad (1)$$

using the quartz tube technique of Zafonte et al. (Reference 25) as discussed in Section II-C-4. The results of all measurements of the NO_2 photolysis made at the light intensity employed in our experiments (i.e., 70 percent of maximum), and with the set of lamps employed during these experiments, are plotted against the ITC run number in Figure 2. This figure includes runs conducted before and during this program, with the arrow in the figure indicating the first experiment. The lines on the figure indicate least squares regressions or averages of the data for the periods indicated. Although the light intensity fell relatively rapidly when the lamps were new, and had an unexpected ~10 percent increase shortly after the beginning of this program, it appeared to be relatively constant during the period most of the runs reported here. The data indicated that an NO_2 photolysis rate of 0.30 min^{-1} is appropriate for runs ITC-690 through 716, with a rate of 0.32-0.33 min^{-1} being appropriate for run ITC-717 and those following, with an estimated uncertainty of ~10 percent in both cases.

To calculate rates of the other photolysis reactions, the relative spectral distribution must also be known. The spectral distribution of the blacklights in this indoor Teflon chamber was measured using a Spex Model 1667 spectrometer with a IP28 photomultiplier, calibrated against an NBS standard lamp, and the relative light intensities (in terms of photons per unit area per unit time) at selected wavelengths are given in Table 3.

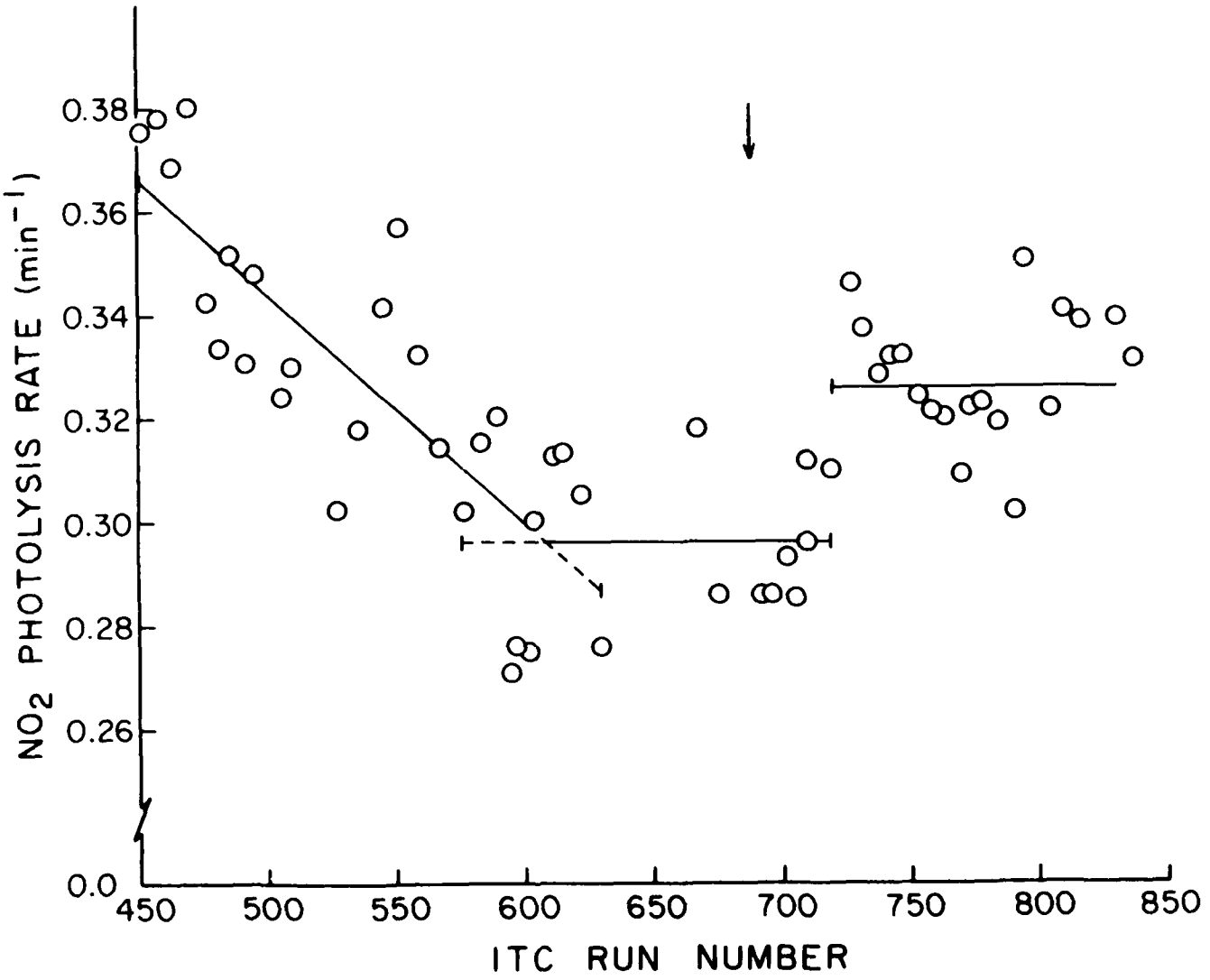

Figure 2. Plot of NO_2 Photolysis Rates Measured in the Indoor Teflon Chamber Against Run Number. Lines Shown are Linear Least Squares Regressions or Averages of the Data Over the Indicated Ranges. Arrow Indicates the Start of the Series of Experiments in this Program.

TABLE 3. RELATIVE SPECTRAL DISTRIBUTION FOR THE BLACKLIGHTS IN THE SAPRC 6400-LITER INDOOR TEFLON CHAMBER.[a]

Wavelength (nm)	Intensity[b]	Wavelength (nm)	Intensity[b]	Wavelength (nm)	Intensity[b]
295.7	0.0	347.8	0.952	405.0	0.258
296.7	0.0019	350.0	0.972	406.0	0.264
298.0	0.0024	351.7	0.990	406.7	0.251
300.7	0.0018	353.7	1.00	408.7	0.0596
302.1	0.0043	356.7	0.982	412.0	0.0387
304.3	0.0058	360.0	0.925	416.7	0.0348
306.3	0.0057	363.3	0.829	423.3	0.0298
310.0	0.0140	364.3	0.859	430.0	0.0227
313.0	0.0728	364.7	0.869	434.3	0.0217
313.7	0.0846	365.5	0.870	436.1	0.641
315.0	0.0879	366.9	0.835	436.7	0.709
315.3	0.0856	368.5	0.685	437.3	0.712
316.7	0.0581	370.0	0.639	438.1	0.651
317.3	0.0564	376.7	0.442	439.7	0.0169
318.7	0.0858	383.3	0.261	443.3	0.0140
323.3	0.1495	390.0	0.1423	450.0	0.0081
330.0	0.331	396.7	0.0885	460.0	0.0
336.7	0.563	393.0	0.0535		
343.3	0.851	404.3	0.223		

[a]As measured on June 30, 1983.

[b]Intensity in terms of photons per unit area per unit time, normalized so the maximum intensity = 1.0 units.

The wavelengths in Table 3 were chosen such that the true light intensity spectrum can be well approximated by a series of straight lines between each of the tabulated points for the purpose of computing the photolysis rates. The data in Table 3 were actually obtained prior to the beginning of this program, but a subsequent spectral measurement indicated that the change of spectral distribution during these experiments was insignificant.

2. NO_x-Air Irradiations

A number of NO_x-air irradiations were carried out periodically throughout this program to obtain a measurement of the chamber radical source and of offgassing of reactive contaminants during our experiments. These runs, the purpose of which has been discussed in detail elsewhere (Reference 19), consisted of irradiations for at least 2 hours of NO_x-air mixtures containing traces (~10 ppb) of propene and n-butane. In the absence of chamber radical sources and reactive contaminants, this system is expected to be completely unreactive, and is thus highly sensitive to these chamber effects. Because the chamber radical source has been shown to be, at least in certain chambers, dependent on the NO_x levels (References 19 and 26), the NO_x levels employed in these runs were representative of those employed in the single-component-NO_x or fuel-NO_x runs.

Radical initiation rates were obtained by equating the initiation rates to termination rates due to the OH + NO_2 reaction [the major termination mechanism in this system (Reference 19)], with the rate of the latter being estimated from the known OH + NO_2 rate constant (Reference 17) and the measured NO_2 and OH radical levels. The OH radical levels were monitored by measuring the relative rates of decay of the two organic tracers (propene and n-butane), which were consumed primarily by reaction with OH radicals:

$$\text{OH + n-butane} \rightarrow \text{products} \qquad (2)$$

$$\text{OH + propene} \rightarrow \text{products} \qquad (3)$$

However, propene was also consumed to some extent in this system by reaction with O_3 and $O(^3P)$ atoms (Reference 17),

$$O_3 + \text{propene} \rightarrow \text{products} \qquad (4)$$

$$O(^3P) + \text{propene} \rightarrow \text{products} \qquad (5)$$

and a correction for this must be made in the data analysis.

For propene and n-butane as the tracers, the relevant kinetic differential equations are:

$$d\ln[\text{n-butane}]/dt = -k_2[OH] \qquad (I)$$

$$d\ln[\text{propene}]/dt = -k_3[OH] - k_4[O_3] - k_5[O(^3P)] \qquad (II)$$

where k_2 and k_3 are the rate constants for the reaction of n-butane and propene with OH radicals, respectively, k_4 and k_5 are the rate constants for the reaction of propene with O_3 and $O(^3P)$ atoms, respectively, and the O_3 and $O(^3P)$ atom concentrations can be estimated, based on the following assumptions. Since $O(^3P)$ is formed primarily from NO_2 photolysis and is consumed primarily by its rapid reaction with O_2, it can, to a very good approximation, be considered to be in photostationary state governed by these two reactions, and thus:

$$[O(^3P)] \simeq \frac{k_1[NO_2]}{k_6[O_2][M]} \qquad (III)$$

where k_1 and k_6 are the rate constants for the photolysis of NO_2 and for the third-order reaction of $O(^3P)$ atoms with O_2, respectively:

$$NO_2 + h\nu \rightarrow NO + O(^3P) \qquad (1)$$

$$O(^3P) + O_2 + M \rightarrow O_3 + M \qquad (6)$$

Similarly, O_3 is also formed by NO_2 photolysis and, under the conditions of our experiments, was consumed primarily by its rapid reaction with NO. Thus it also can be assumed to be in photostationary state, and,

$$[O_3] \simeq \frac{k_1[NO_2]}{k_7[NO]} \qquad (IV)$$

where k_7 is the rate constant for the reaction of O_3 with NO,

$$NO + O_3 \rightarrow NO_2 + O_2 \qquad (7)$$

Equations (I) through (IV) can be combined and rearranged to yield

$$[OH] = (k_3-k_2)^{-1} \frac{d}{dt} \ln \frac{[n\text{-butane}]}{[propene]} - k_1[NO_2] \left\{ A + \frac{B}{[NO]} \right\} \qquad (V)$$

where

$$A = \frac{k_5}{(k_3-k_2)k_6[O_2][M]}$$

and

$$B = \frac{k_4}{(k_3-k_2)k_7}$$

Equation (V) shows that the correction for consumption of propene by reaction with O_3 and $O(^3P)$ atoms increases with $[NO_2]$ and $[NO_2]/[NO]$, respectively.

The radical flux, R_u, required to fit the data for a given run can be estimated from the fact that radical initiation and radical termination rates must balance. Since the only significant radical termination processes in this system are the reactions of OH radicals with NO and NO_2, and since HONO is in photoequilibrium after ~60 minutes of irradiation (Reference 19) then

$$R_u = k_8[OH]_{avg}[NO_2]_{avg} \qquad (VI)$$

where k_8 is the rate constant for the reaction of OH radicals with NO_2,

$$OH + NO_2 \xrightarrow{M} HNO_3 \qquad (8)$$

and $[OH]_{avg}$ and $[NO_2]_{avg}$ (the average OH radical and NO_2 concentrations for $t > 60$ minutes) are experimentally determined. In general, in these

irradiations the OH radical levels were approximately constant after the first hour of irradiation.

In addition to measuring chamber radical sources, NO_x-air irradiations can also be used to obtain an estimate of the extent of contamination by reactive organics, since in general these will cause enhanced rates of NO oxidation due to the following reactions,

$$\text{organic}_i + OH \rightarrow R_i \tag{9}$$

$$R_i + O_2 \xrightarrow{M} R_iO_2 \tag{10}$$

$$R_iO_2 + NO \rightarrow \rightarrow \text{products} \tag{11}$$

In the absence of such contamination, NO oxidation rates are expected to be low, at least at the relatively low NO_x concentrations employed in these experiments. To estimate the extent of this contamination, reactions (9)-(11) can be represented by the following,

$$\text{organic}_i + OH \xrightarrow{k_i} -\alpha_i\ NO + \text{products} \tag{12}$$

where k_i is the OH + organic rate constant, and α_i is the number of molecules of NO oxidized by the overall process (which in general may be greater than 1, since usually the oxidation of organics involves sequential formation of several different peroxy radicals [see, for example Reference 17]). Thus if we assume that the above reactions are the major processes affecting changes in concentration in NO (i.e., that the NO_x and O_3 levels are sufficiently low that the reactions

$$NO + NO + O_2 \rightarrow 2\ NO_2 \tag{13}$$

$$O(^3P) + NO_2 \xrightarrow{M} NO_3 \tag{14}$$

$$O_3 + NO_2 \rightarrow NO_3 + O_2 \tag{15}$$

$$NO_3 + NO \rightarrow 2\ NO_2 \qquad (16)$$

have an insignificant effect on the NO concentrations) then we can write:

$$-\frac{d[NO]}{dt} = \Sigma_i k_i \alpha_i [organic_i][OH]$$

or

$$\text{"Organic Reactivity"} = \Sigma_i k_i \alpha_i [organic_i] = \frac{\frac{-d[NO]}{dt}}{[OH]} \qquad (VII)$$

Thus the ratio of the NO consumption rate to the observed OH radical levels can be considered to be a measurement of the total "organic reactivity" which is the sum of the concentration of the reactive organics present (including the propene and n-butane tracers, and the CO present in the matrix air), weighted by their OH rate constant (k_i) and their efficiency in oxidizing NO (α_i). Note that 10 ppb of each of the tracers and 1 ppm of CO in the matrix air (the typical levels in these experiments) will contribute ~1 x 10^3 min^{-1} to this quantity, which means that any excess over ~1 x 10^3 min^{-1} is due to contaminants.

The results of the NO_x-air irradiations carried out in this program are summarized in Table 4. This table also includes data from the NO_x-air + alkane, or NO_x-air + aromatic, runs (see following section) obtained prior to the addition of the alkane or the aromatic. This table shows that the radical input rates and total organic reactivities are quite variable, though in general they are within the range observed previously for this chamber (References 19 and 26). In contrast to the results of NO_x-air irradiations carried out in the SAPRC 5800-liter evacuable chamber (Reference 19), no significant dependence of the radical input rates on the NO_2 levels was observed in these experiments; though it should be noted that the NO_2 levels were not varied over as wide a range as our previous studies (References 19 and 26).

The data in Table 4 suggest the radical input rates and organic reactivity depend to some extent on whether the reaction bag was new and

TABLE 4. SUMMARY OF RESULTS OF NO_x-AIR IRRADIATIONS.

Bag no.	ITC run no.	Initial conc. NO (ppm)	Initial conc. NO_2 (ppm)	Average[a] [OH] (10^6 cm^{-3})	Rates[a] (ppb min^{-1}) Radical input[b]	Rates[a] (ppb min^{-1}) NO Oxidation	Organic reactivity[c] (10^3 min^{-1})
101	692	0.39	0.11	1.82	0.15	0.12	1.6
	695	0.40	0.10	1.79	0.13	0.23	3.1
	700	0.39	0.14	2.81	0.26	0.39	3.4
	704	0.39	0.13	2.61	0.22	0.29	2.7
	707	0.80	0.21	1.67	0.24	0.26	3.8
	712	0.41	0.10	3.00	0.22	0.43	3.5
	714	0.81	0.20	1.37	0.18	0.43	7.6
	717	0.40	0.12	2.10	0.18	0.30	3.5
	723	0.41	0.10	2.99	0.29	0.62	5.0
	724	0.26	0.06	1.51	0.06	0.36	5.8
	726	0.39	0.12	1.54	0.13	0.28	4.4
	731	0.40	0.13	2.45	0.21	0.30	3.0
	734	0.21	0.05	3.65	0.17	0.37	2.5
102	737	0.39	0.10	0.96	0.06	0.27	6.8
	740	0.40	0.11	1.02	0.08	0.15	3.6
	745	0.41	0.11	1.70	0.13	0.13	1.9
	749	0.19	0.04	2.23	0.10	0.25	2.7
	752	0.44	0.11	2.20	0.20	0.28	3.1
	757	0.20	0.05	4.89	0.28	0.49	2.4
	760	0.42	0.13	1.93	0.17	0.29	3.7
	761	0.42	0.11	1.68	0.14	0.27	4.9
	762	0.22	0.06	2.25	0.12	0.24	2.6
	763	0.22	0.04	2.38	0.11	0.20	2.0
	765	0.36	0.15	1.83	0.16	0.37	4.9
	766	0.21	0.05	2.22	0.10	0.18	2.0
	767	0.43	0.13	1.07	0.09	0.12	2.7
	770	0.41	0.14	1.09	0.10	0.20	4.4
	772	0.34	0.12	2.87	0.30	0.58	4.0
	776	0.44	0.12	2.55	0.22	0.39	3.7
	780	0.41	0.13	2.33	0.20	0.23	2.4
	782	0.39	0.13	2.41	0.21	0.23	2.3
	787	0.21	0.05	3.57	0.19	0.48	3.3
	789	0.44	0.11	2.51	0.21	0.38	3.9
103	793	0.36	0.12	1.68	0.13	-0.03	-0.4
	797	0.44	0.11	1.49	0.13	-0.01	-0.2
	800	0.40	0.14	1.66	0.16	0.13	1.9
	803	0.22	0.07	3.25	0.19	0.25	1.9
	808	0.33	0.13	1.70	0.15	0.22	3.1
	814	0.43	0.10	1.42	0.10	0.12	2.0
	824	0.33	0.07	1.51	0.08	0.06	1.0
	826	0.72	0.17	0.77	0.08	0.03	1.0
	827	0.88	0.17	0.86	0.11	0.09	2.5
	828	0.83	0.18	0.55	0.07	0.07	3.2
	829	0.21	0.05	1.79	0.06	0.08	1.1
	831	0.84	0.17	1.32	0.16	0.14	2.6
	832	0.84	0.16	0.98	0.11	0.11	2.6

[a]Values given are for the second hour of the irradiation.

[b]Calculated using equation (VI).

[c]Calculated using equation (VII).

perhaps also on the chamber-flushing procedure employed between runs. In particular, the lowest organic reactivities for Bags 101 and 103, and the lowest radical input rates for Bag 102 were observed when the reaction bag was new. On the other hand, the first NO_x-air run for Bag 102 suggested some initial contamination of that bag (which subsequently decreased after several runs were carried out), and the initial radical input rates for Bags 101 and 103 were not significantly lower than observed in most subsequent runs. Other than the first run employing Bag 102, the highest organic reactivities were observed in Bag 101, which may be due to the fact that a less complete flushing procedure was employed between runs in that bag, compared to the standard procedure subsequently used (see Section II-B and Appendix A). On the other hand, the radical input rates tended to vary randomly between ~0.1 and 0.3 ppb/min, and did not appear to be strongly influenced by the chamber-flushing procedure or other known factors.

3. Ozone Dark Decay Determinations

Another chamber-dependent parameter which must be known when using these chamber data for model testing purposes is the rate of O_3 destruction on the walls of the chamber. Thus, two O_3 dark decay rate determinations were carried out in this program, one (Run ITC-692) near the beginning, and the other (ITC-803) near the end. These two runs gave O_3 dark decay rates of 1.1 percent/hr and 0.5 percent/hr, respectively. These values are within the range previously observed for this chamber, and indicate that O_3 is quite stable in this chamber, with a half-life of over 60 hours.

4. Acetaldehyde Irradiation

In order to measure the rate of off-gassing of NO_x (NO or NO_2) from the chamber walls upon irradiation, an acetaldehyde-air irradiation (Run ITC-825) was carried out around the end of this program. When irradiated in environmental chamber systems, acetaldehyde is consumed either

by direct photolysis or by reaction with OH radicals (which are always present during irradiations in environmental chambers), with the latter process giving rise to acetyl peroxy radicals.

$$CH_3CHO + OH \rightarrow CH_3\dot{C}O \xrightarrow{O_2} CH_3\overset{O}{\overset{\|}{C}}-OO\cdot \qquad (17)$$

If any NO_x is present in the system, even at sub-ppb levels, the primary fate of the acetyl peroxy radicals will be reaction with NO or NO_2, with the latter process giving rise to PAN, which is relatively stable in these systems, and whose formation can be readily monitored.

$$CH_3\overset{O}{\overset{\|}{C}}-OO\cdot + NO \rightarrow CH_3\overset{O}{\overset{\|}{C}}-O\cdot + NO_2 \qquad (18)$$

$$CH_3\overset{O}{\overset{\|}{C}}-OO\cdot + NO_2 \rightleftarrows CH_3\overset{O}{\overset{\|}{C}}-OONO_2 \text{ (PAN)} \qquad (19)$$

If measurable ozone is present in the system (as was the case for most of these runs, including the one carried out in this program) then NO reacts rapidly with O_3 forming NO_2, leading to an NO_2 concentration greater than that of NO. Thus PAN is the dominant product. Therefore, since PAN formation can only occur if NO_x is present in the system, and since formation of PAN is expected to be the major fate of NO_x under these high acetaldehyde, low NO_x conditions, then the PAN formation rate in acetaldehyde-air irradiations can be equated to the NO_x off-gassing rate from the chamber walls.

The PAN yield observed in run ITC-825 after 180 minutes of irradiation was 5 ppb, indicating a NO_x off-gassing rate of 0.03 ppb/min. This is entirely within the 0.02-0.04 ppb/min range observed in a series of four such experiments carried out for a previous program (Reference 27) employing different bags in this chamber. This NO_x off-gassing rate, though relatively minor, should be taken into account when using these data for model testing.

5. Propene-NO_x Irradiations

To ensure that chamber effects not measured in the above discussed characterization runs are not significantly affecting the results of the experiments to be used for model testing, propene-NO_x-air irradiations were carried out at various times for control purposes. The chemistry of propene in NO_x-air irradiations is among the best characterized of the reactive organics, and models for its reactions have been shown to fit the results of experiments carried out in a variety of chambers (References 9-11 and 13-15). Thus, if any propene-NO_x-air irradiations carried out in this program give results not consistent with model predictions, the possibility of anomalous effects would be indicated.

Table 5 summarizes the initial concentrations and the observed and calculated final or maximum O_3 yields for all of the propene-NO_x irradiations carried out during this program, and Figure 3 shows the observed and calculated concentration-time plots for species monitored in a representative run (run ITC-693). The model calculations were derived, using the mechanism of Atkinson and Lloyd (Reference 17), with the photolysis rates calculated based on the light intensity and spectral distribution data given in Section III-A-1. An O_3 dark decay rate of 0.5 percent/hour, no initially present nitrous acid, and the radical input rates listed in Table 5 (the latter being adjusted to within the nearest 0.05 ppb/min to give the best fit to the data) were used in these calculations.

The calculated O_3 yields were generally ~10 percent lower than observed, and the calculated acetaldehyde yields were high (as seen in Figure 3), but there were no systematic discrepancies between calculation and experiment beyond those expected from uncertainties in the initial reactant concentrations, analytical techniques employed, and the chamber-dependent parameters. The radical input rates required for the model calculations to fit the observed NO oxidation and O_3 formation rates (shown in Table 5) were similar in magnitude and variability to those measured in the NO_x-air irradiations (shown in Table 4). The discrepancy between the observed and calculated acetaldehyde time-concentration profiles is probably due to problems with calibration of this compound in

TABLE 5. INITIAL CONCENTRATIONS AND SELECTED RESULTS OF PROPENE-NO_x-AIR EXPERIMENTS AND MODEL CALCULATIONS.

ITC run no.	Initial concentrations NO (ppm)	NO_2 (ppm)	propene (ppm)	Experimental Final or Max O_3 (hr)	(ppm)	Model Calculations O_3 (ppm)	Radical Input (ppb min^{-1})
690[a]	0.24	0.23	0.76	5.0	0.60	0.61	0.20
693	0.38	0.11	1.10	6.0	0.78	0.65	0.15
716	0.38	0.11	1.04	6.0	0.71	0.65	0.15
728	0.37	0.10	1.05	6.0	0.63	0.67	0.05
736[a]	0.36	0.09	0.51	7.25	0.28	0.28	0.05
754	0.43	0.13	0.98	6.0	0.81	0.70	0.20
759	0.41	0.15	1.02	6.0	0.80	0.70	0.20
791	0.42	0.11	0.95	7.0	0.77	0.69	0.20
792[a]	0.34	0.13	0.98	6.25	0.75	0.66	0.05
810	0.40	0.12	0.93	6.25	0.78	0.68	0.20

[a]Conditioning run for a new reaction bag.

the GC analysis employed (Reference 23), and to the fact that calibration was not current at the time of the experiments. (Acetaldehyde is not a significant product from any of the fuel constituents studied in this program, other than n-butane.) The reason for the ~10 percent discrepancy between the observed and calculated O_3 yields is unclear, but in general a ~10 percent fit between experiment and model calculation is considered acceptable, given the current state of the art.

Propene-NO_x irradiations were also used for conditioning new reaction bags. These runs were not as well-characterized as the other propene runs in that fewer chromatographic analyses were made, as shown by the footnote to Table 5. However, despite the fact that those runs were carried out in an unconditioned chamber and are somewhat less well-characterized, the results of these conditioning runs are not significantly different from the other propene runs, other than the fact that most (though not

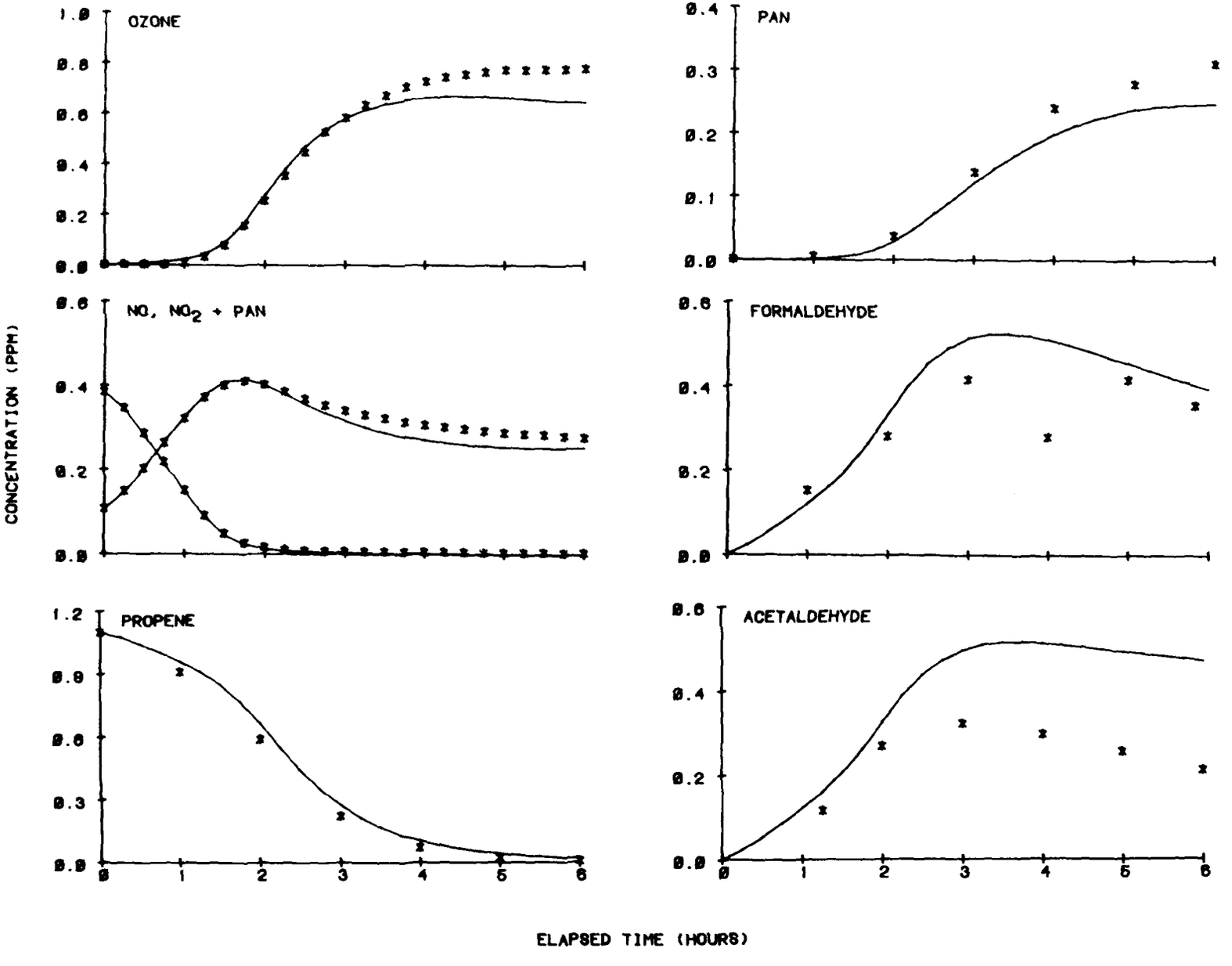

Figure 3. Experimental (*) and Calculated (——) Concentration-Time Plots for Species Monitored in Propene-NO_x-Air Run ITC-693.

all) of them required lower radical input rates to be assumed in the model calculations in order to fit the data.

B. SINGLE COMPONENT RUNS

The majority of experiments carried out in this program, other than control or characterization runs, consisted of NO_x-air irradiations of single representative fuel constituents or potential fuel impurities. Four classes of compounds were studied: (1) benzene and the methylbenzenes toluene, m-xylene, and mesitylene; (2) the bicyclic aromatics tetralin, naphthalene, and 2,3-dimethylnaphthalene; (3) the alkanes n-butane, n-octane, and methylcyclohexane; and (4) the heteroatom-containing potential fuel impurities furan, pyrrole, and thiophene. In many cases, traces (~10 ppb) of propene and n-butane were included in the reaction mixture to monitor OH radical levels from their relative rates of consumption, as employed in NO_x-air irradiations (see Section III-A-2). For the more reactive compounds such as the methylbenzenes or the heteratom-containing organics, the use of these tracers was not necessary, since the OH radical levels could be readily derived from the rate of consumption of the organic itself and its known OH rate constant (Section IV and References 18, 28-30). In addition, for most alkane runs and some aromatic runs, the experiments were carried out by irradiating the NO_x and the tracers for 2 hours before injecting the organic (i.e., carrying out a NO_x-air irradiation) to obtain a measurement of the radical input rates under the exact conditions of the experiment, and to directly measure the effect of the presence of the organic on radical levels.

A summary of the initial concentrations and procedures employed in all single component-NO_x irradiations carried out in this program is given in Table 6, together with selected results of those experiments. The results of these experiments are discussed in more detail in the following sections. In Section III-B-1, the overall reactivities of the various compounds in NO_x-air irradiations are compared, and in Sections III-B-2 and III-B-3, their efficiencies in converting NO to NO_2 and their effects

on radical levels in NO_x-air irradiations are discussed and compared. These are among the factors which need to be considered when developing models for the atmospheric reactions of these compounds.

1. Comparison of Overall Reactivities

The results shown in Table 6 indicate significant differences among the compounds studied in their effectiveness in causing NO conversion and O_3 formation. Since the major initial reaction of these compounds in NO_x-air irradiations is reaction with the OH radical, these differences can be attributed, at least in part, to differences in their OH rate constants, which are summarized in Table 7 for all of the compounds studied in this program. This table shows that there is indeed a wide range in the OH radical rate constants for these compounds; and, for compounds within a given class, these differences can qualitatively account for the observed differences in overall reactivity. For example, Figure 4 shows plots of the concentration-time O_3 profiles for runs employing benzene and the alkylbenzenes, carried out with similar initial NO_x levels. It can be seen that the reactivity of those compounds increases monotonically with the degree of substitution on the aromatic ring, as is the case with their OH rate constants. Similarly, Figure 5 compares the O_3, NO, and NO_2 (where the NO_2, as noted in Section II-C-3, is uncorrected for the presence of organic and inorganic nitrates and PAN) concentration-time profiles for runs employing naphthalene and 2,3-dimethylnaphthalene at similar NO_x levels. Again the more substituted compound, which has the higher OH radical rate constant, is the more reactive, since less of the compound is required to produce similar O_3 and NO_x concentration-time profiles. Finally, Figure 6 compares the O_3 concentration-time profiles for runs containing furan, thiophene, and pyrrole at similar NO_x levels, and the order of reactivity is pyrrole > furan > thiophene, which is also the same as the ranking of their OH radical rate constants (Table 7).

However, in comparing the reactivities of compounds of different types, it is clear that the OH rate constant cannot be the only factor

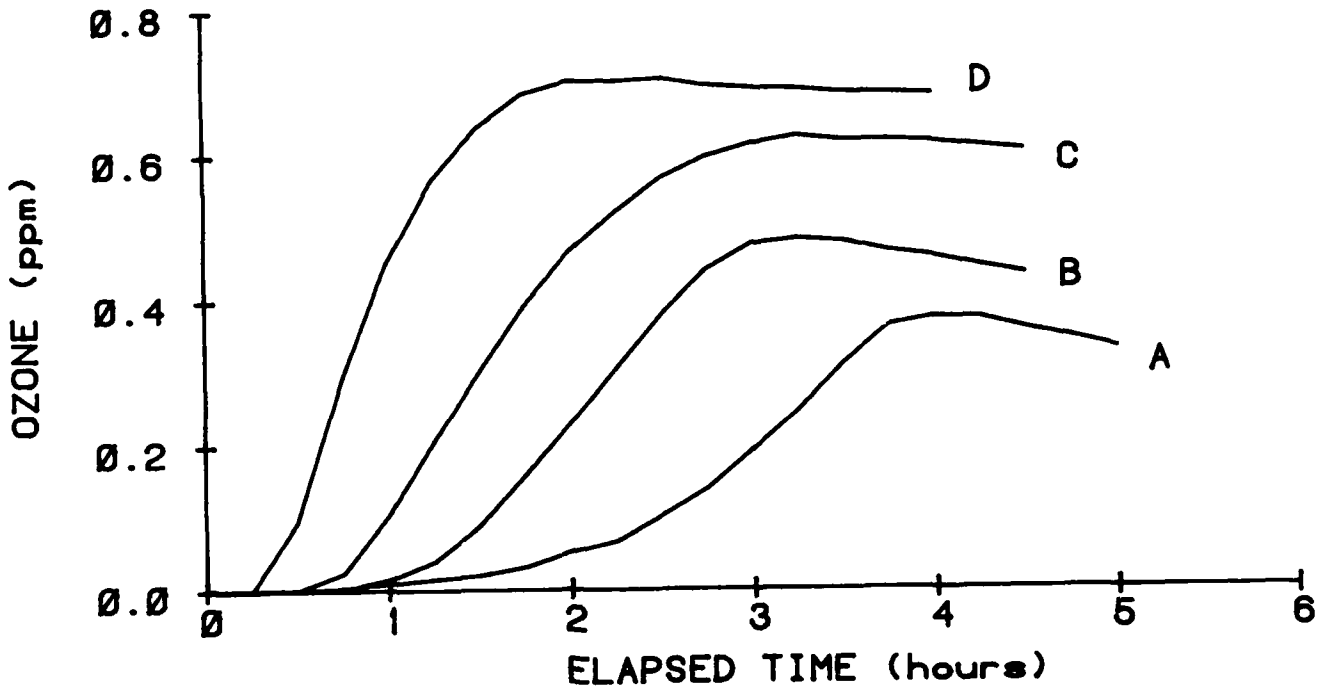

A. ITC-698, 13.9 ppm Benzene
B. ITC-699, 1.5 ppm Toluene
C. ITC-702, 0.5 ppm m-Xylene
D. ITC-703, 0.6 ppm Mesitylene

Figure 4. Concentration-Time Plots from the Following Aromatic-NO_x-Air Runs (Initial $NO_x \simeq 0.5$ ppm):

influencing an organic's reactivity in NO_x-air irradiations. For example, Figure 7 compares the O_3 and NO_x concentration-time profiles for toluene and methylcyclohexane at similar NO_x levels. This figure shows that despite the fact that methylcyclohexane reacts with OH radicals ~60 percent faster than does toluene (Table 7) and is present at ~30 times higher concentration, essentially no O_3 formation had occurred in the methylcyclohexane run after 5 hours of irradiation, while the toluene run produced a maximum yield of ~0.5 ppm O_3 in less than 3.5 hours. The results of the

TABLE 6. INITIAL CONCENTRATIONS, RUN TYPES, AND SELECTED RESULTS OF THE SINGLE COMPONENT-NO_x-AIR IRRADIATIONS.

Organic	ITC run no.[a]	Run type[b]	Initial conc. NO_x[c] (ppm)	Initial conc. Organic (ppm)	Initial NO consumption rate[d] (ppb min^{-1})	Reaction time (hr)	Maximum O_3 (hr)	Maximum O_3 (ppm)	Final yields O_3 (ppm)	Final yields PAN (ppm)
Benzene	698	N	0.50	13.9	2.0	5.0	4.0	0.37	0.33	-
	710	N	0.55	13.9	1.9	6.25	4.5	0.37	-	-
	831	TA	1.01	2.0	0.4	4.0	-	-	0.02	0.00
Toluene	699	N	0.51	1.50	3.8	4.5	4.5	0.49	0.43	0.15
	828	TA	1.01	0.43	0.4	4.0	-	-	0.02	0.00
m-Xylene	702	N	0.52	0.50	6.6	4.5	3.25	0.63	0.61	0.37
	827	TA	1.05	0.14	0.8	4.0	-	-	0.02	0.00
Mesitylene	706	N	0.49	0.29	5.0	6.25	-	-	0.64	0.42
	742	N	0.48	0.52	>6	4.5	-	-	0.77	0.46
	703	N	0.50	0.58	6.3	4.0	2.5	0.71	0.68	0.59
	826	TA	0.89	0.09	1.3	4.0	-	-	0.02	0.00
	709	N	0.99	0.52	12	6.0	-	-	0.78	0.59
Tetralin	748	N	0.22	8.4	1.7	5.75	3.75	0.37	0.34	0.00
	739	N	0.52	0.24	0.8	6.0	-	-	0.00	0.00
	750	T	0.53	4.4	2.0	6.0	-	-	0.46	0.00
	747	N	0.50	9.3	2.1	6.5	6	0.48	-	0.00
	832	TA	1.00	3.9	2.1	4.25	-	-	0.07	0.00
Naphthalene	755	T	0.24	1.41	1.1	6.0	5.5	0.29	0.19	-
	756	T	0.26	2.7	1.9	5.25	4.5	0.28	0.27	-
	751	N	0.52	0.75	1.0	7.0	-	-	0.11	-
	802	T	0.53	0.84	1.2	6.0	-	-	0.12	0.00
	798	T	0.55	1.93	1.3	6.25	-	-	0.20	0.00
2,3-Dimethylnaphthalene	775	T	0.29	0.14	1.4	6.0	-	-	0.29	0.03
	771	N	0.27	0.40	2.1	5.25	-	-	0.33	0.06
	806	N	0.33	0.49	2.5	6.0	-	-	0.35	0.03
	774	T	0.57	0.33	2.0	6.0	-	-	0.34	0.07
n-Butane	770	T'A	0.55	9.4	1.7	4.25	-	-	0.04	0.00

TABLE 6. INITIAL CONCENTRATIONS, RUN TYPES, AND SELECTED RESULTS OF THE SINGLE COMPONENT-NO_x-AIR IRRADIATIONS (CONCLUDED).

n-Octane	763	TA	0.26	0.96	0.5	5.25	-	-	0.04	0.00
	762	TA	0.28	9.3	0.8	5.0	-	-	0.11	0.00
	797	TA	0.55	0.91	0.7	4.5	-	-	0.00	0.00
	761	TA	0.53	9.4	[e]	5.0	-	-	0.03	0.00
Methylcyclohexane	766	TA	0.27	8.7	0.9	5.0	-	-	0.12	0.01
	765	TA	0.51	0.92	1.0	5.0	-	-	0.02	0.00
	800	TA	0.54	1.10	0.8	4.0	-	-	0.01	0.00
	767	TA	0.56	8.8	1.1	7.25	-	-	0.04	0.00
Furan	715	N	0.50	0.21	2.7	6.0	-	-	0.06	0.00
	743	N	0.50	0.37	7.3	6.25	5.5	0.6	0.58	0.01
	711	N	0.52	0.40	5.4	4.75	2.75	0.47	0.46	0.02
	713	N	0.99	0.38	4.7	6.0	-	-	0.04	0.00
Thiophene	733	N	0.25	0.43	1.2	7.75	7.5	0.25	0.24	0.01
	729	N	0.49	0.43	1.1	6.0	-	-	0.07	0.00
	730	N	0.47	1.78	3.6	5.0	3.25	0.41	0.29	0.01
	744	N	0.52	1.64	4.7	4.5	3.25	0.48	0.40	0.01
Pyrrole	780	TA	0.49	~0.1[f]	2.2	2.0[f]	-	-	0.02[f]	0.00
	779	N	0.49	0.27	5.9	1.5	-	-	0.07	0.00
	735	N	0.49	0.53	>14	4.75	0.5	0.32	0.11	-
	778	N	0.49	0.97	>30	1.0	1.0	0.52	0.52	-

[a] Listed in order of increasing NO_x then increasing organic.

[b] Codes for run types: T = propene and n-butane tracers present, T' = propene and propane tracers present, A = organic added after a 2-hour tracer-NO_x-air irradiation, N = no tracers present.

[c] Average initial $[NO_2]/[NO_x] = 0.21 \pm 0.03$.

[d] Average $-d[NO]/dt$ for first hour or until $[NO] \leq [O_3]$, whichever occurred first.

[e] NO_x data not reliable due to apparent interference by n-octane on the NO-NO_x analyzer. A different analyzer was employed in subsequent runs.

[f] Two injections of pyrrole were made. Data shown is for the first injection only.

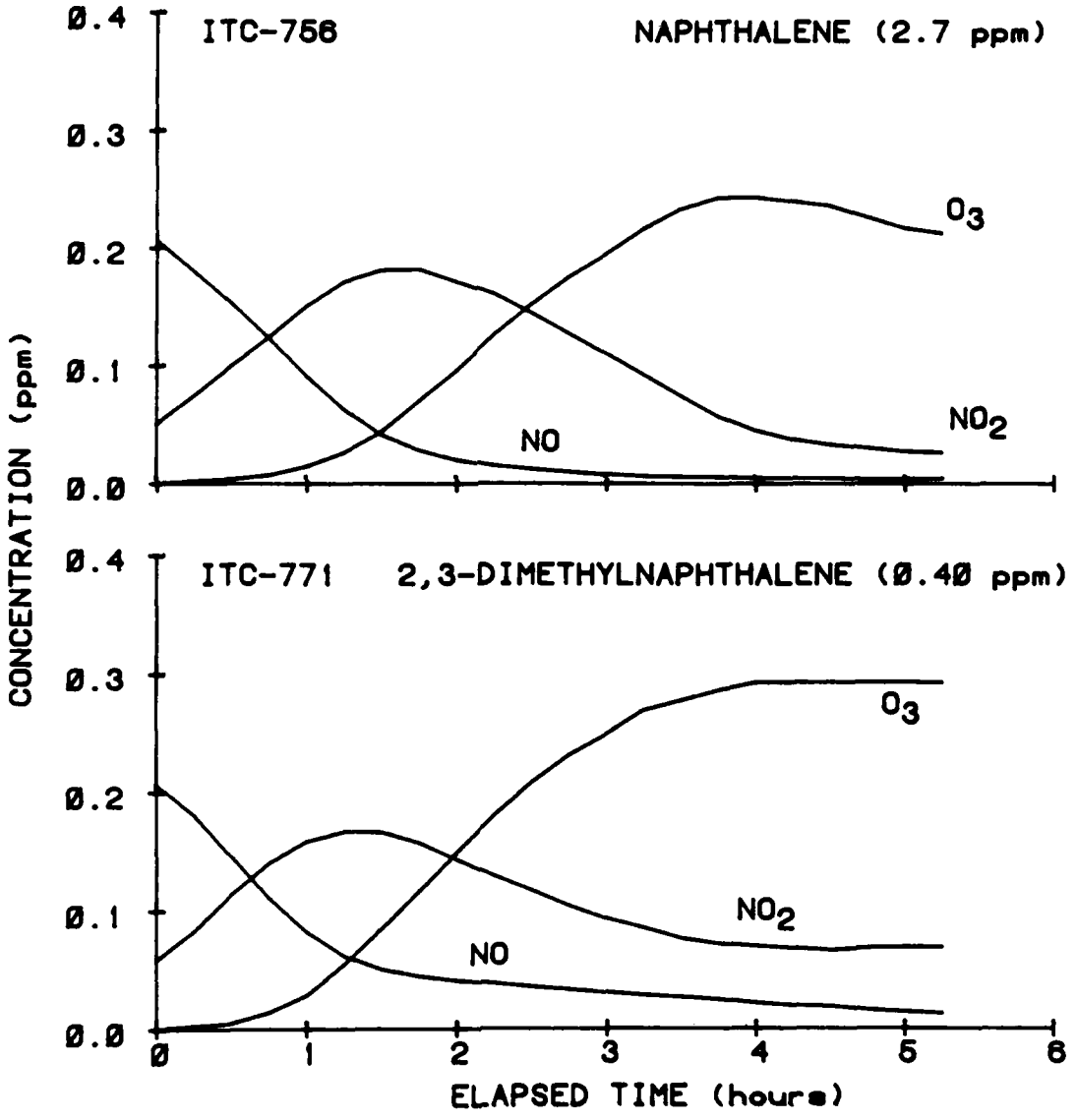

Figure 5. Comparison of O_3, NO, and NO_2 Concentration-Time Profiles for Naphthalene-NO_x-Air Run ITC-756 and 2,3-Dimethylnaphthalene-NO_x-Air Run ITC-771.

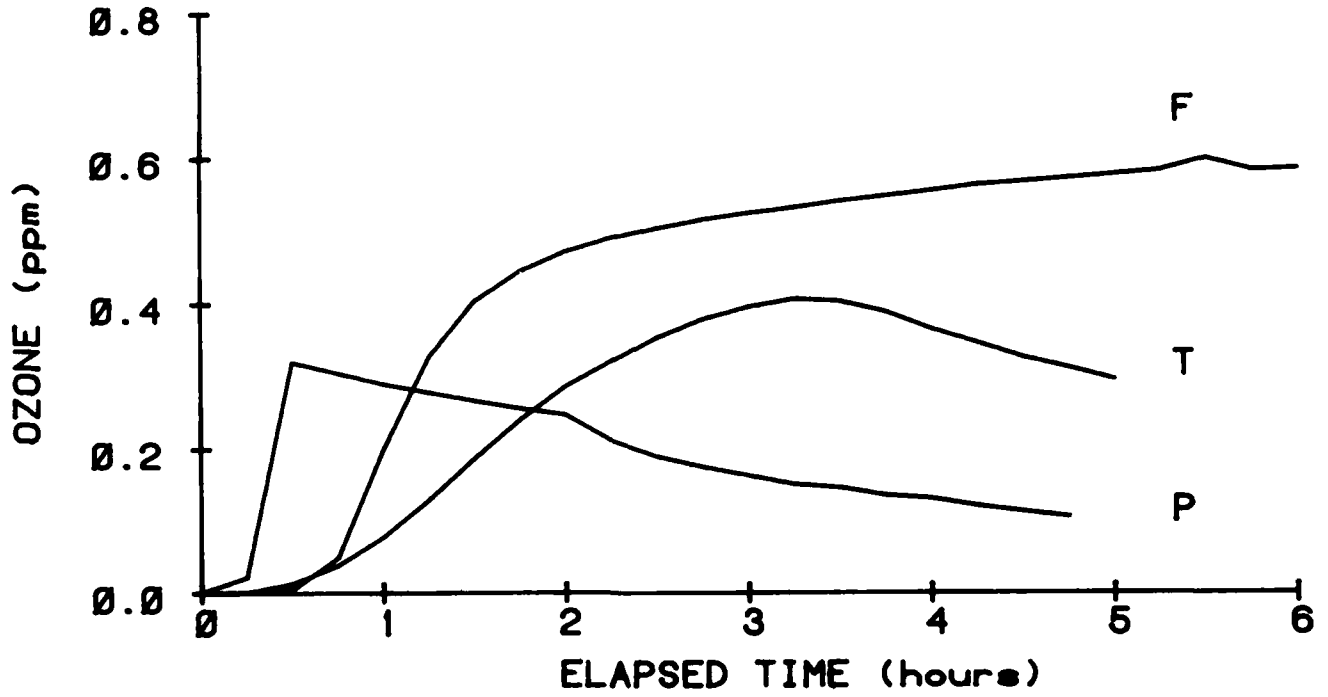

F. ITC-743, 0.4 ppm Furan
T. ITC-730, 1.8 ppm Thiophene
P. ITC-735, 0.6 ppm Pyrrole

Figure 6. Comparison of O_3 Concentration-Time Profiles for the Following Heterocyclic Organic-NO_x-Air Runs (Initial NO_x ≈ 0.5 ppm).

experiments with n-octane were similar to those for methylcyclohexane and in general the alkanes are the least reactive of all the compounds studied in this program.

The bicyclic aromatics tetralin, naphthalene, and 2,3-dimethylnaphthalene, while more reactive than the alkanes, were found to be significantly less reactive than the alkylbenzenes. For example, tetralin, which might be expected to be similar to a xylene in its reactivity [since for the alkylbenzenes essentially all of the reaction with OH radicals occurs at the aromatic ring (References 17 and 18)], is much less reactive

TABLE 7. RATE CONSTANTS FOR THE REACTIONS OF OH RADICALS WITH THE FUEL CONSTITUENTS AND MODEL COMPOUNDS STUDIED IN THIS PROGRAM.

Compound	$10^{12} \times k_{OH}$ (cm^3 $molecule^{-1}$ sec^{-1})	References
Benzene	1.2	Reference 18
Toluene	6.4	
m-Xylene	24	
1,3,5-Trimethylbenzene	62	
Tetralin	39	This work (Section IV)
Naphthalene	24	Reference 28
2,3-Dimethylnaphthalene	115	This work (Section IV-3)
n-Butane	2.6	Reference 29
n-Octane	9.0	
Methylcyclohexane	10.3	
Furan	40	Reference 30
Thiophene	9.6	
Pyrrole	120	This work (Section IV)

than m-xylene. This is shown in Figure 8, which compares results of a m-xylene run, and a tetralin run which has similar initial NO_x levels. In addition, Figures 9 and 10 give comparable comparisons of a m-xylene and a naphthalene run, and of a mesitylene and a 2,3-dimethylnaphthalene run, respectively. These figures show that in all cases, despite the fact that the bicyclic aromatics have comparable (in the case of napthalene versus m-xylene) or higher (in the cases of tetralin versus m-xylene or 2,3-dimethylnaphthalene versus mesitylene) OH radical rate constants, the runs employing the bicyclic aromatics either exhibit significantly less reactivity than those with the alkylbenzenes, or else significantly higher levels of the bicyclic aromatic are required to produce comparable O_3 and NO_x time-concentration profiles. Clearly, the reaction mechanisms of the

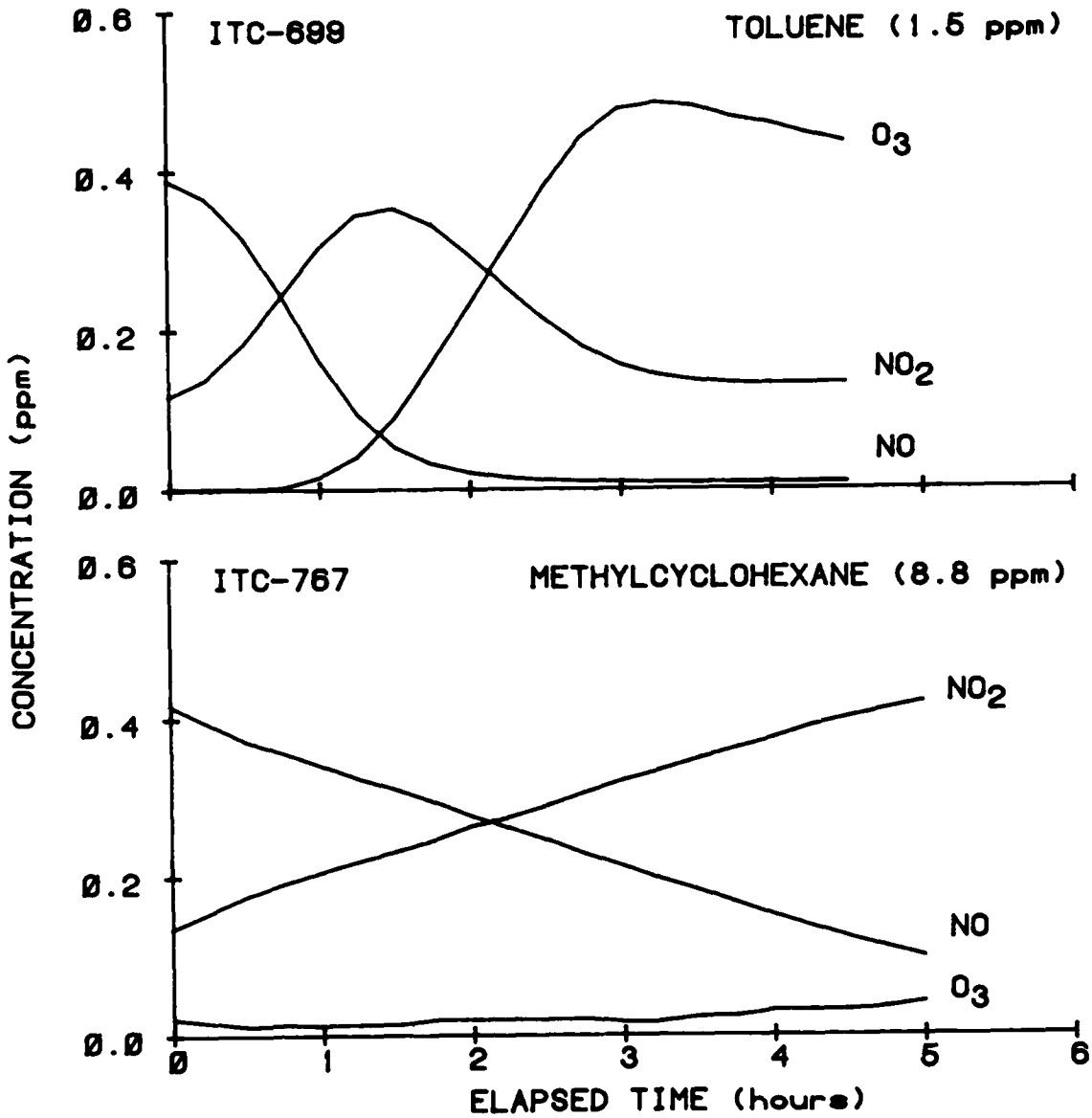

Figure 7. Comparison of O_3, NO, and NO_2 Concentration-Time Profiles for Toluene-NO_x-Air Run ITC-699 and Methylcyclohexane-NO_x-Air Run ITC-767.

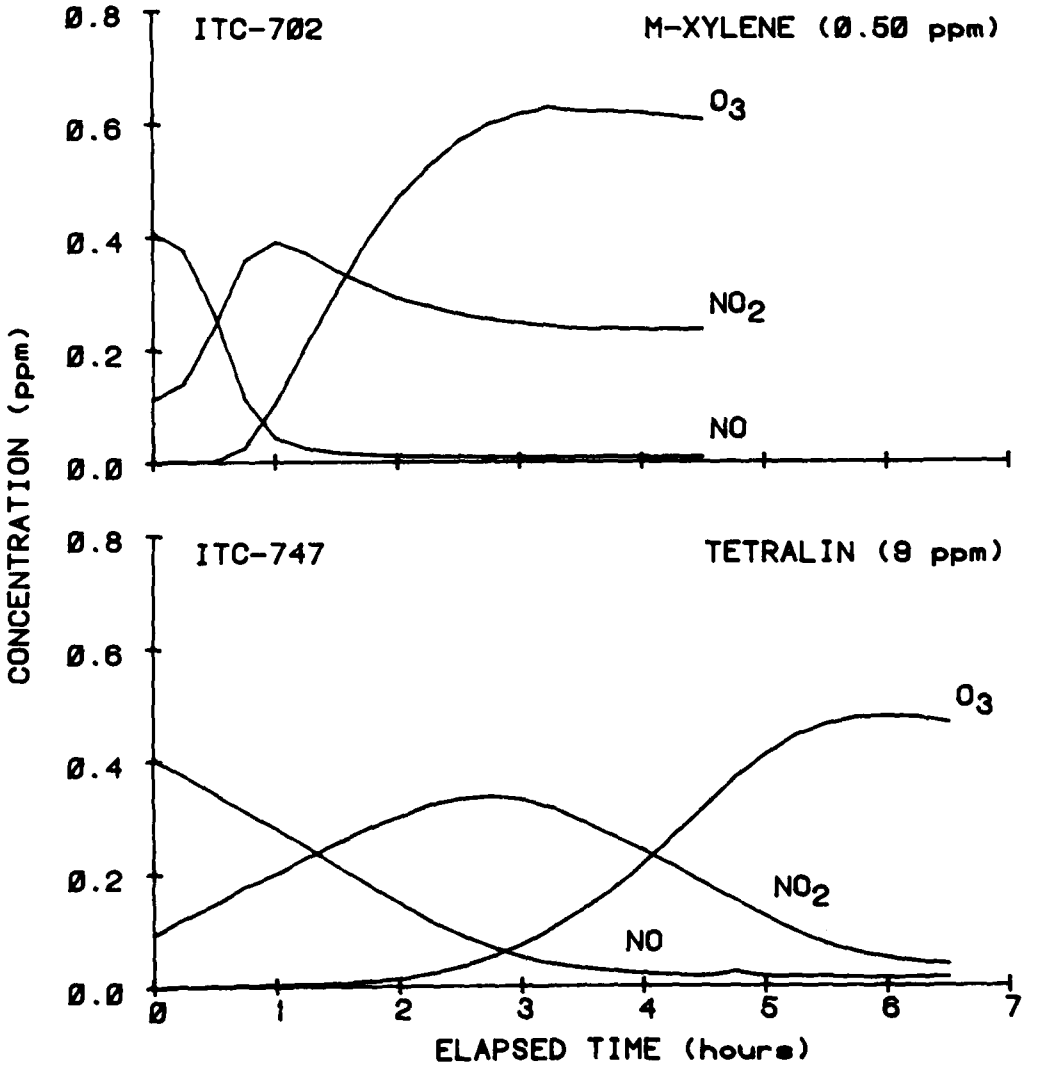

Figure 8. Comparison of O_3, NO, and NO_2 Concentration-Time Profiles for m-Xylene-NO_x-Air Run ITC-702 and Tetralin-NO_x-Air Run ITC-747.

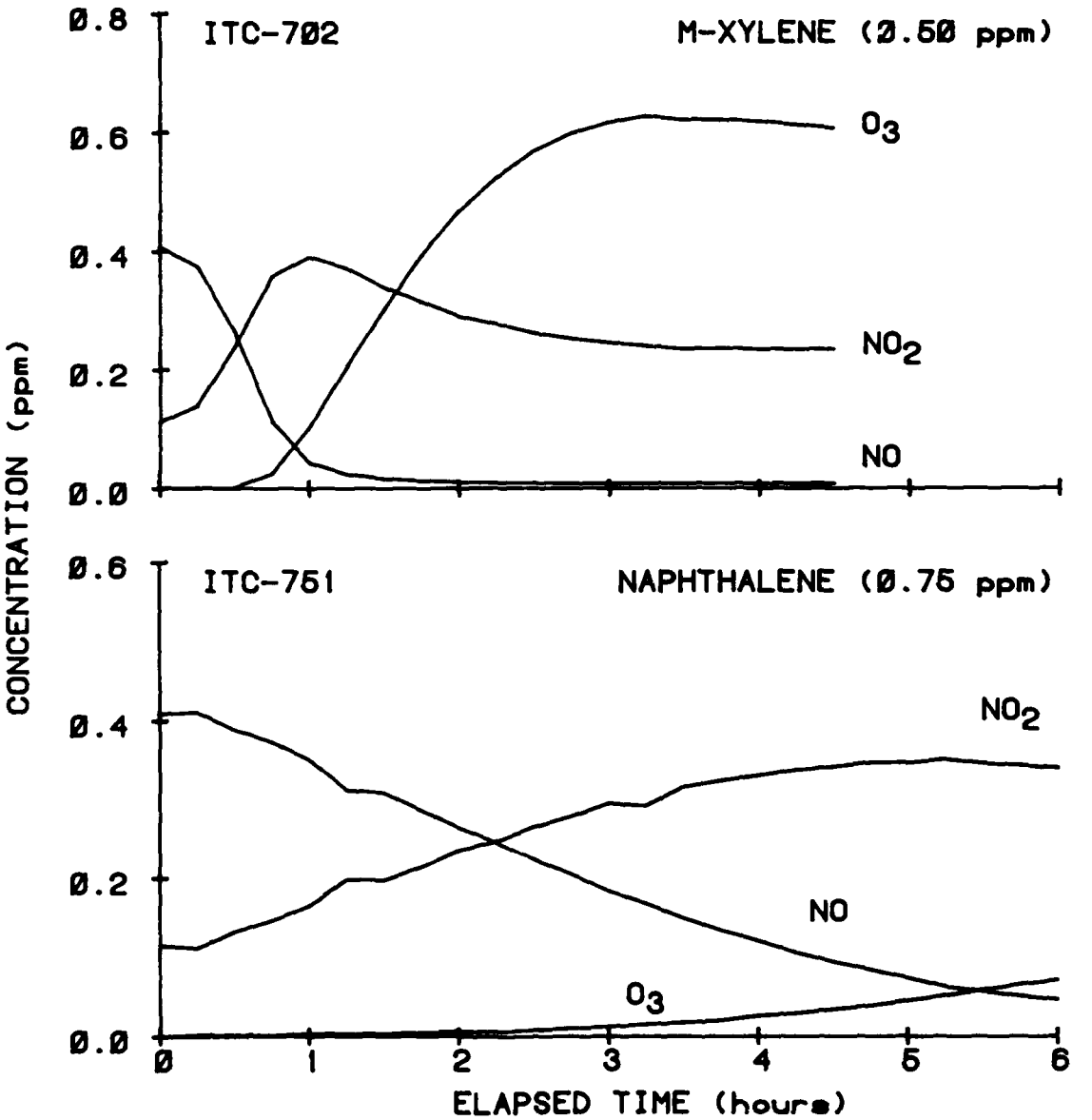

Figure 9. Comparison of O_3, NO, and NO_2 Concentration-Time Profiles for m-Xylene-NO_x-Air Run ITC-702 and Naphthalene-NO_x-Air Run ITC-751.

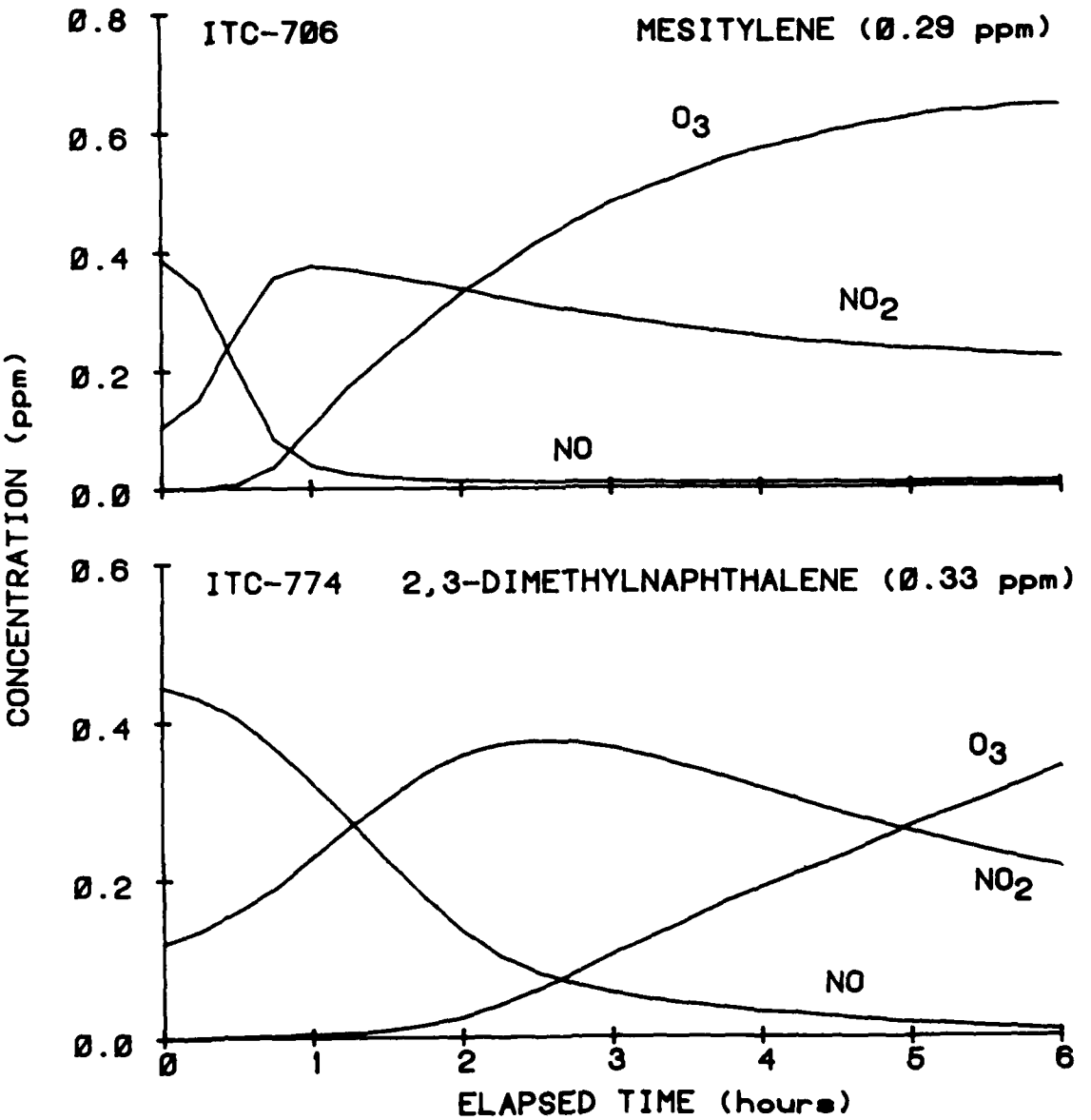

Figure 10. Comparison of O_3, NO, and NO_2 Concentration-Time Profiles for Mesitylene-NO_x-Air Run ITC-706 and 2,3-Dimethylnaphthalene-NO_x-Air Run ITC-774.

bicyclic aromatics, including tetralin, are significantly different from those for the simple alkylbenzenes.

The heteroatom-containing organics furan, pyrrole, and thiophene appear to be approximately comparable to the alkylbenzenes in their reactivity. For example, Table 7 shows that the OH radical rate constant for thiophene is similar (to within a factor of ~1.7) to that for toluene, and the rate constant for furan is similar to that for m-xylene, and Figures 11 and 12 show that these sets of compounds have similar reactivities in terms of the rates of O_3 formation and NO oxidation, at least under the conditions of the experiments shown in these figures. However, the reactivities of these heterocyclic organics have a very different dependence on the initial NO_x and organic levels than do the alkylbenzenes. For example, Figures 13 and 14 compare the results of experiments employing pyrrole with those employing mesitylene (which reacts with OH radicals ~2 times slower than pyrrole) at two different levels of the organic (the initial NO_x levels were ~0.5 ppm for all four runs). These figures show that when the organics are irradiated at the ~0.5-0.6 ppm level with ~0.5 ppm NO_x, pyrrole forms O_3 more rapidly than does mesitylene (though less O_3 is formed). However, when the concentrations of pyrrole and mesitylene are each reduced by a factor of 2 at the same initial NO_x level, the relative rates of O_3 formation change markedly, with mesitylene now forming O_3 far more rapidly than does pyrrole. This is apparently due to the fact that once all the pyrrole is reacted (which occurred between 60 and 90 minutes in run ITC-779 shown in Figure 14), no further conversion of NO to NO_2 or O_3 formation occurred. Thus, in run ITC-735 (Figure 13), the pyrrole concentration was high enough to consume all of the NO before the pyrrole was consumed, allowing O_3 formation to occur, while in run ITC-779 (Figure 14), the lower pyrrole concentration was consumed before the NO was all consumed, and thus essentially no O_3 formation occurred. Note also that even in the run with the higher pyrrole concentration (Figure 13), no further O_3 was formed after the pyrrole was consumed, despite the fact that NO_2 still remained in the system (as evidenced by the fact that the total uncorrected NO_2 levels and O_3 simultaneously declined, due

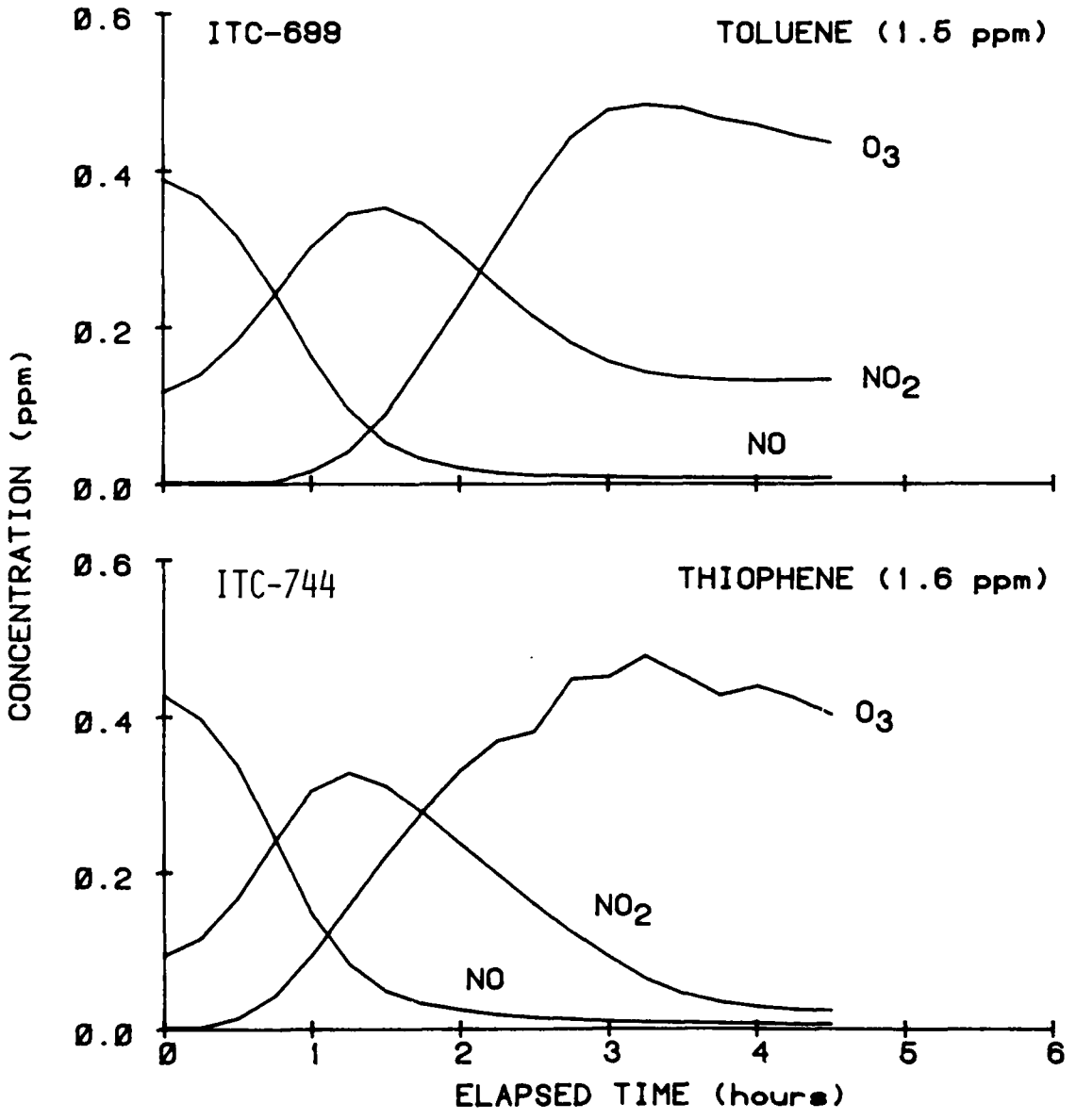

Figure 11. Comparison of O_3, NO, and NO_2 Concentration-Time Profiles for Toluene-NO_x-Air Run ITC-699 and Thiophene-NO_x-Air Run ITC-744.

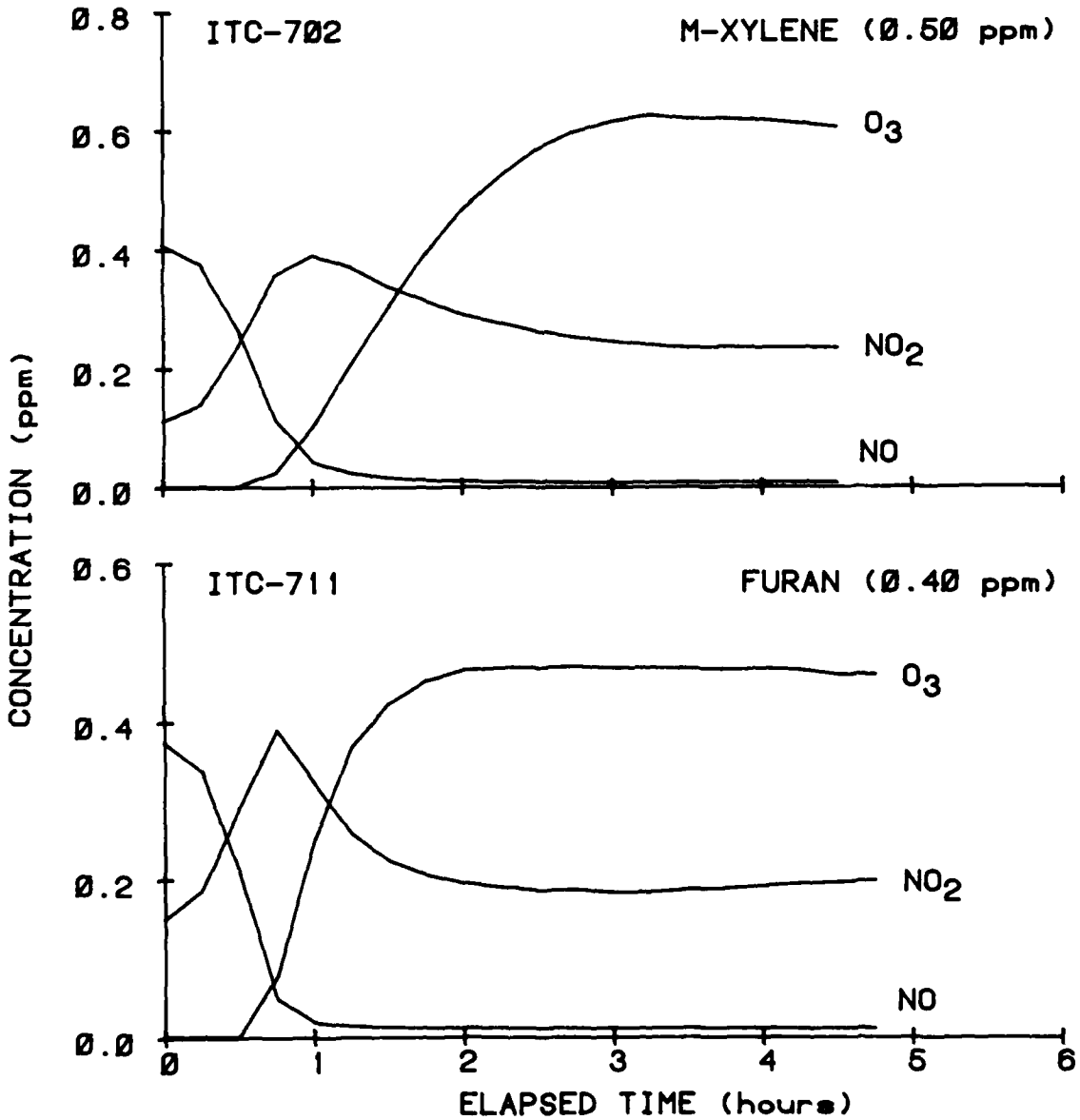

Figure 12. Comparison of O_3, NO, and NO_2 Concentration-Time Profiles for m-Xylene-NO_x-Air Run ITC-702 and Furan-NO_x-Air Run ITC-711.

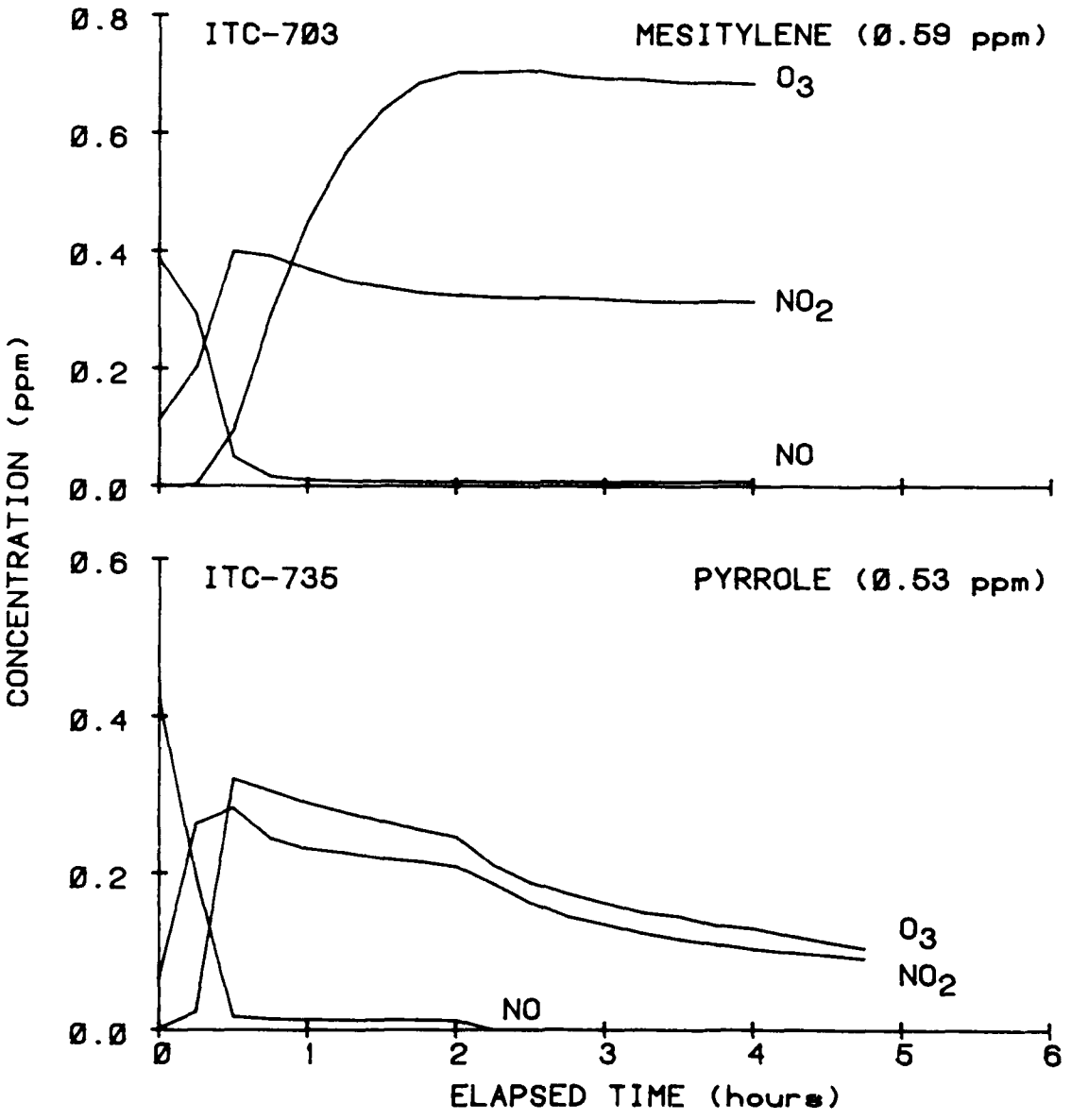

Figure 13. Comparison of O_3, NO, and NO_2 Concentration-Time Profiles for Mesitylene-NO_x-Air Run ITC-703 and Pyrrole-NO_x-Air Run ITC-735.

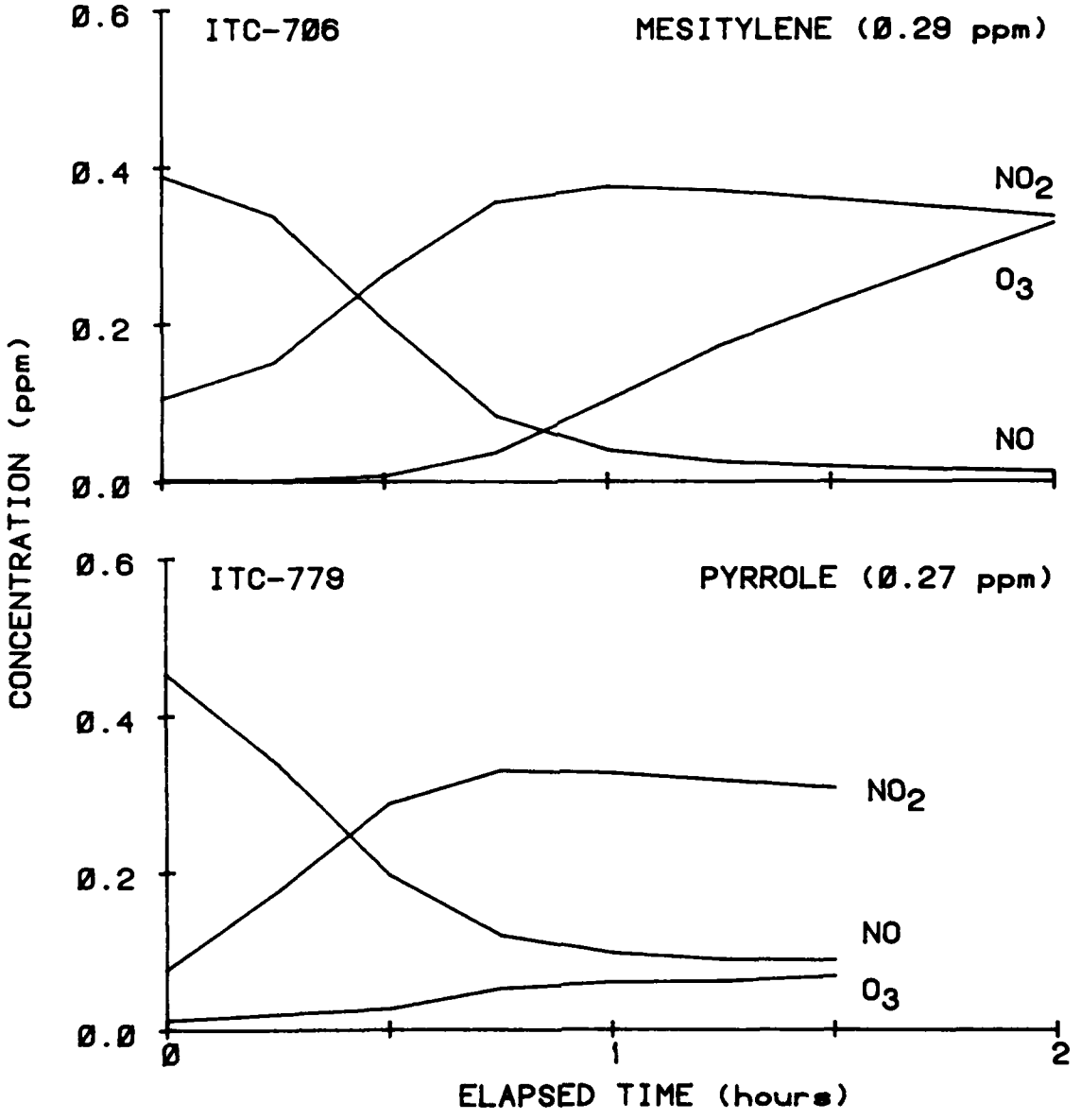

Figure 14. Comparison of O_3, NO, and NO_2 Concentration-Time Profiles for Mesitylene-NO_x-Air Run ITC-706 and Pyrrole-NO_x-Air Run ITC-779.

to the $NO_2 + O_3$ reaction). This is probably the primary reason that the pyrrole run formed much less O_3 than was formed in the corresponding mesitylene run (as shown in Figure 13).

Furan was observed to be similar to pyrrole in that after it was completely reacted, no further oxidation or NO or O_3 formation occured. For example, Figure 15 shows the O_3, NO_x, and furan concentration-time profiles for a run where the furan level was reduced by a factor of ~2, and for a run where the NO_x level was increased by a factor of ~2, relative to those in run ITC-711. It can be seen that, despite the relatively high reactivity of the furan-NO_x system in run ITC-711, essentially no O_3 formation occurs in the runs ITC-715 and 713. Apparently there was either insufficient furan or too much NO for all the NO to be oxidized before the furan was consumed. No such behavior was observed for thiophene, but this may be due to the fact that because of its lower OH radical rate constant, no runs were carried out in which the thiophene was completely consumed prior to the end of the irradiations.

This characteristic of the pyrrole and furan-NO_x-air photooxidation system is quite unusual, since for most other organics which have been studied to date, O_3 formation continues until all of the NO_x has been consumed. Many compounds react too slowly to be completely consumed within the time scale of the experiments. However, for organics such as the more reactive alkenes, which are generally consumed relatively early in the irradiations, continued formation of O_3 will occur after the initially present organic is consumed, due to the reactions of the oxygenated products formed (see, for example, the data in Reference 23). Apparently the photooxidation products of furan and pyrrole are either totally unreactive, or, more likely, they form products which react so rapidly that they are removed from the system essentially instantaneously. Thus, once the furan or pyrrole and their major products have reacted, the system reverts to a NO_x-air irradiation, where no peroxy radicals are generated to cause NO consumption and thus O_3 formation.

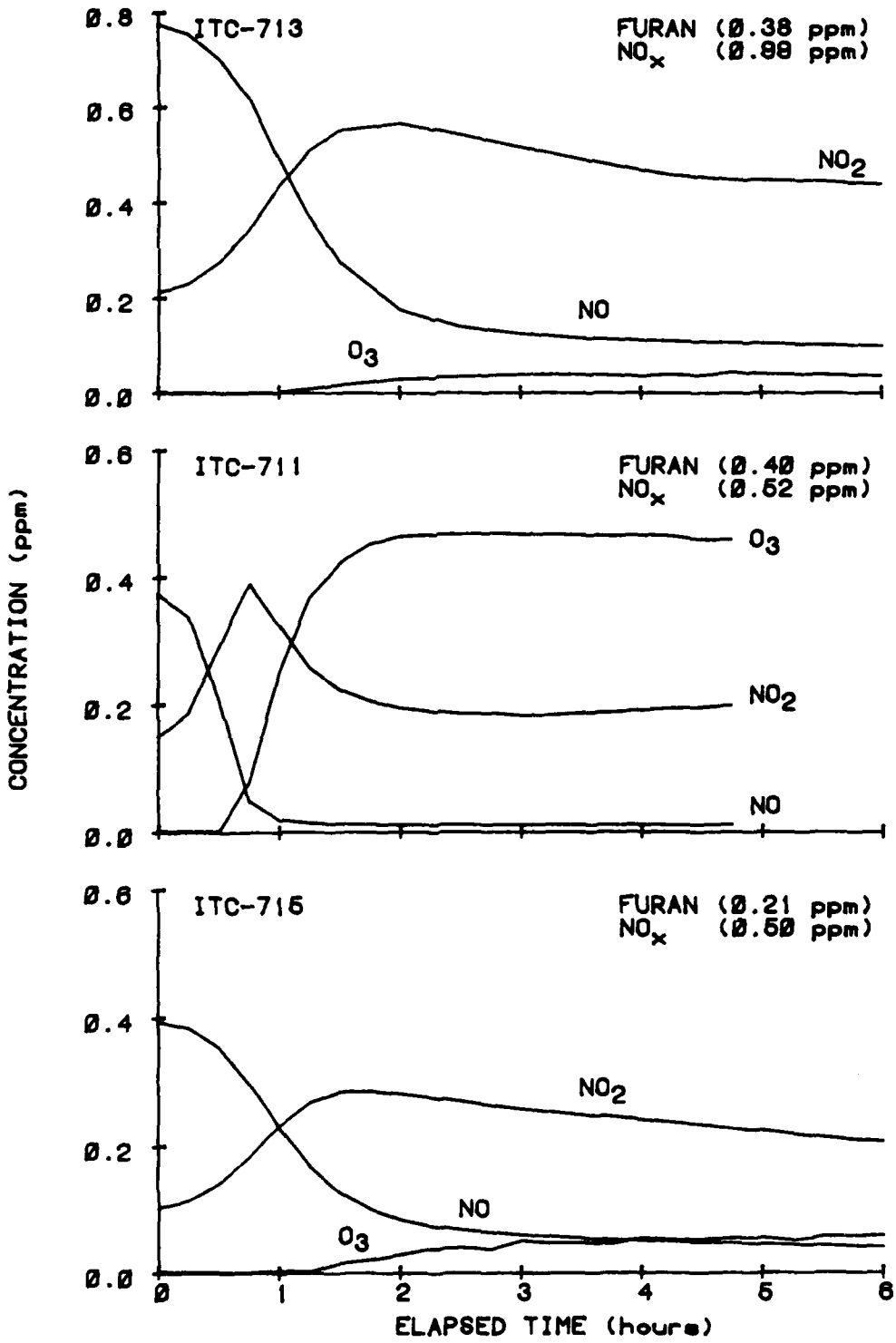

Figure 15. Comparison of O_3, NO, and NO_2 Concentration-Time Profiles for Furan-NO_x-Air Runs ITC-711, 713, and 715.

2. NO Oxidation Efficiency

One aspect in which the reactivities of various organics can differ is in their efficiency of converting NO to NO_2, which causes O_3 formation. Ozone is formed in NO_x-air irradiations by the reactions of O_2 with the $O(^3P)$ atoms formed from NO_2 photolyses, and its concentration is influenced by the following rapid reactions.

$$NO_2 + h\nu \rightarrow O(^3P) + NO \qquad (1)$$

$$O(^3P) + O_2 \xrightarrow{M} O_3 + M \qquad (6)$$

$$O_3 + NO \rightarrow NO_2 + O_2 \qquad (7)$$

This results in the O_3 concentration being essentially determined by the $[NO_2]/[NO]$ ratio. In the absence of a reactive organic, as in a NO_x-air irradiation, the change in NO or NO_2 concentrations is relatively slow. Hence their ratio remains approximately constant, and essentially no O_3 is formed. However, in the presence of reactive organics, peroxy radicals are produced which either consume NO or convert NO to NO_2, causing the $[NO_2]/[NO]$ ratio and thus O_3 levels to increase.

$$\text{organic} + OH \xrightarrow{O_2} RO_2\cdot \qquad (20)$$

$$RO_2 + NO \rightarrow RO\cdot + NO_2 \qquad (21)$$

$$\xrightarrow{M} RONO_2 \qquad (22)$$

In a typical experiment, this is first manifested by the consumption of the initially present NO [with O_3 being present in only low levels, in a steady state determined by reactions (1), (6), and (7)], followed by the formation of measurable levels of O_3 after the initially present NO is consumed. Since the alkoxy radicals formed in Reaction (21)

will usually react further to generate additional peroxy radicals (or HO_2) which can react with additional molecules of NO, several molecules of NO may be consumed for each molecule of the organic reaction, and, in general, the efficiency will depend on the organic's NO_x-air photooxidation mechanism.

A semiquantitative estimate of the efficiency of the organics in oxidizing NO (and thus in forming O_3) can be obtained from our data if it is assumed that reactions (1), (6), (7), and (20)-(22) are the major processes influencing NO oxidation and O_3 formation. [Other reactions are known to influence the O_3 and the NO_x levels (Reference 17); but it can be shown that, at least in the initial stages of the experiment when O_3 levels are relatively low, these are second-order effects.] Thus if we define α as the overall NO oxidation efficiency of the organic, for the purposes of this discussion the reactions of the organic can be represented by

$$\text{organic} + OH \xrightarrow{k_{OH}} -\alpha\ NO + \text{products} \qquad (12)$$

(where k_{OH} is the organic + OH rate constant). Thus the kinetic differential equations for O_3 and NO can be approximated by:

$$\frac{d[O_3]}{dt} \simeq k_1[NO_2] - k_7[NO] \qquad \text{(VIII)}$$

$$\frac{d[NO]}{dt} \simeq k_1[NO_2] - k_7[NO] - \alpha k_{OH}[\text{organic}][OH] \qquad \text{(IX)}$$

(where the $O(^3P)$ atom concentration is assumed to be in steady state, as defined by Equation (IV) in Section III-A-2.) In addition, since in these experiments the organic is consumed primarily by reaction with OH radicals and dilution due to sampling is negligible (due to the flexible design of the chamber employed), the differential equation for the organic can be represented by

$$\frac{d[\text{organic}]}{dt} = -k_{OH}[OH][\text{organic}]. \qquad (X)$$

The above equations can be combined, integrated, and rearranged to yield

$$\alpha \simeq \frac{\Delta([O_3]-[NO])}{-\Delta[\text{organic}]} \qquad (XI)$$

which allows an estimate of the NO oxidation efficiency to be made directly from the experimental data, provided, of course, that sufficiently accurate values of Δ[organic] are available.

For experiments employing the less reactive organics, where the amounts consumed were relatively small, accurate values of α cannot be obtained. For these compounds, providing that tracer organics were present in the reaction mixture, Δ[organic] can be estimated using (a) the integrated form of equation (X),

$$-\Delta[\text{organic}] = \int_o^t k_{OH}[OH][\text{organic}]dt \qquad (XII)$$

(b) the tracer decay rates to obtain the average hydroxyl radical concentrations, and (c) the following approximation,

$$\int_o^t k_{OH}[OH][\text{organic}]dt \simeq k_{OH}[OH]_{avg} \cdot [\text{organic}]_{avg}\Delta t \qquad (XIII)$$

which is reasonably valid for those runs where relatively little of the organic is consumed, and OH radical concentrations are relatively constant. Thus for experiments where $-\Delta$[organic] cannot be obtained directly, α can be estimated from the relation

$$\alpha \simeq \frac{\Delta([O_3]-[NO])}{k_{OH}[OH]_{avg} \cdot [\text{organic}]_{avg}\Delta t} \qquad (XIV)$$

where $[OH]_{avg}$ is obtained from the tracer data as described in Section III-A-2.

The NO oxidation efficiencies estimated using equations (XI) or (XIV) from the data from the initial periods of the experiments are summarized in Table 8, together with the average NO_2 and organic concentrations during this time period. (The lengths of the initial period used to derive these values depended on the reactivities of the organic and in some cases on the availability of useable tracer data, as indicated in Table 8.) The major result is that, despite the wide range of reactivities for the organics studied, the NO oxidation efficiencies, α, are not greatly different from a value of 2 for all of the compounds studied. This clearly indicates that differences in NO oxidation efficiency cannot be the cause for the significant differences in reactivity which were observed.

3. Effects on Radical Levels

Another aspect of the photooxidation mechanisms of the organics which will effect their reactivity in NO_x-air irradiations is their tendency to remove or add radicals to the system. If the presence of the compound tends to suppress radical levels, then less of the compound will be consumed in a given period of time, and consequently less NO oxidation and O_3 formation will occur. Conversely, if the presence of the compound leads to enhanced radical levels, either directly or (more likely) by forming products which are radical initiators, then obviously the compound will be much more reactive in NO_x-air irradiations. Since, as discussed in the previous section, most of the organics studied here have very similar efficiencies in converting NO to NO_2, this is the most probable explanation for the wide variations in reactivities between the different classes of compounds studied.

Table 8 lists the average OH radical concentrations observed during the first hour of each experiment. These OH radical levels were obtained by one of three techniques: (1) if tracer data are available,

TABLE 8. AVERAGE NO_2 AND ORGANIC CONCENTRATIONS AND CALCULATED AVERAGE OH RADICAL LEVELS AND VALUES OF THE REACTIVITY PARAMETERS α AND β FOR THE INITIAL PERIODS OF THE SINGLE COMPONENT-NO_x-AIR IRRADIATIONS.

Organic	ITC run no.	Time (hr)	Average $[NO_2]$ (ppm)	Average [Organic] (ppm)	Average $10^6 \times [OH]$ (cm^{-3})	α	β	method[a]
Benzene	698	1	0.15	13.9	1.1	-	-0.09	3
	710	1	0.17	13.9	1.0	-	-0.12	3
	831	1	0.19	2.0	0.5	b	b	1
Toluene	699	1	0.20	1.45	3.0	2.4	0.12	2A
	828	1	0.19	0.43	0.7	b	b	1
m-Xylene	702	1	0.25	0.41	5.4	2.5	0.20	2A
	827	1	0.20	0.14	0.7	b	b	1
Mesitylene	706	1	0.25	0.19	5.0	2.3	0.16	2A
	742	1	0.28	0.34	4.9	2.2	0.13	2A
	703	1	0.30	0.39	5.0	2.1	0.10	2A
	826	1	0.19	0.08	1.1	b	b	1
	709	1	0.45	0.37	3.9	2.4	0.17	2A
Tetralin	748	1	0.08	8.3	0.1	-	-0.12	3
	739	1	0.13	0.22	0.9	1.6	0.02	1A
	750	1	0.17	4.4	0.3	0.7	-0.04	1B
	747	1	0.15	10.0	0.1	-	-0.08	3
	832	1	0.23	~6	0.3	0.7	-0.02	1B
Naphthalene	755	1	0.08	1.4	0.4	1.4	-0.24	1B
	756	1	0.10	2.6	0.3	2.1	-0.22	1B
	751	1	6.13	0.72	~1.0	~0.9	-0.05	2A
	802	1	0.14	0.81	0.4	2.7	-0.32	1B
	798	1	0.15	1.9	0.3	1.5	-0.13	1B
2,3-Dimethylnaphthalene	775	1	0.10	0.10	1.4	1.6	-0.12	1B
	771	1	0.11	0.38	~0.3	~3.8	-0.26	2A
	806	1	0.14	0.45	0.5	1.9	-0.09	2A
	774	1	0.17	0.29	0.7	1.5	-0.13	1B
n-Butane	770	2	0.23	9.4	0.5	1.8	-0.03	1B
n-Octane	763	2	0.11	0.95	0.5	2.1	-0.34	1B
	762	2	0.14	9.4	≥0.1	c	c	1
	797	2	0.17	0.90	0.4	2.8	-0.43	1B
	761	2	0.20	9.5	≥0.1	c	c	1
Methylcyclohexane	766	1.75	0.11	8.8	≥0.1	c	c	1
	765	1.75	0.17	0.91	0.5	3.2	-0.39	1B
	800	1.75	0.19	0.96	0.6	2.2	-0.28	1B
	767	1.75	0.20	8.8	≥0.2	c	c	1B
Furan	715	1	0.16	0.17	4.6	1.6	0.16	2A
	743	1	0.23	[illegible].2	12.2	1.9	0.28	2A
	711	1	0.25	0.23	12.8	1.8	0.26	2A
	713	1	~0.3[d]	0.30	4.3	d	0.21	2
Thiophene	733	1	0.07	0.41	3.7	1.6	-0.02	2A
	729	1	0.13	0.42	1.9	2.5	-0.03	2A
	730	1	0.19	1.68	3.7	1.4	0.08	2A
	744	1	0.19	1.53	4.1	1.7	0.11	2A
Pyrrole	780	1	0.18	0.14	3.7	1.8	0.16	2A
	779	1	0.24	0.13	5.9	1.4	0.13	2A
	735	1	0.22	0.19	12.1	1.3	0.10	2A
	778	0.5	0.17	0.32	26.8	0.9	0.04	2A

[a]Codes for calculation methods:
1 = OH radical concentrations calculated from the tracer data using equation (V).
2 = OH radical concentrations calculated from the amount of organic consumed using equation (XV).
3 = OH radical concentrations calculated assuming $\alpha = 2$ using equation (XVI).
A = α calculated from the amount of organic consumed using equation (XI).
B = α calculated using the calculated amount of organic consumed using equation (XIV).

[b]Δ[organic] too small to reliably calculate α and β.

[c]Could not be estimated due to uncertainties in average [OH].

[d]NO_x analytical problems.

the OH radical levels were estimated as described in Section III-A-2, (2) if no tracer data are available, but values of $-\Delta[\text{organic}]$ could be obtained with reasonable accuracy from the GC measurements, then $[OH]_{avg}$ was estimated using a rearranged form of equations (XII) and (XIII):

$$[OH]_{avg} \simeq \frac{-\Delta[\text{organic}]}{k_{OH}[\text{organic}]_{avg}\Delta t} \simeq \frac{\Delta \ln[\text{organic}]}{k_{OH} \cdot \Delta t} \qquad \text{(XV)}$$

(3) if tracer data are not available and $-\Delta[\text{organic}]$ cannot be obtained directly with reasonable accuracy, than $[OH]^{avg}$ is estimated using a rearranged form of equation (XIV),

$$[OH]_{avg} \simeq \frac{\Delta([O_3]-[NO])}{\alpha \cdot k_{OH} \cdot [\text{organic}]_{avg} \cdot \Delta t} \qquad \text{(XVI)}$$

making the assumption that $\alpha \simeq 2$. As shown in Table 8, this assumption that $\alpha \simeq 2$ is reasonable, but obviously the use of Equation (XVI) is a more approximate way to estimate the OH radical levels than are the other two methods.

The estimated OH radical levels given in Table 8 can be compared with the values observed in NO_x-air irradiations listed in Table 5 of Section III-A-2, which generally ranged from (1-3) x 10^6 cm^{-3}. It can be seen that the different classes of compounds are indeed significantly different with respect to their effects on OH radical levels. Thus the alkanes significantly suppress OH radical levels, while the more reactive alkylbenzenes and heteroatom-containing organics significantly enhance them. Benzene and the bicyclic aromatics have an intermediate effect. This is consistent with the observed differences in overall reactivity discussed above in Section III-B-1, and indicates that the differing effects of the organics on radical levels are largely responsible for these differences.

Since the OH radical levels in organic-NO_x-air irradiations are influenced by other factors which are independent of the nature of the organics, especially the magnitude of the chamber radical source and the NO_2 levels present, it is useful to derive a reactivity index relating to effects on radical levels which reflect primarily the nature of the organic itself. This can be done by analyzing the results of the organic-NO_x-air irradiations in a manner analogous to our analysis of NO_x-air irradiations (discussed in Section III-A-2) except that all of the reactions which affect radical levels involving the organic, its intermediates and its photooxidation products, are represented by the following, highly simplified overall process:

$$\text{organic} + \text{OH} \xrightarrow{k_{OH}} (1 + \beta)\ \text{OH} + \text{products} \qquad (23)$$

where β, which can be positive or negative, reflects the tendency of the organic or its products to remove ($\beta < 0$) or contribute ($\beta > 0$) radicals to the system. As in our analyses of NO_x-air irradiations, we assume that the principal radical sink is the reaction of OH with NO_2

$$\text{OH} + \text{NO}_2 \xrightarrow{M} \text{HNO}_3 \qquad (8)$$

and the principal radical source is the chamber radical source, other than radical sources and sinks associated with the reactions of the organic or its products, which are all lumped together as reaction (23). Thus, since the rates of radical source and sink processes must balance, we can write

$$\begin{pmatrix}\text{nonorganic}\\ \text{radical}\\ \text{sources}\end{pmatrix} + \begin{pmatrix}\text{Net radical input}\\ \text{from organics}\end{pmatrix} = \begin{pmatrix}\text{Nonorganic}\\ \text{radical sinks}\end{pmatrix}$$

or

$$R_u + \beta k_{OH}[OH]_{avg}[\text{organic}]_{avg} = k_8[OH]_{avg}[NO_2]_{avg}, \qquad (XVII)$$

where R_u is the radical input rate from sources independent of the organic and its products (assumed to be the chamber radical source measured in NO_x-air irradiations), k_{OH} is the OH + organic rate constant, and k_8 is the rate constant for the OH + NO_2 reaction. Equation (XVII) can be rearranged to yield

$$\beta \simeq \frac{k_8[OH]_{avg}[NO_2]_{avg} - R_u}{k_{OH}[OH]_{avg}[organic]_{avg}} \qquad \text{(XVIII)}$$

The values of β estimated using equation (XVIII) from the data for the first hour of the single component runs are summarized in Table 8. The radical input rates, R_u, used to calculate these values were obtained in one of two ways. If the run was carried out by adding the organic after irradiation of a tracer-NO_x-air mixture for 2 hours, the radical input rate derived from the data obtained prior to the addition of the organic was used. For the remaining runs, the radical input rates were obtained by averaging the rates from the NO_x-air irradiations carried out before and after the organic-NO_x-air irradiation. Since, as discussed in Section III-A-2, the radical input rates appear to be independent of NO_x in these experiments, this averaging was carried out without regard to the NO_x levels employed. Uncertainties in the appropriate values of R_u tended to be relatively less important in deriving values of β for compounds which tended to contribute radicals ($\beta > 0$), but were a major factor in estimating values of β for compounds which tended to remove radicals ($\beta < 0$).

The modest degree of variability in the estimated values of β shown in Table 8 is expected based on the number of assumptions and approximations involved and the uncertainties in the estimated values of R_u and $[OH]_{avg}$. However, the values obtained are reasonably self-consistent, with different runs employing the same compound giving similar values, with no apparent dependence on initial organic and NO_x values. As expected based on their low reactivities, the alkanes methylcyclohexane and n-octane have the greatest tendency to remove radicals, with values of β ranging from -0.3 to -0.4. Naphthalene and 2,3-dimethylnaphthalene have

the next greatest tendency to remove radicals, with average values of β of -0.19 and -0.15, respectively. On the other hand, the methylbenzenes clearly have a tendency to contribute radicals to the system, with values of β ranging from 0.1 to 0.2, though benzene and tetralin apparently have a slight tendency to remove radicals. Among the heteratom-containing organics, furan has the greatest tendency to contribute radicals, with pyrrole being somewhat less effective and thiophene apparently neither removing nor contributing radicals to a significant extent, at least in the initial hour of the irradiation (but see below). This ordering is generally consistent with the observed ordering of the overall reactivities, as discussed in Section III-B-1, if the additional effect of differences in OH radical rate constants is considered.

However, the representation provided by reaction (23) is almost certainly oversimplistic, especially since it assumes that of all the radical initiation or termination processes associated with the organic are due primarily to reactions of the organic itself, while in many cases the secondary reactions of the products may be the major factor. This is particularly likely to be the case for compounds which tend to contribute radicals ($\beta > 0$), since the most probable organic radical sources in organic-NO_x-air photooxidation are photolyses of oxygenated products [as, for example, is believed to be the case for the alkylbenzenes (References 12 and 17)]. In such cases, the total radical input rates tend to increase with time, due to the buildup of the photoreactive products, and the effective β values will also increase. To examine this possibility, Figures 16 and 17 show plots of the total radical input from all reactions involving organics, calculated in 1-hour or 1/2-hour intervals by using a rearranged form of equation (XVII) for selected runs involving benzene and the alkylbenzenes (Figure 16) and tetralin, naphthalene, n-octane, and

$$\begin{pmatrix}\text{Net radical}\\ \text{input from}\\ \text{organics)}\end{pmatrix} = \begin{pmatrix}\text{(Nonorganic}\\ \text{radical}\\ \text{sinks)}\end{pmatrix} - \begin{pmatrix}\text{(Nonorganic}\\ \text{radical}\\ \text{sources)}\end{pmatrix}$$

$$= k_8[OH]_{avg}[NO_2]_{avg} - R_u \qquad \text{(XIX)}$$

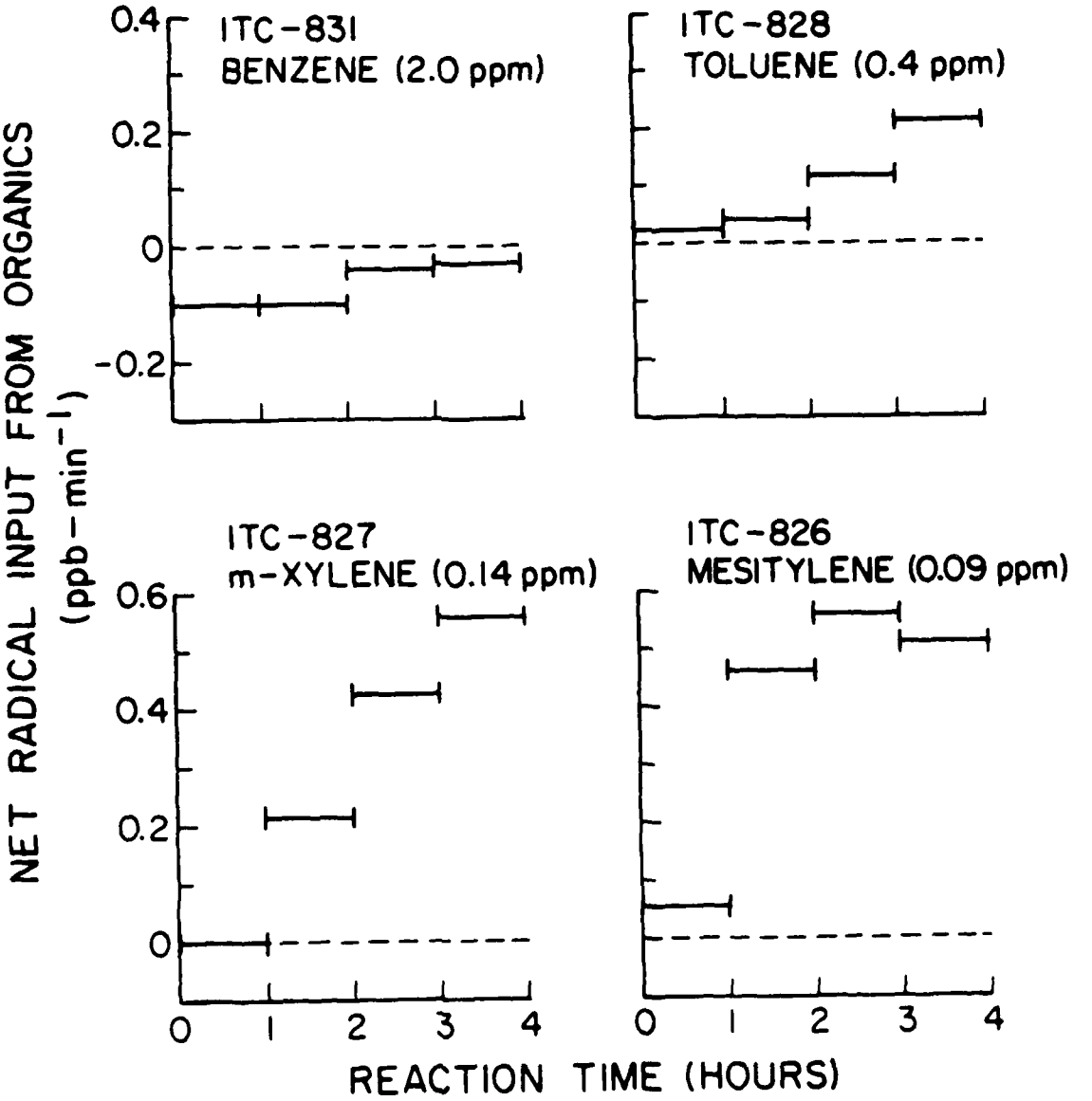

Figure 16. Plots of Net Radical Input Rates from Organics Calculated from Selected Benzene, Toluene, m-Xyelene, and Mesitylene-NO_x-Air Runs.

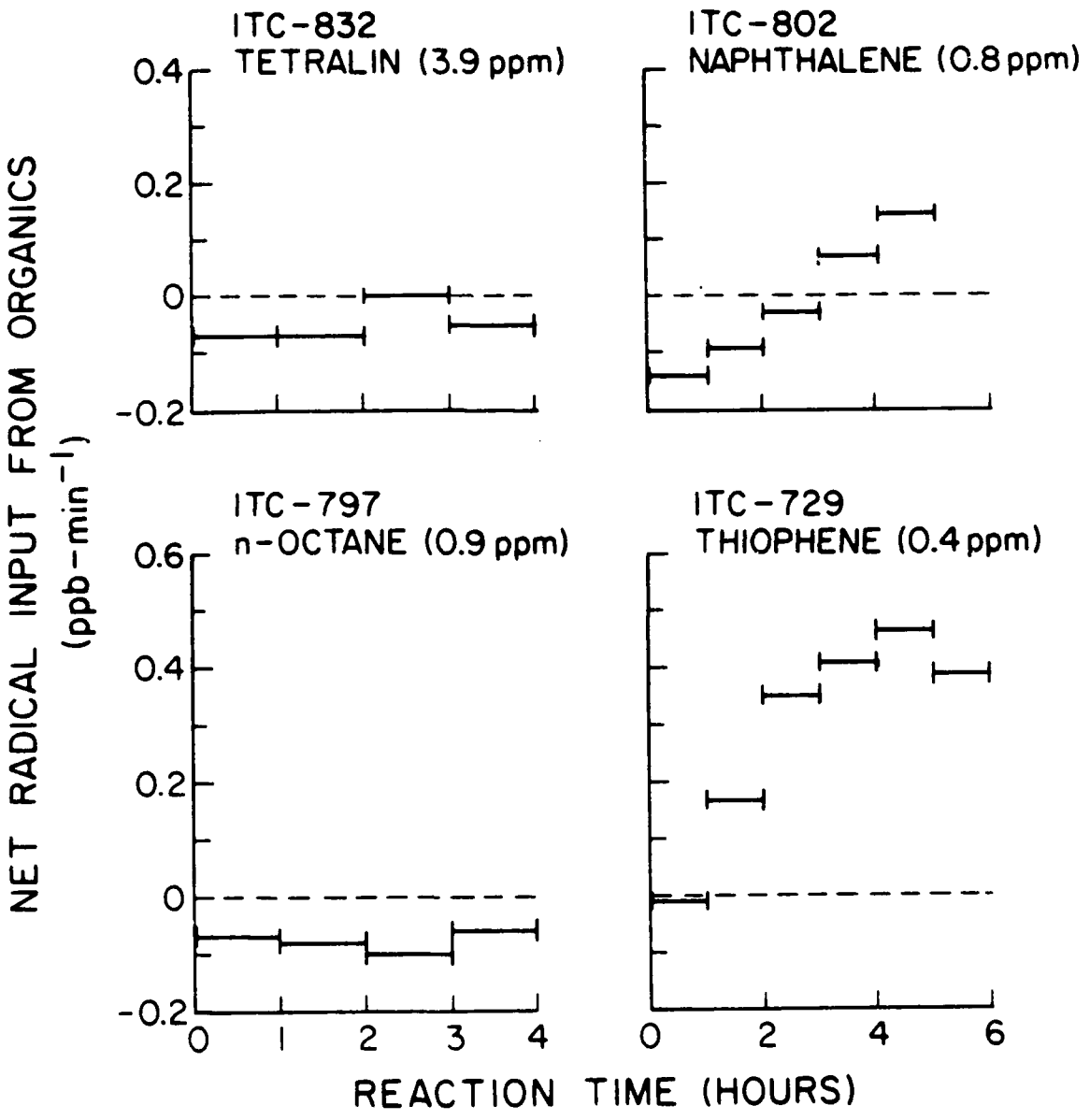

Figure 17. Plots of Net Radical Input Rates from Organics Calculated from Selected Tetralin, Naphthalene, n-Octane, and Thiophene-NO_x-Air Runs.

thiophene (Figure 17). These figures clearly indicate significant increases of radical levels with time for those runs involving the alkylbenzenes and thiophene, and suggest slight increases in radical levels with time in the case of benzene and tetralin. No significant buildup of radicals with time for the alkanes n-octane and methylcyclohexane is indicated.

These results are not inconsistent with our current understanding of the atmospheric photo-oxidation mechanisms of the alkanes and the simple alkylbenzenes. In the case of the alkanes, the data in Figure 17 indicate that the suppression of radicals is immediate, and there is no evidence of any significant buildup of photoreactive products. The immediate suppression of radicals indicates that the radical termination process is involved in the initial reaction of the parent alkane, and not in the formation of products which are radical inhibitors. This is entirely consistent with our assumed mechanism for the photo-oxidations of the alkanes, which are characterized by following competition between radical propagation:

$$RO_2 + NO \rightarrow RO\cdot + NO_2 \qquad (21)$$

and radical termination to form alkyl nitrates.

$$RO_2 + NO \xrightarrow{M} RONO_2 \qquad (22)$$

For n-octane, the rate constant ratio $k_{22}/(k_{21} + k_{22})$ has been measured to be 0.33 (Reference 31), which is entirely consistent with the observed values of β of 0.3-0.4 measured in this study (Table 8). This branching ratio has not been measured for methylcyclohexane, but our observed values of β of 0.3-0.4 for this compound are entirely consistent with $k_{22}/(k_{21} + k_{22})$ ratios obtained for other branched and cyclo-alkanes (Reference 32).

In the case of the aromatics, current models for the atmospheric reactions of toluene and the xylenes (References 12, 15, 16, 17, and 33) attribute the high reactivities of these compounds to the observed formation of photoreactive α-dicarbonyls such as methylglyoxal and (from

o-xylene) biacetyl (References 34-37), though recent modeling studies indicate that formation of additional, as yet uncharacterized, photoreactive products may also be important (Reference 38). Aromatics also form products such as phenols and aromatic aldehydes in their atmospheric photo-oxidations (Reference 17) which are believed to act as radical inhibitors (References 12, 19, 39), but apparently for the alkylbenzenes their formation has a smaller impact on the radical levels than the formation of photoinitiators.

Figures 16 and 17 show that for aromatics such as benzene, tetralin, and naphthalene, the radical initiation rates tend to be suppressed initially, though at least for naphthalene and possibly for the other two compounds, the apparent buildup of photoreactive products causes the radical initiation rates to subsequently increase. Since this suppression of radical input rates is immediate, rather than increasing with time as one might expect if an inhibitor were formed as a product which builds up with time, the data suggest that these aromatics, like the alkanes, may also have a radical termination pathway in their initial photo-oxidation reaction. Indeed, it was originally proposed that a process analogous to the formation of the alkyl nitrates from alkanes was involved in the photo-oxidation of toluene and the xylenes (References 12 and 15), though this process has not been assumed in more recent published models (References 16 and 33). However, at the present time, this and most other aspects of the aromatic photo-oxidation mechanisms remain largely speculative.

For the heterocyclic organics furan, thiophene, and pyrrole, essentially nothing is known concerning their NO_x-air photo-oxidation mechanisms. However, the data obtained in this study clearly indicate that significant formation of photoreactive products is probable. For thiophene, this is indicated by the buildup in radical initiation rates with time shown in Figure 17. For furan and pyrrole, it is probable that the photoreactive products are consumed rapidly, as indicated by the extremely high radical levels observed in runs employing these compounds (Table 8), and also by the observation that once the initially present furan or pyrrole is consumed, no apparent persistent reaction products remain to cause the oxidation of NO and the formation of O_3 to continue (Section

IV-B-1). However, at the present time the identities and reactions of these products are unknown.

C. FUEL RUNS

Environmental chamber experiments were carried out using one whole fuel, from a preproduction batch of shale-derived JP-4 which was supplied by the USAF, and three different "surrogate" jet fuels synthesized by mixing 15 representative fuel components. In addition, experiments were carried out in which small amounts (1-2 percent on a mole carbon basis) of furan, thiophene, or pyrrole were added to one of the synthetic fuels to represent the effects of these potential fuel impurities on the fuel's atmospheric reactivity. The surrogate fuel experiments are needed to test models for the atmospheric reactions of realistic fuel mixtures whose compositions are known exactly (so that the chemical mechanism can be tested without concern for the effects of any uncertainties in the fuel analyses). Obviously experiments with real fuels are needed to test the model's ability to simulate their reactivity. The compositions of the fuels employed in our experiments are discussed in Section III-C-1. Comparison of the reactivities of the fuels studied is discussed in Section III-C-2, and the effects of including the heteroatom-containing impurities in the fuel mixtures are discussed in Section III-C-3.

1. Compositions of the Fuels Employed

a. JP-4

A gas chromatogram taken from the environmental chamber after it was dosed with a sample from the preproduction batch of shale-derived JP-4 employed in this program is shown in Figure 18, with selected fuel components being identified. This chromatogram is qualitatively similar with those obtained using other batches of JP-4 (both petroleum- and shale-derived) employed in our previous studies (reference Appendix - Outdoor), and indicate that a large number of different compounds are

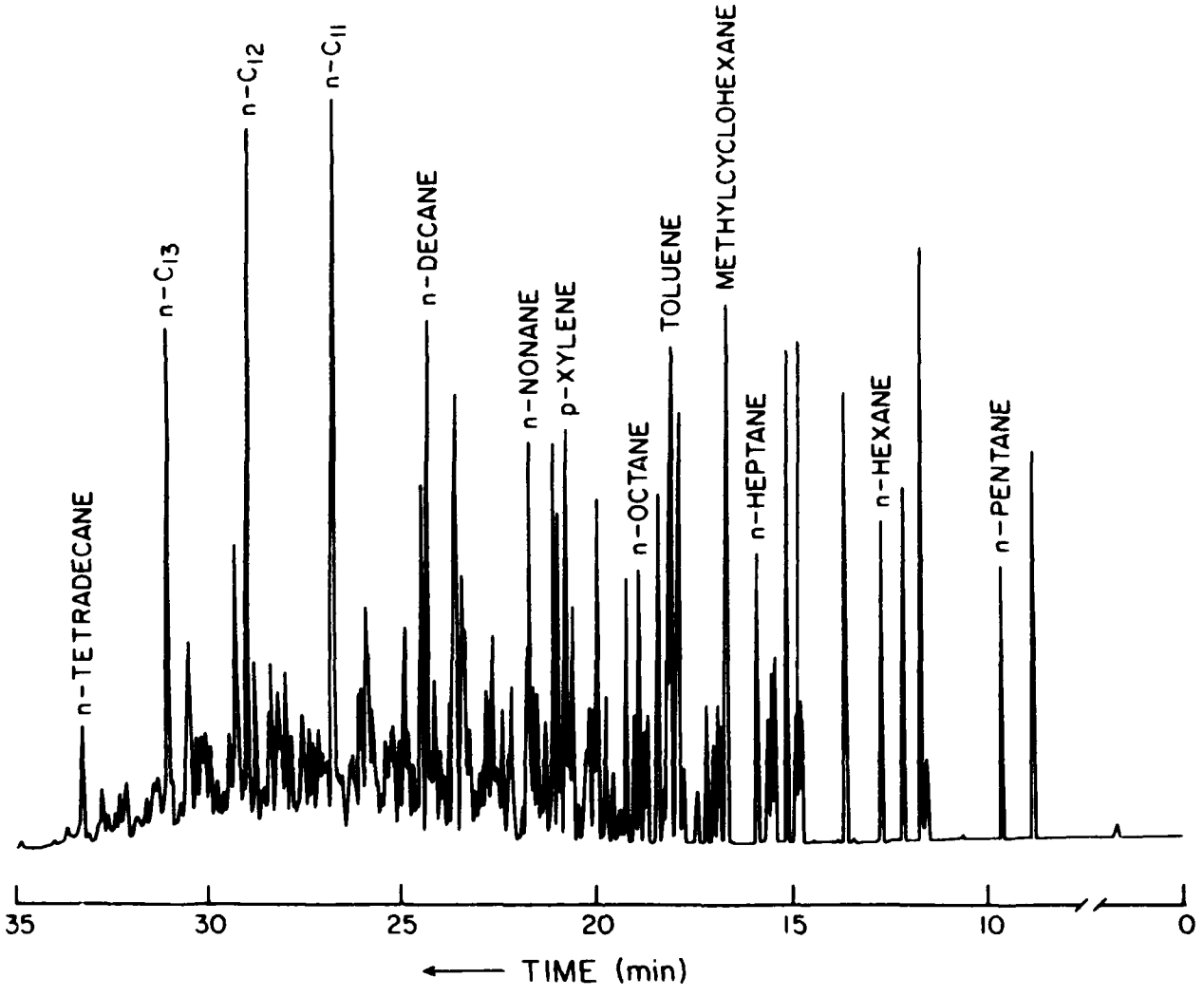

Figure 18. Chromatogram of the Preproduction Batch of Shale-Derived JP-4 After Injection into the Indoor Teflon Chamber, with Selected Constituents Identified.

present, including n-alkanes, cycloalkanes, and aromatics. (The chromatographic technique employed is not suitable for compounds heavier than C_{13}, and the absence of such compounds on this chromatogram does not necessarily mean that they are not present.) Although a detailed quantitative analysis of this fuel was not carried out in this phase of this program, quantitative analyses were routinely carried out for the C_6-C_{13} n-alkanes, methylcyclohexane, and several alkylbenzenes, and the averages of the relative amounts of these compounds measured after the fuel was injected into the chamber for the four JP-4/NO_x/air runs are shown in Table 9. (The n-undecane, dodecane, and tridecane levels in run ITC-725 were low, relative to those measured in the other two runs, and are not counted in the averages.) A more complete analysis of this fuel will be necessary before runs employing it can be used for model testing. Such analyses should be carried out in the second phase of this program.

b. Synthetic Fuels

The synthetic fuels employed in this program consisted of three mixtures of 15 different alkanes, alkylbenzenes, and bicyclic aromatics which are representative of the types of compounds present in jet fuels now in use. The composition of the first mixture, designated "Synthetic Fuel 1" or the "standard" synthetic fuel, was specified by the Air Force. The second mixture was designated Synthetic Fuel 2, or the "high-aromatics" fuel, and consisted of the same 15 compounds with the same relative composition among the seven alkanes and among the eight aromatics, but the percentage of aromatics (on a mole carbon basis) was increased from 27 to 38 percent. For the third formulation, designated Synthetic Fuel 3, or the "modified aromatics" fuel, the composition and levels of the alkane components were the same as in the "standard" synthetic fuel, but the ratio of alkylbenzenes to bicyclic aromatics was increased by a factor of ~2, relative to that in the other fuels. These different formulations were useful for testing the effects of changing fuel composition on their atmospheric reactivity, and for testing models designed to predict these effects.

TABLE 9. COMPOSITION OF THE THREE SYNTHETIC FUELS EMPLOYED IN THIS PROGRAM AND RELATIVE CONCENTRATIONS OF SELECTED COMPOUNDS MEASURED IN THE PRE-PRODUCTION BATCH OF SHALE-DERIVED JP-4.

	Mole % (as carbon)						
	Standard		High aromatics		Modified aromatics		JP-4
Component	Calc[a]	Obs[b]	Calc[a]	Obs[b]	Calc[a]	Obs[b]	Obs[b,c]
Alkanes (total)	78.9	72.9	67.9	62.2	78.1	74.0	75.0
n-Hexane	14.4	11.4	12.4	9.9	14.2	11.7	5.2
n-Heptane	20.5	17.8	17.6	15.2	20.3	18.2	4.6
n-Octane	18.6	18.7	16.0	15.9	18.4	19.1	4.1
n-Nonane	-	-	-	-	-		7.6
n-Decane	-	-	-	-	-		9.5
n-Undecane	-	-	-	-	-		12.1
n-Dodecane	-	-	-	-	-		12.0
n-Tridecane	-	-	-	-	-		9.2
n-Tetradecane	2.1	3.6	1.8	2.9	2.0	3.3	d
Cyclohexane	8.3	6.5	7.1	5.6	8.2	6.6	d
Methylcyclohexane	12.9	12.5	11.2	10.7	12.8	12.8	10.7
Ethylcyclohexane	2.1	2.5	1.8	2.0	2.1	2.4	d
Alkylbenzenes	13.3	14.8	20.2	21.5	16.9	18.6	21.8
Toluene	8.1	7.9	12.3	11.8	10.3	10.2	8.7
p-Xylene	1.9	2.0	2.8	3.0	2.4	2.6	7.8
Cumene	1.4	1.9	2.1	2.6	1.8	2.3	d
Mesitylene	2.0	3.0	2.9	4.1	2.5	3.5	5.3
Bicyclic Aromatics	7.8	12.3	11.[illegible]	16.3	5.0	7.4	d
Tetralin	2.5	4.4	3.9	5.9	1.6	2.7	d
Naphthalene	2.2	3.0	3.3	4.2	1.4	1.8	d
2-Methylnaphthalene	2.2	3.6	3.3	4.5	1.4	e	d
2,3-dimethylnaphthalene	0.9	13	1.4	1.7	0.6	0.8	d

[a]Calculated concentration based on measured weights or volumes of each compound used when synthesizing the fuel.

[b]Averages of the relative gas-phase concentrations measured after the fuel was introduced into the chamber.

[c]Arbitrarily normalized so total measured alkane = 75, for more direct comparison with the "standard" and "modified aromatic" synthetic fuels.

[d]Not measured.

[e]Not measured. Assumed to have the same ratio to the total of the other bicyclic aromatics for the purpose of calculating total percentages.

The three synthetic fuels were prepared by mixing the desired weights (for solids) or volumes (for liquids) of the 15 components. Their relative compositions, calculated based on the amounts of each component added to the mixtures, are given in Table 9. Also shown in Table 9 are the averages of the relative gas phase concentrations measured by gas chromatography after the fuels were injected into the chamber for the fuel-NO_x-air experiments. Although reproducibilities to within 5 percent or better in relative fuel composition were observed in analyses carried out for separate runs, this table shows that some compounds had somewhat greater discrepancies between the observed and expected relative levels, with the observed gas phase levels of the lighter alkanes tending to be somewhat less than expected, and the levels of the bicyclic aromatics tending to be greater. Although this could have been due to evaporation, the fuels were stored under refrigeration and there was no evidence that fuel composition changed with time during this program. This discrepancy, which was similar for all three fuels studied, was not considered to be excessive and should not significantly affect the utility of the data obtained in this program.

The data shown in Table 9 also allow some comparison to be made between the synthetic fuels and the batch of JP-4 employed in this study. The total alkylbenzene/total alkanes ratio for the compounds monitored in JP-4 is closer to those for the high or modified aromatics fuels than that for the standard fuel, but it is not clear whether this would be the case if a more complete analysis of JP-4 were carried out. It is clear, however, that the synthetic fuels all have much higher levels of lighter alkanes compared to heavy alkanes than the JP-4 fuel, and this may have an effect on their relative reactivity.

2. Comparisons of Fuel Reactivities

The initial concentrations and selected results of all fuel-NO_x runs carried out in this program are summarized in Table 10, and plots of O_3, NO_2, and PAN concentration-time profiles for runs employing each of the fuels with comparable initial total fuel and NO_x concentrations are

TABLE 10. INITIAL CONCENTRATIONS AND SELECTED RESULTS OF THE FUEL-NO_x-AIR IRRADIATIONS.

Fuel	ITC run no.[a]	Initial concentration		Initial[c] NO consumption rate	Maximum O_3		6-Hour yields	
		NO_x[b] (ppm)	Fuel (ppmC)	(ppb min^{-1})	(hr)	(ppm)	O_3 (ppm)	PAN (ppm)
Shale-Derived JP-4	725	0.22	50[d]	1.2	-	-	0.45	0.03
	722	0.54	50[d]	2.0	-	-	0.45	0.03
	721	0.54	100[d]	2.9	-	-	0.68	0.05
	768	0.53	100[d]	2.3	-	-	0.82	0.04
"Standard" Synthetic Fuel	785	0.26	45	2.1	~6	0.60	0.60	0.03
	781	0.51	43	2.8	-	-	0.75	0.04
	784	0.50	88	3.2	5.5	0.75	0.73	0.05
	805	0.52	98	2.4	5.75	0.79	0.78	0.03
"High Aromatics" Synthetic Fuel	795	0.50	45	2.9	-	-	0.76	0.03
	796	0.53	97	3.3	4.25	0.60	0.47	0.04
"Modified Aromatics Synthetic Fuel	801	0.55	41	2.3	-	-	0.78	0.03
	799	0.55	94	3.7	5.25	0.84	0.81	0.05
"Standard" Fuel								
+ 0.37 ppm Furan	786	0.49	72	4.8	2.25	0.64	0.50	0.03
+ 0.37 ppm Thiophene	788	0.48	89	2.8	5.0	0.72	0.69	0.05
+ 0.19 ppm Pyrrole	807	0.48	77	5.9[e]	3.0	0.64	0.57[f]	0.03[f]

[a]Listed in order of increasing initial NO_x, then increasing initial fuel.

[b]Average initial $[NO_2]/[NO_x] = 0.20 \pm 0.06$.

[c]$-d[NO]/dt$ for first hour of the run, unless indicated otherwise.

[d]Nominal value expected based on amount of fuel injected.

[e]Calculated for first 45 minutes of run.

[f]5.25-Hour yields.

shown in Figures 19 and 20. In all experiments, substantial yields of O_3 (at least 0.45 ppm) and non-negligible levels of PAN (generally 20-30 ppb) were formed, but it should be noted that relatively high levels of fuels, i.e., 50-100 ppmC, were employed. In terms of overall reactivity, the fuels were much more reactive than the alkanes, where essentially no O_3 and PAN formation resulted in experiments employing comparable hydrocarbons and NO_x levels, but were much less reactive than the alkylbenzenes, where substanial O_3 and PAN formation could occur when these compounds were present at much lower levels. Thus, as one might reasonably expect, the reactivity of these fuels is intermediate between that of its most reactive and its least reactive components.

Although the differences in reactivities between the four fuels studied were less than the differences in reactivities of the different classes of individual components, the results of these experiments indicate that differences in fuel composition will indeed affect their atmospheric reactivity. In particular, increasing the overall levels of the aromatics in the fuels will, as expected, increase the rate at which O_3 is formed, but it will also decrease the final yield of O_3 observed in the higher fuel/NO_x runs, where O_3 maxima are obtained. (Compare the data for the "standard" synthetic fuel and the "high aromatics" fuel in Figure 19 and Table 10.) This suppression of maximum O_3 yields caused by increasing levels of aromatics in multicomponent-NO_x-air irradiation has been observed previously (References 33 and 40). It is believed that this is because the photooxidation of the aromatics involves a number of significant NO_x sinks, which means that less O_3 can be formed before NO_x is consumed (References 17, 33, and 40).

The ratio of alkylbenzenes to bicyclic aromatics within the aromatic fraction of the fuels appears to be almost as important as the total level of aromatics in the fuel, particularly at the higher fuel/NO_x ratios. In particular, the "modified aromatics" synthetic fuel, with approximately the same total aromatics level as the standard fuel, with a higher ratio of alkylbenzenes to bicyclics, is considerably more reactive than the standard fuel in the ~100 ppmC fuel -0.5 ppm NO_x experiments.

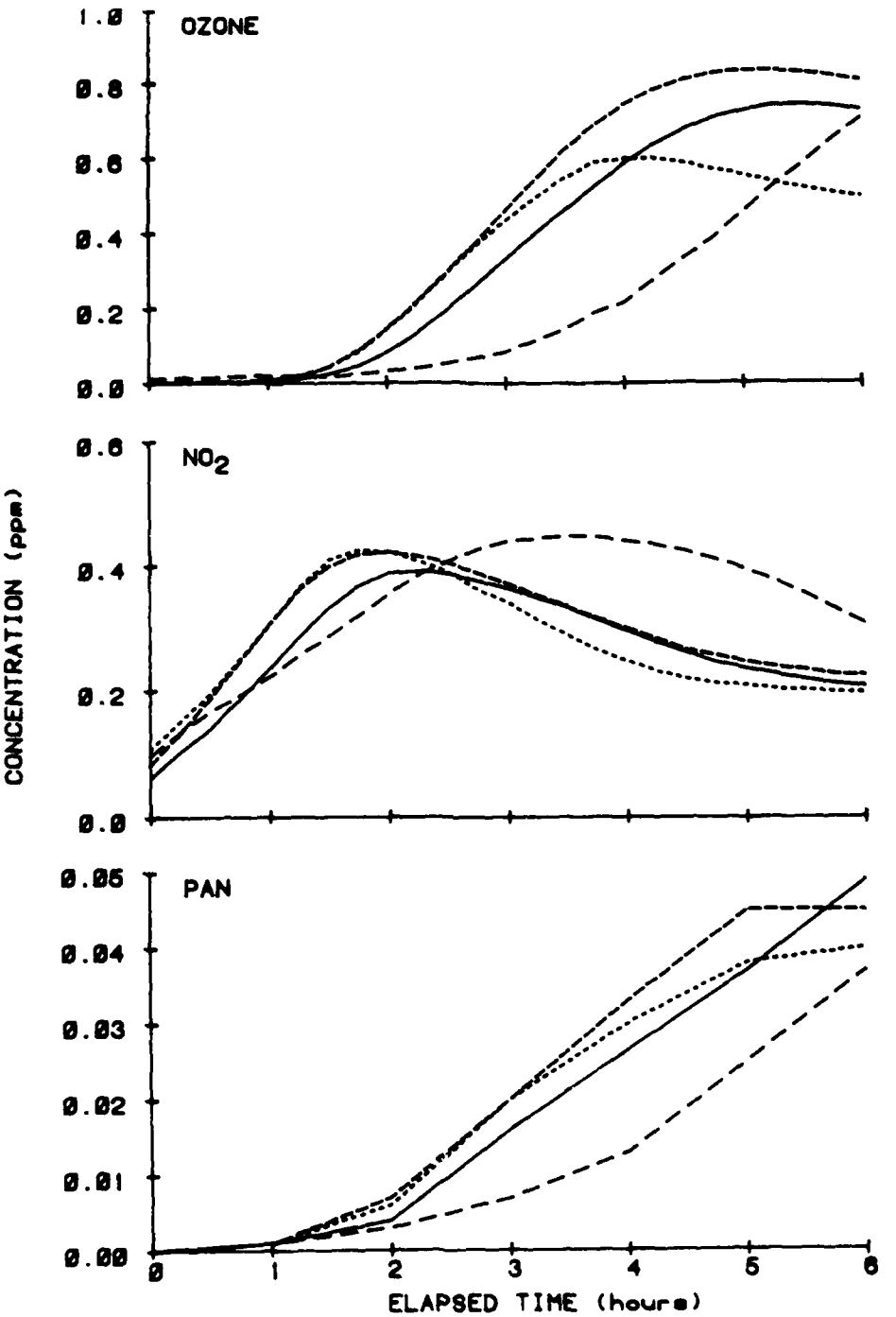

——— Standard Synthetic Fuel Run ITC-784
..... "High Aromatics" Fuel Run ITC-796
----- "Modified Aromatics" Fuel Run ITC-799
- - - JP-4 Run ITC-768

Figure 19. Concentration-Time Plots for O_3, NO_2, and PAN Observed in Selected ~100 ppmC fuel - 0.5 ppm NO_x runs.

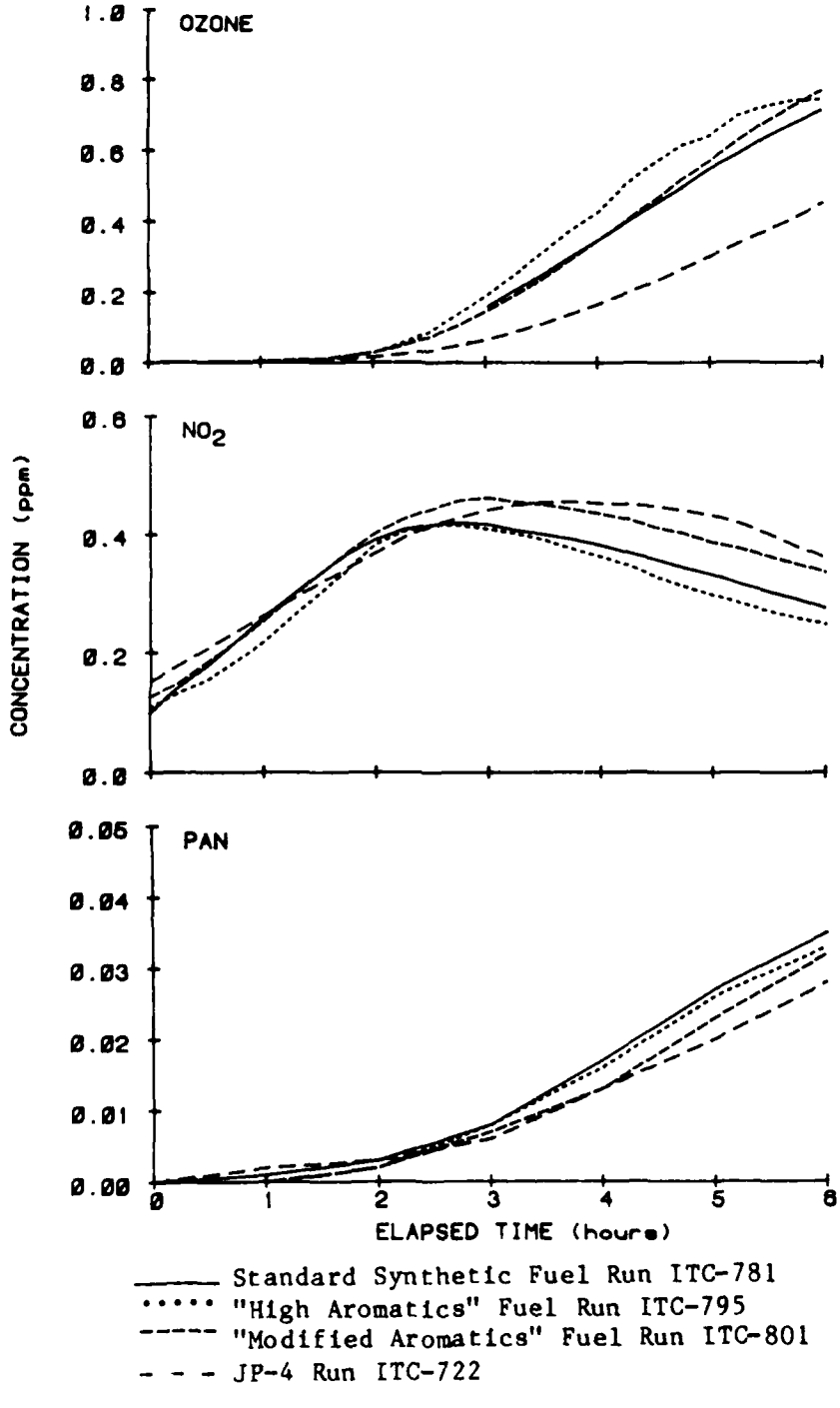

Figure 20. Concentration-Time Plots for O_3, NO_2, and PAN Observed in the ~50 ppmC Fuel -0.5 ppm NO_x Runs.

Thus the "modified aromatics" synthetic fuel exhibits both a shorter initiation time for O_3 formation (comparable to that for the "high aromatics" fuel), and also (unlike the "high aromatics" fuel) forms somewhat more O_3 than the standard fuel (see Figure 19). On the other hand, in the ~50 ppmC fuel/0.5 ppm NO_x experiments, the initiation time for O_3 formation in the "modified aromatics" fuel was comparable to that for the standard fuel, indicating that the composition of the aromatics will also influence how the reactivity changes with changing fuel/NO_x ratios. The fact that at higher fuel/NO_x ratios the maximum O_3 is suppressed when the levels of both alkylbenzenes and bicyclic aromatics are increased, but not when bicyclics are reduced and alkylbenzenes are increased, indicates that the suppression of O_3 observed when aromatics are increased is caused to a larger extent by the increased levels of the bicyclics than by the increased levels of the alkylbenzenes. This suggests that NO_x sinks may be even more important in the NO_x-air photooxidations of the bicyclic aromatics than is the case for the alkylbenzenes. This must be taken into account when developing models for the atmospheric reactions of these fuel constituents.

In order to determine the reproducibility of the results of these fuel-NO_x-air irradiations, two duplicate experiments were carried out employing both the standard synthetic fuel and the shale-derived JP-4, and the O_3 and NO_x concentration-time profiles obtained are plotted together in Figure 21. The results indicate that experiments employing this fuel are more difficult to carry out reproducibly than is the case for the synthetic fuels. In particular, Figure 20 shows that although JP-4 runs ITC-721 and ITC-768 had comparable initial NO_x and fuel levels, the former run had a shorter initiation time for O_3 formation, and appeared to approach a lower maximum O_3 yield than is the case for run ITC-768. In contrast, Figure 20 shows reasonably good reproducibility in O_3 profiles for the two replicate runs employing the standard synthetic fuel (runs ITC-784 and ITC-805). The fact that JP-4 runs have more problems with reproducibility is probably due to difficulties in reproducibly introducing the heavier fuel constituents into this chamber, as was observed in our previous study with JP-8 (Reference 6). The problem with this JP-4

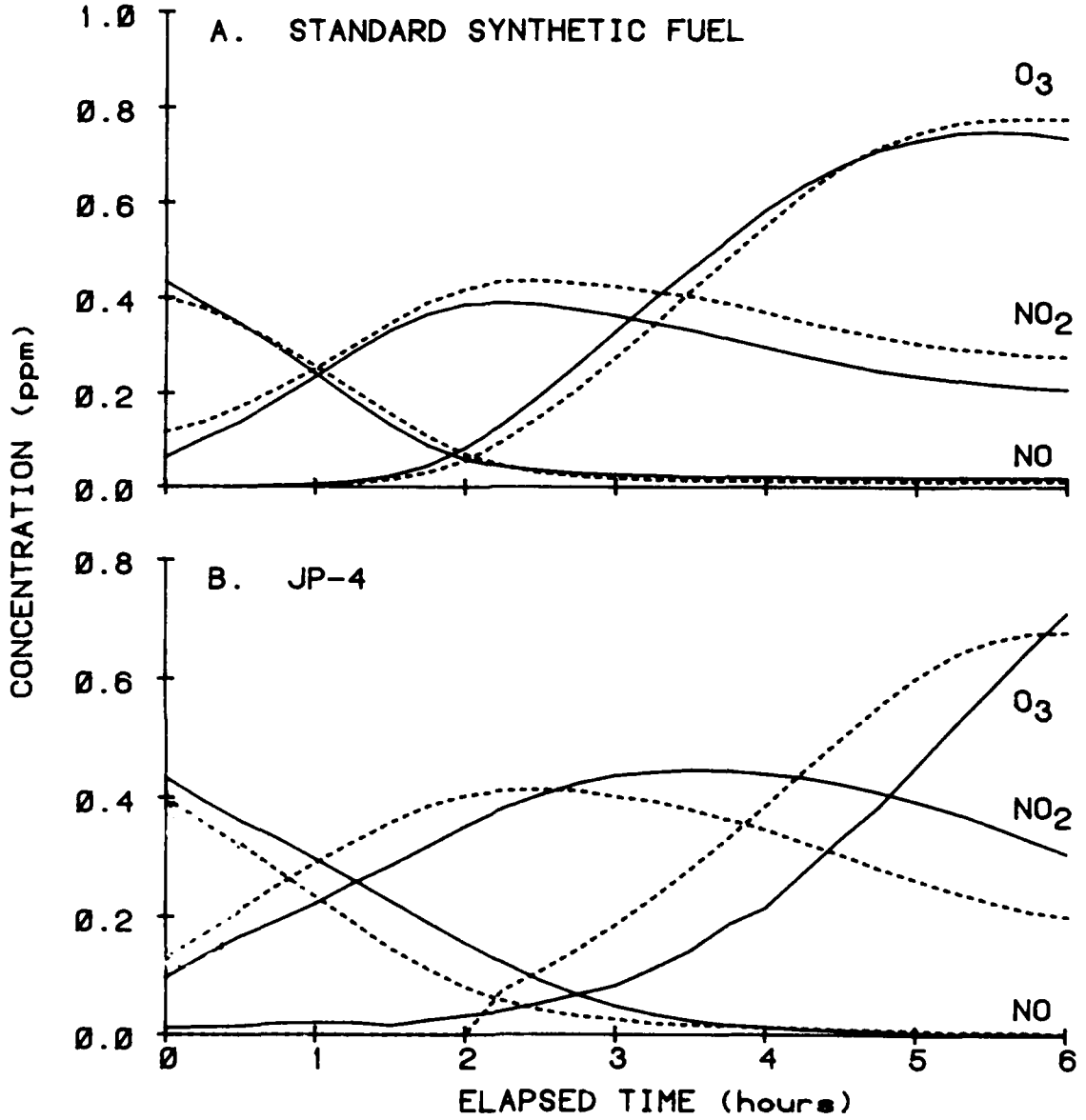

A. Plots for "Standard" Synthetic Fuel Runs
——— ITC-784
----- ITC-805
B. Plots for JP-4 Fuel Runs
——— ITC-768
----- ITC-721

Figure 21. Comparisons of O_3, NO, and NO_2 Concentration-Time Profiles for Replicate Fuel-NO_x-Air Irradiations.

sample was not as great as that observed previously with JP-8 (Reference 6), but we did observe greater variability in levels of n-undecane and the higher n-alkanes monitored after injection of JP-4 than was the case for the lighter constituents, with run ITC-725 having anomalously low monitored levels of these compounds compared with those measured in the other runs. Thus the conditions of the runs employing JP-4 are somewhat less well-characterized than is the case for the other runs carried out in this program, and this must be taken into account when using the results of these experiments for model testing.

Despite these variations in reproducibility, the results of these experiments clearly indicate that the shale-derived JP-4 employed in this study was less reactive in terms of rates of O_3 formation than were any of the synthetic fuels studied. This could be due to lower overall levels of aromatics, but more complete data concerning the composition of this fuel, as well as modeling studies, are required to determine if this is indeed the cause. It is clear that the JP-4 fuel has a higher level of heavier alkanes compared to light alkanes than do the synthetic fuels (see Table 9), and this is another possible cause for the observed differences in reactivity between the different fuels studied.

3. Effects of Added Furan, Thiophene, or Pyrrole

To test the effects of potential heteroatom-containing fuel impurities on the atmospheric reactivities of jet fuels, one run each was carried out in which furan, thiophene, or pyrrole was added to the standard synthetic fuel. The amount of furan or thiophene added corresponded to ~2 percent of the total fuel concentration on a mole carbon basis, while the amount of pyrrole added corresponded to only ~1 percent of the fuel. Selected results of these experiments are given in Table 10, and comparisons of the O_3, NO, and NO_2 concentration-time profiles with and without these added "impurities" are given in Figures 22-24.

The data in Table 10 and Figures 22-24 clearly indicate that the inclusion of 1-2 percent of furan or pyrrole has large effects on atmospheric reactivities of the fuels, while the effect of a comparable amount

AD-A148 716 ATMOSPHERIC PHOTOCHEMICAL MODELING OF TURBNNE ENGINE FUELS PHASE I EXPERI..(U) CALIFORNIA UNIV RIVERSIDE STATEWIDE AIR POLLUTION RESEARCH CE.. 2/2

UNCLASSIFIED W P CARTER ET AL. SEP 84 F/G 4/1 NL

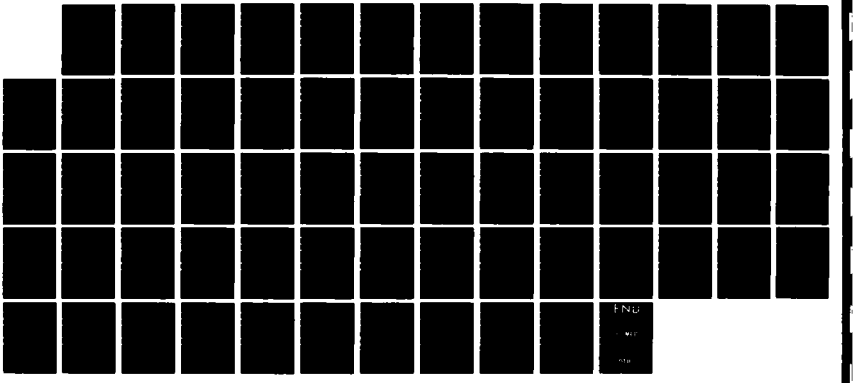

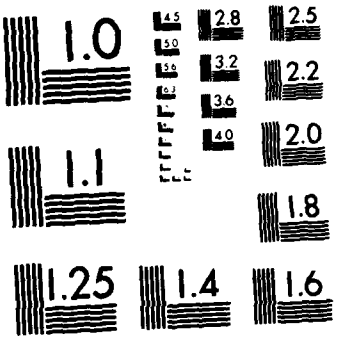

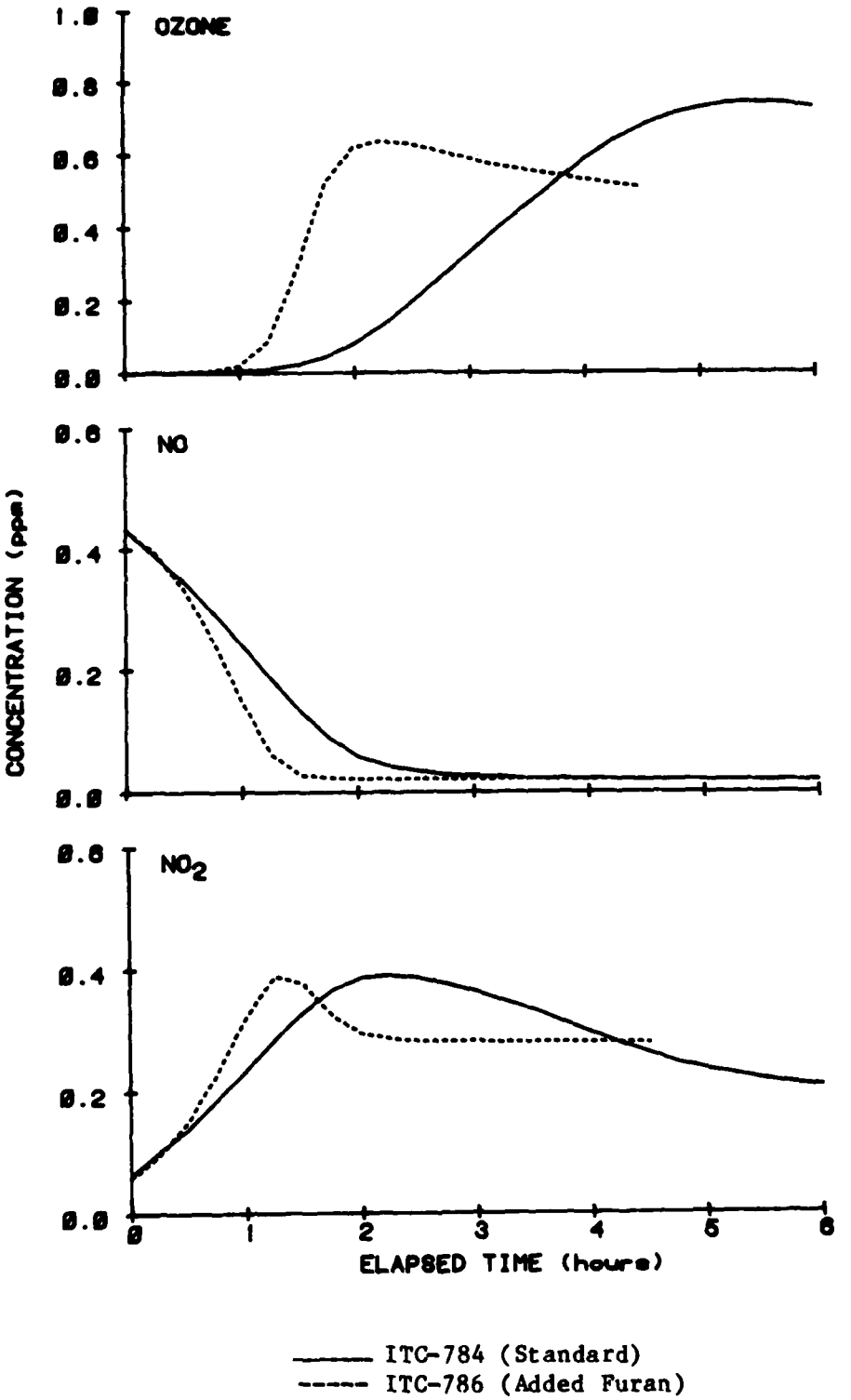

Figure 22. Comparison of Concentration-Time Plots for O_3, NO, and NO_2 for "Standard" Synthetic Fuel Runs With and Without ~2 Percent Added Furan.

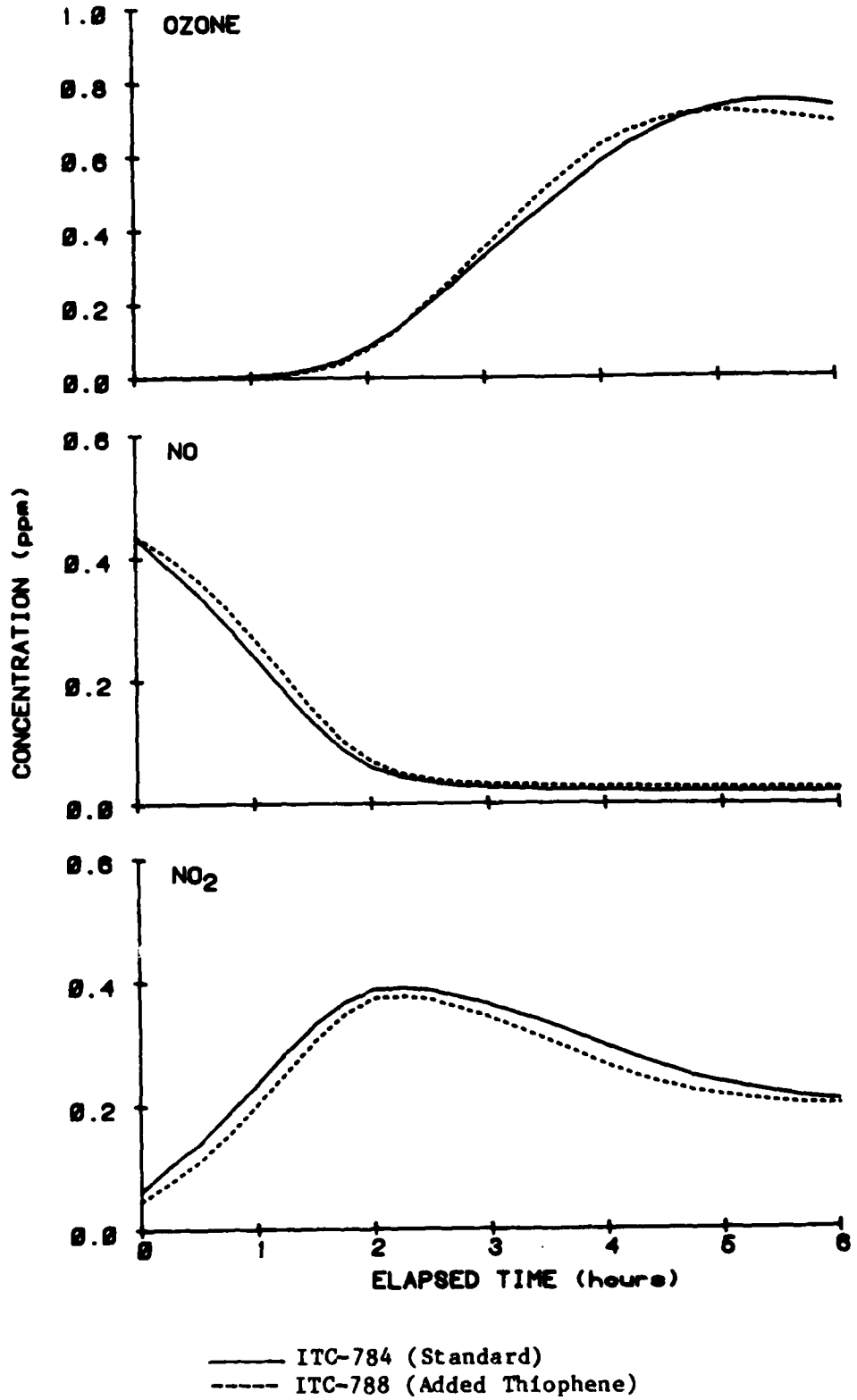

Figure 23. Comparison of Concentration-Time Plots for O_3, NO, and NO_2 for Standard Synthetic Fuel Runs With and Without ~2 Percent Added Thiophene.

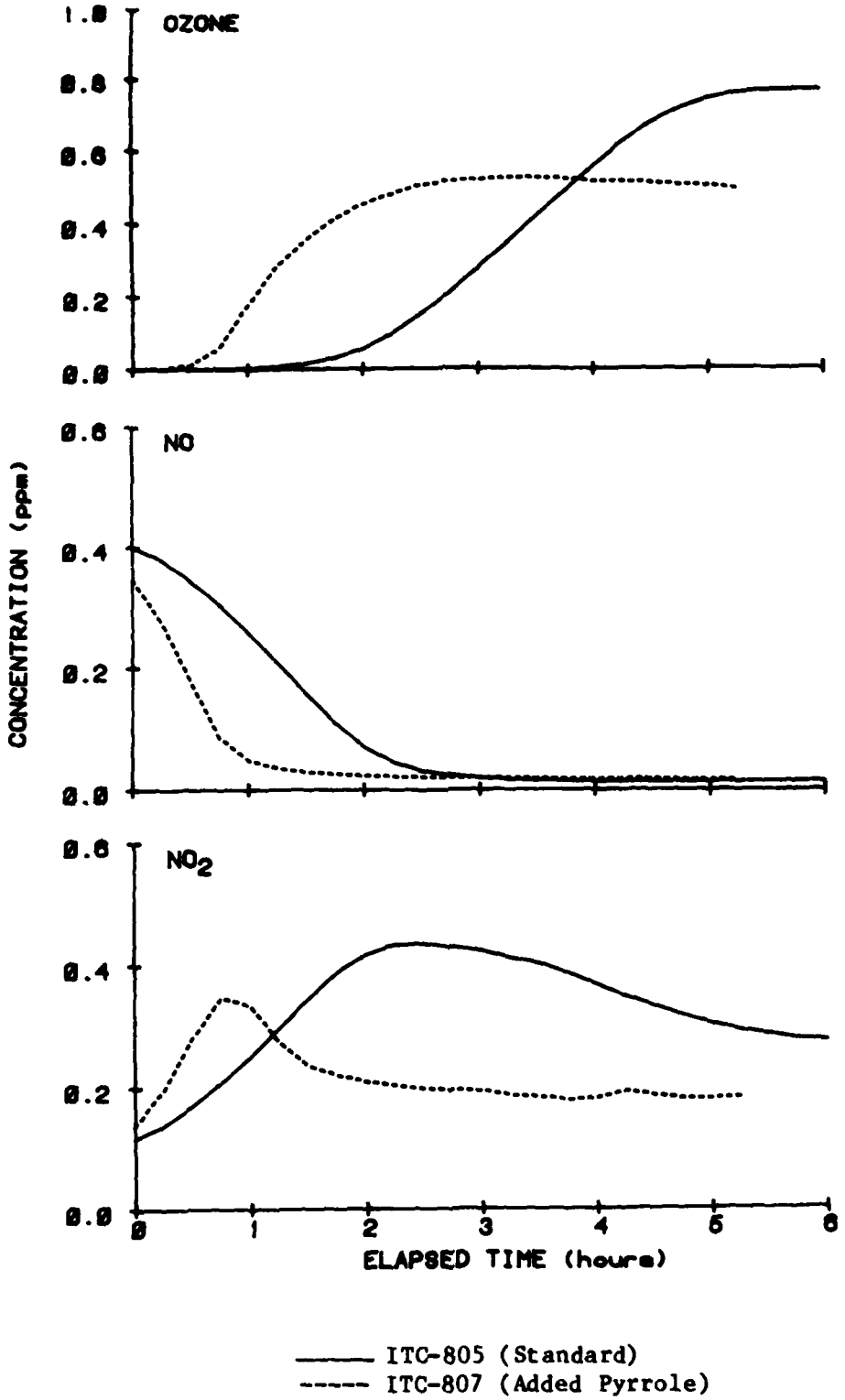

Figure 24. Comparison of Concentration-Time Plots for O_3, NO, and NO_2 for Standard Synthetic Fuel Runs With and Without ~1 Percent Added Pyrrole.

of added thiophene is relatively minor. (Figure 24 shows that the initial NO_2/NO ratio was not well replicated between the added pyrrole run and the corresponding standard fuel run, but the effect of this is expected to be much smaller than the observed differences between the two runs. Good replication of the injections was obtained in the added furan and thiophene runs as shown in Figures 22 and 23.) Although the large magnitude of the effect with added furan or pyrrole is somewhat suprising, considering the relatively small quantities of the compounds added, the fact that the effect is positive is as expected, since, as discussed in Section III-B, these compounds are among the most reactive studied in this program, both in terms of their relatively high OH radical rate constants, and in terms of their tendency to enhance radical levels. Their high OH radical rate constants cause them to be rapidly consumed relatively early in the run (all the pyrrole had reacted by 1.5 hours in run ITC-807), giving them a disproportionately high impact on the chemistry during that period. The radicals formed in the photooxidations of furan and pyrrole thus enhance the initial rates of consumption of all fuel constituents present, causing more rapid rates of NO oxidation and thus O_3 formation. The much smaller effect in the case of thiophene can be attributed to the fact that it reacts more slowly with OH radicals, resulting in less of it reacting and thus less of an effect on the overall chemistry of the system at any given time. In particular, of the 0.37 ppm initial thiophene in run ITC-788, less than 49 ppb reacted. Thiophene also appears to contribute radicals more slowly to NO_x-air irradiations than did the other heterocyclics (as discussed in Section III-B-3), but in this case its lower OH radical rate constant is probably the more important factor.

It is interesting to note from Figures 22 and 24 that in addition to decreasing the initiation time for O_3 formation, the presence of furan and pyrrole also appears to suppress the yield of O_3 formed. This effect seems to be the greatest with pyrrole, despite the fact that less pyrrole was added than was the case for furan (and despite the fact that the higher initial NO_2/NO ratio in the added pyrrole run would be expected to result in <u>more</u> O_3 being formed). This could be due to a tendency of these

compounds to remove NO_x from the system, but this effect seems to be surprisingly large, considering the small amounts of furan or pyrrole added. The model calculations to be carried out in the second phase of this program should be useful in elucidating this effect.

SECTION IV

KINETIC STUDIES

In order to develop chemical models to treat the atmospheric chemistry of selected constituents of jet fuels, it is necessary to know accurately the rate constants for the major loss processes of these fuel constituents under atmospheric conditions. It is now well-recognized (Reference 15) that the potential atmospheric loss processes for organics can be photolysis, reaction with OH and NO_3 radicals, or reaction with O_3. For the alkane and aromatic fuel constituents, reaction with OH radicals is believed to be the only significant removal process (Reference 18), but for certain of these compounds the rate constants for this process are unknown. For the three heterocyclics involved in this study (furan, thiophene, and pyrrole), removal by direct photolysis is believed to be negligible, but their rate constants for reaction with NO_3 radicals are not known, nor is it known how rapidly pyrrole reacts with O_3 and with OH radicals. This information must be obtained before data from chamber experiments employing these compounds can be used for model testing.

Therefore, as an integral part of this program but at no additional cost to the U. S. Air Force, we have carried out the necessary kinetic studies to determine the rate constants for the reactions of NO_3 radicals with furan and thiophene, and for the reactions of O_3 and OH and NO_3 radicals with pyrrole. In addition, we have derived rate constants for the reactions of OH radicals with tetralin, 1-methylnaphthalene, 2,3-dimethylnaphthalene, ethylcyclohexane, and tetradecane from their rates of decay observed in the synthetic fuel-NO_x-air irradiations whose other results are discussed in the previous section. The experimental procedures, data analysis techniques, and results of the kinetic studies and analyses carried out in this program are discussed in the following sections.

A. DETERMINATION OF OH RADICAL RATE CONSTANTS

1. Experimental Procedures and Data Analysis

Hydroxyl radical rate constants were determined by a reactive rate technique in which the decay rates of the organic of interest (e.g., pyrrole, tetralin, n-tetradecane, etc.), and that of a reference organic whose OH radical rate constant is known are monitored under conditions where the organics are consumed primarily by reaction with OH radicals. In the case of the alkanes and the bicyclic aromatics, the data from the synthetic fuel-NO_x runs were employed, with 1,3,5-trimethylbenzene being used as the reference organic, and the chamber radical source and internal organic radical sources being used as the source of OH radicals. In the case of pyrrole, separate experiments were carried out in which OH radicals were generated by the photolysis of methylnitrite in air,

$$CH_3ONO + h\nu \rightarrow CH_3O + NO \qquad (24)$$

$$CH_3O + O_2 \rightarrow HCHO + HO_2 \qquad (25)$$

$$HO_2 + NO \rightarrow OH + NO_2 \qquad (26)$$

with propene being employed as the reference organic.

The analysis of the data was the same, regardless of which experimental technique was employed, provided that both the organic of interest (designated "organic" in the following discussion) and the reference organic (designated "reference") was consumed primarily by reaction with OH radicals, and that dilution was negligible (as was the case for all these experiments, since flexible Teflon reactors were employed). In this case, we can write

$$\frac{d[\text{organic}]}{dt} = -k_{org}[\text{organic}][OH] \qquad (XX)$$

and

$$\frac{d[\text{reference}]}{dt} = -k_{ref}[\text{reference}][OH] \qquad \text{(XXI)}$$

where k_{org} and k_{ref} are the rate constants for reactions of OH radicals with the organic of interest and the reference organic, respectively. The above equations can be rearranged, integrated, and combined to yield

$$\ln \frac{[\text{organic}]_{t_o}}{[\text{organic}]_t} = \frac{k_{org}}{k_{ref}} \ln \frac{[\text{reference}]_{t_o}}{[\text{reference}]_t} \qquad \text{(XXII)}$$

where $[\text{organic}]_{t_o}$ and $[\text{reference}]_{t_o}$ are the initial concentrations of the two organics, respectively, and $[\text{organic}]_t$ and $[\text{reference}]_t$ are their concentrations observed at time t. Hence plots of $\ln([\text{organic}]_{t_o}/[\text{organic}]_t)$ against $\ln([\text{reference}]_{t_o}/[\text{reference}]_t)$ should yield lines of slope k_{org}/k_{ref} and zero intercept. Since k_{ref} is known, k_{org} can thus be derived.

The experimental conditions and procedures employed in the synthetic fuel-NO_x-air experiments used to derive the kinetic data for the alkanes and bicyclic aromatics have been discussed in Section II. In order to determine the OH + pyrrole rate constant, CH_3ONO-pyrrole-propene-NO-air irradiations were carried out at 1 atmosphere pressure and 298 ± 1 K in an ~75-liter FEP Teflon cylindrical reaction bag surrounded by 24 GE F15T8-BL 15-watt blacklights (Reference 41). NO was included in the reaction mixture to minimize the formation of O_3 and NO_3 radicals, which otherwise could cause a significant amount of consumption of propene and pyrrole. In this work, eight of these blacklights were used, corresponding to a photolytic half-life of CH_3ONO of ~30 minutes. Prior to irradiation, the reaction bag/lamp assembly was covered to avoid any photolysis of the reactants. Pyrrole and propene were monitored before and during the irradiations by gas chromatography, using the techniques described in Section II-C-1).

2. Results for Pyrrole

The data obtained from irradiations of CH_3ONO-pyrrole-propene-NO-air irradiations are plotted in accordance with equation (XXII) in Figure 25. These data yield an excellent straight-line fit with, within one least-squares standard deviation, a zero intercept. The rate-constant ratio obtained from the slope of this plot by a least-squares analysis is $k_{org}/k_{ref} = 4.55 \pm 0.13$, where the indicated error limit is two standard deviations.

From the OH radical concentrations estimated from the observed propene decay rates, and the O_3 concentrations calculated from the light intensity and the $[NO_2]/[NO]$ ratios using equation (IV) in Section III-A-2, it was calculated that under the experimental conditions employed the O_3 reactions contributed $<<$ 1 percent of the OH radical reaction for both propene and pyrrole. Similarly, for the NO and NO_x concentrations and the observed light intensities employed in these irradiations, it was calculated that $O(^3P)$ atom reaction contributed $\lesssim$ 1 percent of the OH radical reaction for propene and $\lesssim$ 4 percent for pyrrole [assuming, in the absence of experimental data, an upper limit rate constant of 1×10^{-10} cm^3 $molecule^{-1}$ sec^{-1} for the reaction of $O(^3P)$ atoms with pyrrole]. Thus the assumptions implicit in the derivation of Equation (XXII) appear to be valid for this system.

The rate constant ratio k_{org}/k_{ref} can be placed on an absolute basis by using a rate constant for the reaction of OH radical with propene of $k_{ref} = 2.63 \times 10^{-11}$ cm^3 $molecule^{-1}$ sec^{-1} (Reference 42) yielding

$$k_{org} = (1.20 \pm 0.04) \times 10^{-10} \text{ cm}^3 \text{ molecule}^{-1} \text{ sec}^{-1}$$

at $295 \pm 1^{\circ}K$ and 1 atmosphere total pressure, where the indicated error is two least squares standard deviations and does not take into account any errors in the value of k_{ref} used.

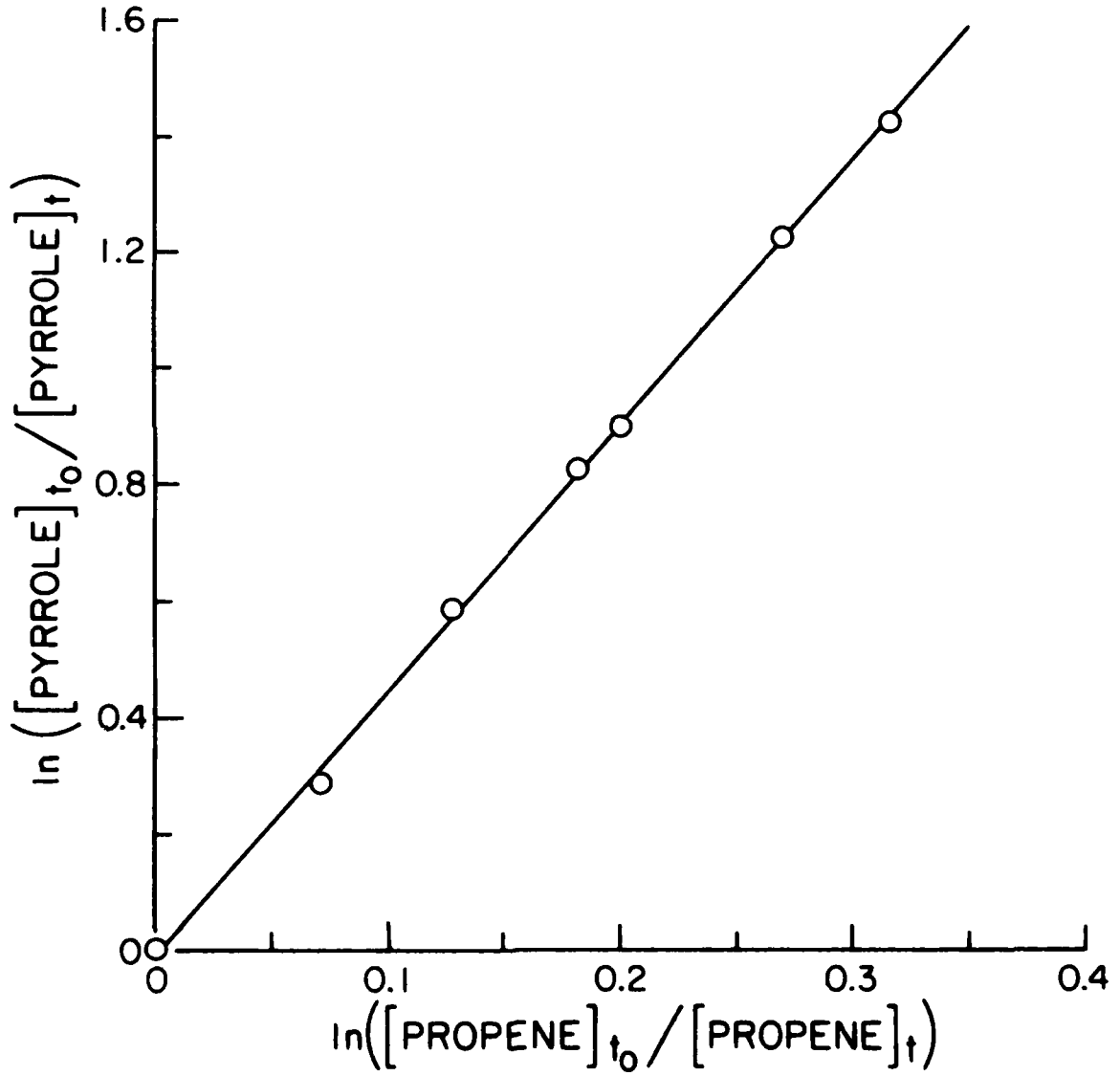

Figure 25. Plot of Equation (XXII) for the Reaction of OH Radicals with Pyrrole and Propene.

3. Results for the Synthetic Fuel Constituents

The data obtained from the 10 synthetic fuel-NO_x-air experiments were used to obtain estimates for the OH radical rate constants for ethylcyclohexane, n-tetradecane, tetralin, and the naphthalenes present in those fuels. However, the kinetic data were of much lower precision than those from the CH_3ONO-pyrrole-propene-NO-air experiments. This is attributed to the greater difficulty in precise monitoring of the higher molecular weight compounds present in these synthetic fuels, and to the fact that the OH radical levels were lower in these experiments than is the case with those employing CH_3ONO, which means that less of the organics are consumed. However, the data were of sufficient quality to at least obtain a preliminary estimate of the rate-constant ratios.

The data were analyzed by carrying out a least-squares regression in accordance with equation (XXII) for each compound of interest, with 1,3,5-trimethylbenzene as the reference organic, and with a separate regression being calculated for each run and (in the case of tetralin, where two GC analysis techniques were employed) for each analysis technique. The slopes and (1 σ) standard deviations obtained are summarized in Table 11. In most cases the intercepts of these regressions were within two standard deviations of zero. As indicated by equation (XXII), the slopes are equated with the OH radical rate constant ratios for the compounds of interest, relative to the 1,3,5-trimethylbenzene reference organic. The rate constant ratios, obtained by weighed least squares analysis of the ratios from the individual runs and (for tetralin) analysis techniques, are also given in Table 11.

The rate constants can be placed on an absolute basis using the accepted (Reference 18) literature value of 6.2×10^{-11} cm^3 $molecule^{-1}$ sec^{-1} for 1,3,5-trimethylbenzene. The resulting absolute rate constants (with indicated errors being two standard deviations of the weighed average, not reflecting uncertainties in the OH + 1,3,5-trimethylbenzene rate constant) are summarized in Table 12. Also shown in Table 12 is the literature value for the OH + naphthalene rate constant (the only one for which literature data are available) and the OH ethylcyclohexane and

TABLE 11. OH RADICAL RATE CONSTANT RATIOS DERIVED FROM THE RESULTS OF THE SYNTHETIC FUEL-NO_x-AIR IRRADIATIONS.

ITC run no.	Rate constant ratio relative to 1,3,5-trimethylbenzene[a]						
	Tetralin[b]	Tetralin[c]	Naphthalene	2-Methyl-naphthalene	2,3-Dimethyl-naphthalene	Ethyl-cyclohexane	n-tetradecane
781	0.59 ± 0.03	0.61 ± 0.06	0.45 ± 0.09	1.19 ± 0.05	2.16 ± 0.10	0.19 ± 0.01	0.40 ± 0.06
784	0.73 ± 0.03	0.66 ± 0.13	0.70 ± 0.15	1.54 ± 0.14	2.14 ± 0.21	0.18 ± 0.03	0.46 ± 0.10
785	0.61 ± 0.02	0.58 ± 0.10	0.29 ± 0.07	0.83 ± 0.11	1.47 ± 0.14	0.44 ± 0.14	0.39 ± 0.14
786	0.63 ± 0.12	0.83 ± 0.92	0.58 ± 0.10	1.09 ± 0.32	1.79 ± 0.20	0.23 ± 0.07	0.45 ± 0.19
788	0.66 ± 0.07	0.40 ± 0.06	0.25 ± 0.03	0.64 ± 0.09	1.29 ± 0.13	0.58 ± 0.04	0.28 ± 0.05
795	0.63 ± 0.04	0.59 ± 0.13	0.38 ± 0.06	1.03 ± 0.13	1.80 ± 0.18	0.30 ± 0.06	0.36 ± 0.03
796	0.70 ± 0.05	0.74 ± 0.12	0.47 ± 0.08	1.25 ± 0.05	2.27 ± 0.17	0.32 ± 0.06	0.46 ± 0.09
799	0.73 ± 0.08	0.74 ± 0.12	0.34 ± 0.07	1.15 ± 0.11	2.57 ± 0.24	0.28 ± 0.10	0.54 ± 0.06
801	0.59 ± 0.03	0.52 ± 0.07	0.39 ± 0.06	-	1.87 ± 0.33	0.26 ± 0.09	-0.13 ± 0.08
805	0.78 ± 0.07	0.31 ± 0.09	0.23 ± 0.04	0.26 ± 0.29	1.09 ± 0.34	0.63 ± 0.13	0.28 ± 0.06
Weighed Average	0.62 ± 0.09		0.31 ± 0.10	1.13 ± 0.23	1.85 ± 0.40	0.23 ± 0.11	0.34 ± 0.15

[a]Indicated errors are single standard deviations.

[b]Tetralin data from the "DB-5C" capillary GC system with syringe sampling.

[c]Tetralin data from the "SP C-II," GC system with Tenax tube sampling.

TABLE 12. SUMMARY OF OH RADICAL RATE CONSTANTS OBTAINED FROM THE SYNTHETIC FUEL EXPERIMENTS.

Compound	$k_{org} \times 10^{12}$ (cm^3 $molecule^{-1}$ sec^{-1}		
	This work	Literature[a]	Calculated[b]
Tetralin	38 ± 11		
Naphthalene	19 ± 12	24 ± 2	
2-Methylnaphthalene	70 ± 29		
3,3-Dimethylnaphthalene	115 ± 25		
Ethylcyclohexane	14 ± 14		11
n-Tetradecane	21 ± 19		18

[a]From Reference 28.

[b]Calculated from group rate constants derived from existing data on OH + alkanes derived by Atkinson et al. (Reference 29).

n-tetradecane rate constants calculated using the estimation technique derived previously by Atkinson et al. (Reference 29), based on the existing large data base of OH + alkane rate constants. Considering the relatively large uncertainties associated with our data, the agreement between our value and the literature value for naphthalene and our values and the estimated values for the alkanes is surprisingly good, and suggest we may be overestimating our error limits. In terms of which values of rate constants are appropriate to use for model calculations and data analysis, it is clear that the literature value for naphthalene is much more precise than that obtained here, and the calculated values for the alkanes should also be considered more precise and thus are preferred. However, for tetralin and the methylnaphthalenes, ours are the only values available, and these can be used until more precise data are obtained.

B. DETERMINATION OF THE O_3 + PYRROLE RATE CONSTANT

The rate constant for the reaction of O_3 with pyrrole was obtained by measuring the enhanced rate of decay of O_3 in the presence of known excess concentrations of pyrrole in one atmosphere of air. Under these conditions, the reactions removing O_3 are

$$O_3 + \text{wall} \rightarrow \text{loss of } O_3 \tag{27}$$

$$O_3 + \text{pyrrole} \rightarrow \text{products} \tag{28}$$

and hence

$$-d[O_3]/dt = k_w + k_{O_3}[\text{pyrrole}][O_3] \tag{XXIII}$$

where k_w and k_{O_3} are the rate constants for reactions (1) and (2), respectively. With the pyrrole concentration being in large excess over the initial O_3 concentration ($[\text{pyrrole}]/[O_3]_{\text{initial}} \geq 10$), the reactant concentration remained essentially constant throughout the reaction, and Equation (XXIII) may be rearranged to yield:

$$-d\ln[O_3]/dt = k_w + k_{O_3}[\text{pyrrole}] \tag{XXIV}$$

Thus, from the dependence of the ozone decay rate, $-d\ln[O_3]/dt$, on the pyrrole concentration, and with a knowledge of k_w, the background ozone decay rate, the rate constant k_{O_3} may be readily obtained.

As described previously (Reference 30), reactions were carried out in an ~175-liter volume Teflon bag, constructed out of a 2-mil thick (180 by 140 cm) FEP Teflon sheet, heat-sealed around the edges and fitted with Teflon injection and sampling ports at each end of the bag. The reaction bag was initially divided into two subchambers, with O_3 being injected into one subchamber and pyrrole into the other. The reactions were initiated by removing the bag divider and rapidly mixing the contents of the bag by pushing down on alternate sides of the entire bag for ~1 minute. Initial O_3 concentrations after mixing were typically ~1 ppm and, after mixing of the reactants, the O_3 concentrations were monitored as a

function of time by a Monitor Labs Model 8410 chemiluminescence ozone analyzer. Background ozone decay rates in the absence of the reactants were determined during these rate-constant determinations, and were ~3 x 10^{-6} sec^{-1}. Pyrrole was quantitatively monitored in the reaction bag by gas chromatography as described in Section III-C-1.

In all cases, the O_3 decays monitored in the presence of varying concentrations of pyrrole were exponential, within the experimental error limits. As shown in Figure 26, these O_3 decay rates increased linearly with the pyrrole concentrations, in accordance with equation (XXIV). The rate constant k_{O_3} obtained from the slope of this plot by a least-squares analysis is

$$k_{O_3} = (1.57 \pm 0.20) \times 10^{-17} \text{ cm}^3 \text{ molecule}^{-1} \text{ sec}^{-1}$$

where the indicated error is two least-squares standard deviations of the slope of Figure 26 combined with an estimated 10 percent overall uncertainty in the pyrrole concentrations.

C. DETERMINATION OF NO_3 RADICAL RATE CONSTANTS FOR FURAN, THIOPHENE, AND PYRROLE

1. Experimental Technique and Data Analysis

The experimental technique used for the determination of NO_3 radical reaction rate constants was a relative rate method which has been described in detail previously (References 43-45). This technique is analogous to that described above for OH radicals, and is based upon monitoring the relative decay rates of a series of organics, including at least one organic whose NO_3 radical reaction rate constant is reliably known, in the presence of NO_3 radicals. NO_3 radicals were generated by the thermal decomposition of N_2O_5 in air:

$$N_2O_5 \xrightarrow{M} NO_2 + NO_3 \qquad (29)$$

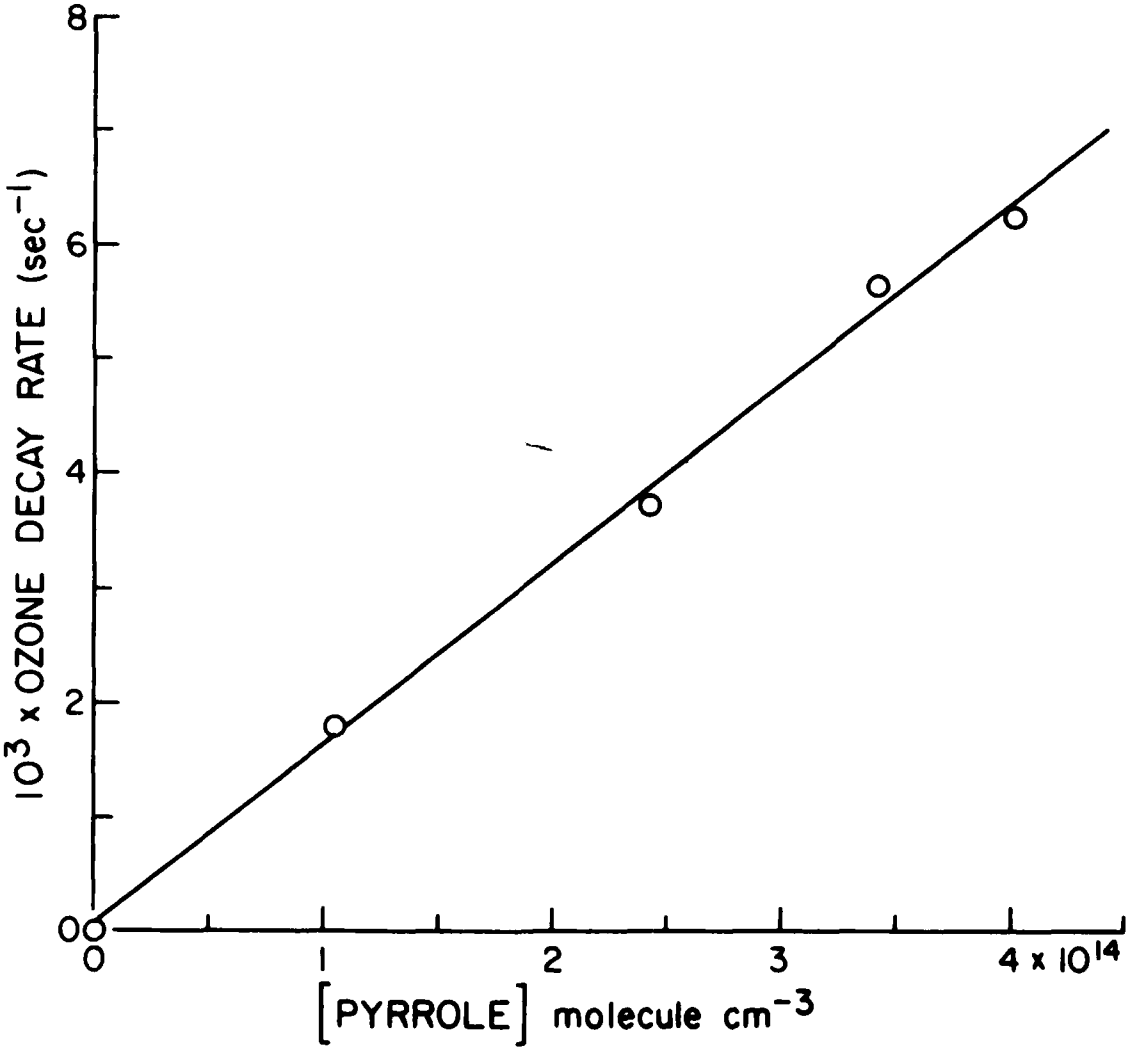

Figure 26. Plot of Equation (XXIV) for the Reaction of O_3 with Pyrrole.

$$NO_2 + NO_3 \xrightarrow{M} N_2O_5 \qquad (30)$$

Providing that furan, thiophene, and pyrrole and the reference organics reacted only with NO_3 radicals (see below),

$$NO_3 + \text{heterocycle} \rightarrow \text{products} \qquad (31)$$

$$NO_3 + \text{reference organic} \rightarrow \text{products} \qquad (32)$$

then (References 43-45)

$$\ln \frac{[\text{heterocycle}]_{t_o}}{[\text{heterocycle}]_t} - D_t = \frac{k_{31}}{k_{32}} \ln \frac{[\text{reference organic}]_{t_o}}{[\text{reference organic}]_t} - D_t \qquad \text{(XXV)}$$

where $[\text{heterocycle}]_{t_o}$ and $[\text{reference organic}]_{t_o}$ are the concentrations of the heterocycle and the reference organic, respectively, at time t_o, $[\text{heterocycle}]_t$ and $[\text{reference organic}]_t$ are the corresponding concentrations at time t, k_{31} and k_{32} are the NO_3 radical rate constants for reactions (31) and (32), respectively, and D_t is the dilution factor at time t, due to the small amounts of dilution occurring from the incremental additions of N_2O_5 to the reactant mixtures. [During these experiments, the dilution factor D_t was typically 0.0015 (i.e., ~0.15 percent) per N_2O_5 addition.] Hence plots of $[\ln([\text{heterocycle}]_{t_o}/[\text{heterocycle}]_t)-D_t]$ against $[\ln([\text{reference organic}]_{t_o}/[\text{reference organic}]_t)-D_t]$ should yield straight lines of slope k_{31}/k_{32} and zero intercepts.

With this experimental technique, the initial concentrations of the heterocycles and the reference organics were ~1-4 ppm, and up to five incremental amounts of N_2O_5 [~(0.1-3) ppm per addition] were added to the chamber during an experiment. In order to extend the reaction times beyond the mixing time, 2-10 ppm of NO_2 were also included in the reaction mixtures to drive the equilibrium between NO_3 radicals, NO_2, and N_2O_5 towards N_2O_5.

These rate-constant determinations were carried out at 295 ± 1°K and atmospheric pressure (~735 torr) in a ~4000-liter all-Teflon chamber, with dry purified matrix air as the diluent gas. As described previously (References 43-45), N_2O_5 was prepared by the method of Schott and Davidson (Reference 46). Known pressures of N_2O_5 (as measured by an MKS Baratron capacitance manometer) in 1-liter Pyrex bulbs were flushed into the chamber for 3 minutes by a 2-liter min^{-1} flow of N_2 (≥ 99.995 percent purity level), with simultaneous rapid stirring by a fan rated at 300 liters sec^{-1}.

The heterocyclics and the reference organics were quantitatively monitored during the experiments by GC-FID. Propene and the heterocyclics were monitored as discussed in Section II-C-1, with the analysis for trans-2-butene and 2-methyl-2-butene being carried out using the same system as employed for furan and thiophene (Section II-C-1).

Furan, thiophene, and pyrrole were obtained from the Aldrich Chemical Company, with stated purity levels of ≥ 99 percent, ≥ 99 percent, and 98 percent, respectively. No impurities were observed by GC-FID analyses.

2. Results

The technique described above was employed using trans-2-butene as the reference organic for furan, using 2-methyl-2-butene for pyrrole, and using both trans-2-butene and propene for thiophene. In all cases, duplicate experiments were carried out with differing initial NO_2 concentrations, to assure that the reaction was indeed with NO_3 and not NO_2 or N_2O_5 (see below). The data obtained for furan and thiophene using trans-2-butene as the reference organic and plotted in accordance with equation (XXV) in Figures 27, and the data obtained for pyrrole with 2-methyl-2-butene as the reference organic are plotted in Figure 28. Because of the small amounts of thiophene consumed (< 7 percent) during the initial experiments using trans-2-butene as the reference organic, a further set of experiments for thiophene were carried out using propene as the reference organic, and the data from these experiments are plotted in Figure 29.

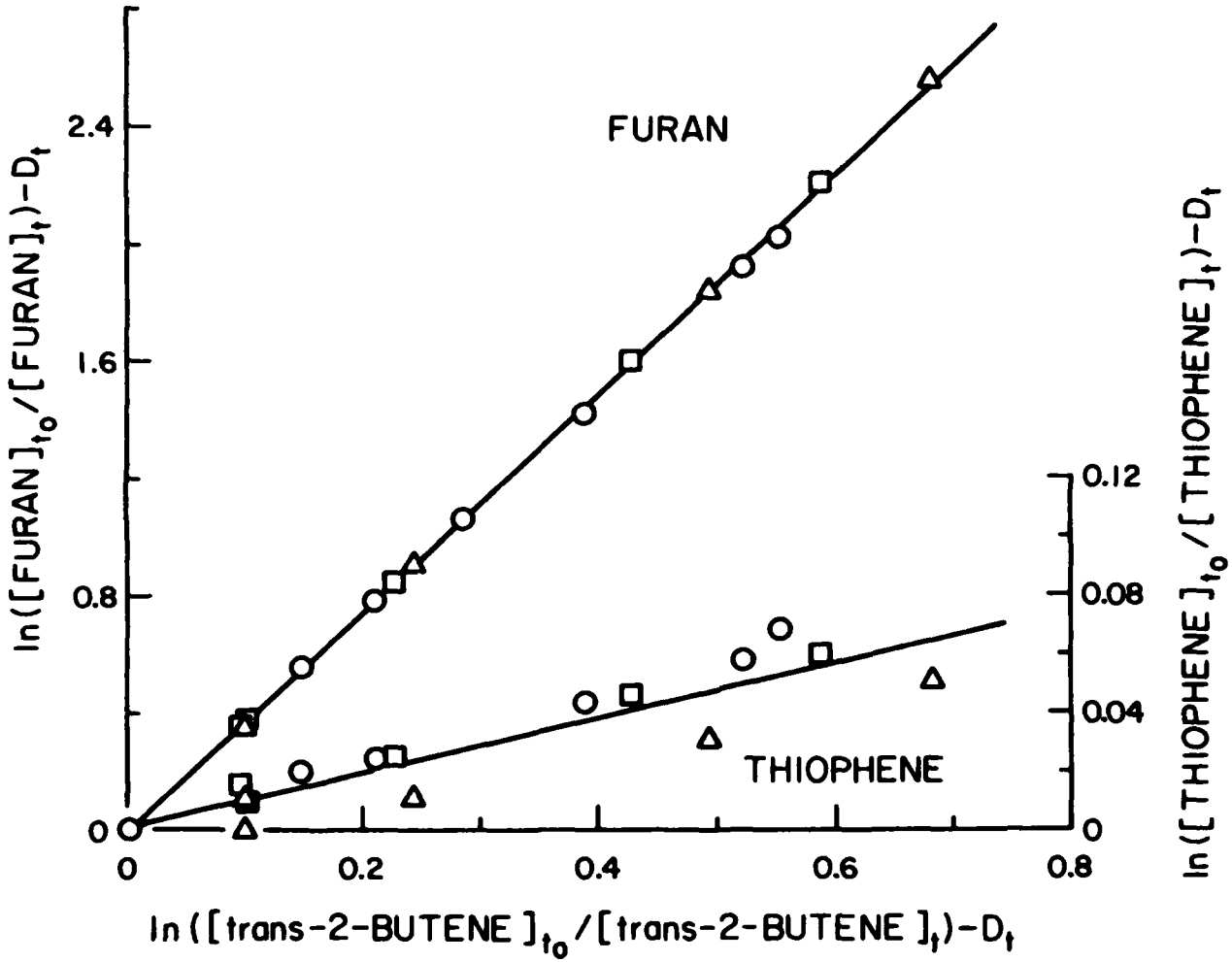

Figure 27. Plot of Equation (XXV) for Furan and Thiophene, with trans-2-Butene as the Reference Organic (Initial NO_2 Concentrations: ○ - 5 ppm; △ - 2 ppm; □ - 8 ppm).

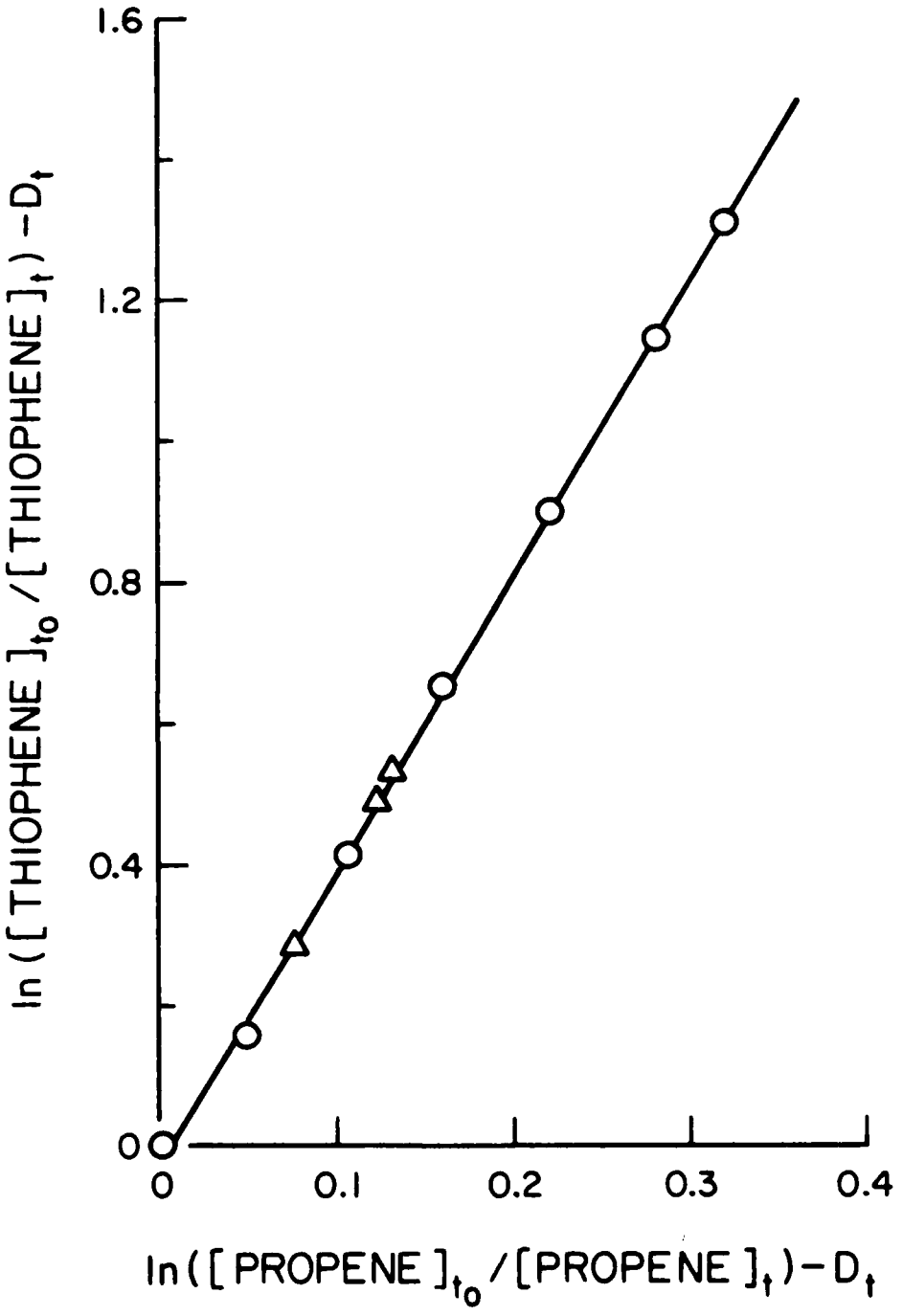

Figure 28. Plot of Equation (XXV) for Pyrrole, with 2-Methyl-2-butene as the Reference Organic (Initial NO_2 Concentrations: ○ - 5 ppm; △ - 10 ppm).

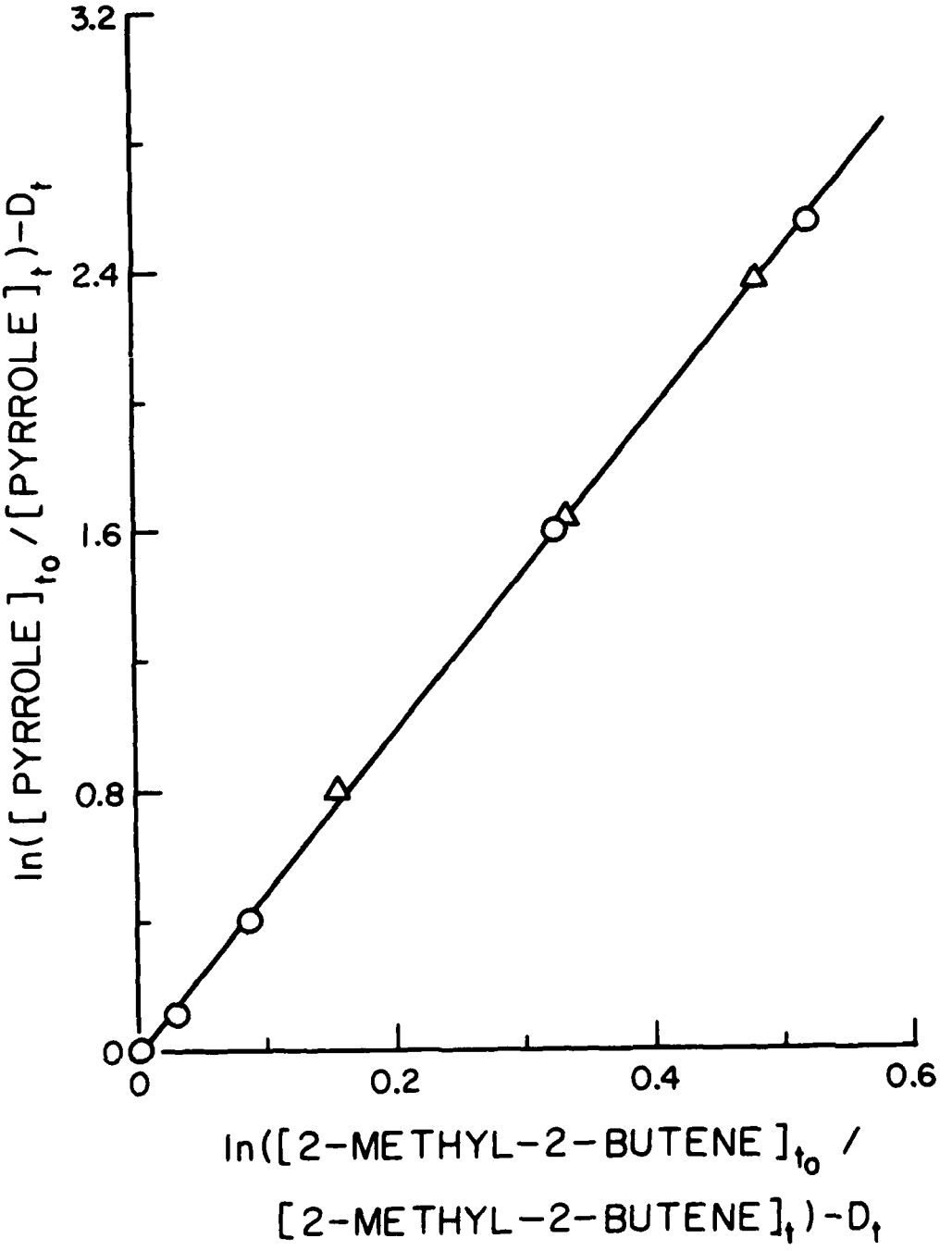

Figure 29. Plot of Equation (XXV) for Thiophene, with Propene as the Reference Organic (Initial NO_2 Concentrations: ○ - 4 ppm, △ - 2 ppm).

The rate constant ratios k_{31}/k_{32} obtained by the least squares analyses according to equation (XXV) are summarized in Table 13. In all cases the least squares intercepts of these plots were within three standard deviations of zero. These rate constants can be placed on a more absolute basis using the published rate constants, k_{32}, for propene, trans-2-butene, and 2-methyl-2-butene (References 43 and 44), but it should be noted that these values are still linearly dependent on the value used for the equilibrium constant for the reactions $NO_2 + NO_3 \rightleftarrows N_2O_5$. In this work we use our recently determined equilibrium constant of 3.4×10^{-11} cm^3 $molecule^{-1}$ at 298°K (Reference 47), which is a factor of 1.8 higher than that given by Malko and Troe (Reference 48). The rate constants k_{31} so obtained are also given in Table 13.

In previous studies the reference organics propene, trans-2-butene, and 2-methyl-2-butene have been shown to react with NO_3 radicals, and not with N_2O_5 (References 44 and 49). Since the $[N_2O_5]/[NO_2]$, and hence the $[N_2O_5]/[NO_3]$, ratios were varied by factors of 2-4 in the present study, the excellent straight line plots in Figures 27-29 show that furan, thiophene, and pyrrole also react with NO_3 radicals, and not with N_2O_5. Furthermore, no observable decays of these heterocycles ($< 5 \times 10^{-4}$ min^{-1}) were observed in the presence of 2-10 ppm of NO_2, showing that no significant dark reaction of NO_2 with these organics occurs. This was also confirmed by the excellent agreement of the sets of data obtained at differing initial NO_2 concentrations (Figures 27-29).

TABLE 13. RELATIVE RATE CONSTANT RATIOS k_3/k_4 AND RATE CONSTANTS k_3 FOR THE REACTION OF NO_3 RADICALS WITH FURAN, THIOPHENE, AND PYRROLE AT 295 ± 1°K AND ATMOSPHERIC PRESSURE.

	k_{28}/k_{29}[a]				
Heterocycle	Propene	Relative to *trans*-2-Butene	2-Methyl-2-butene	k_{28} (cm^3 $molecule^{-1}$ sec^{-1})[b]	
Furan		3.72 ± 0.05		$(1.4 \pm 0.2) \times 10^{-12}$	
Thiophene	4.14 ± 0.09	0.092 ± 0.023		$(3.1 \pm 0.7) \times 10^{-14}$[c] $(3.5 \pm 1.0) \times 10^{-14}$[d]	$(3.2 \pm 0.7) \times 10^{-14}$[e]
Pyrrole			4.92 ± 0.09	$(4.9 \pm 1.1) \times 10^{-11}$	

[a] Indicated errors are two least-squares standard deviations derived from the slopes of the plots shown in Figures 1-3.

[b] Based upon an equilibrium constant for the reactions $NO_2 + NO_3 \rightleftharpoons N_2O_5$ of $2.4 \times 10^{-27} (T/300)^{0.32} e^{11080/T}$ cm^3 $molecule^{-1}$ (References 47 and 48). The indicated errors are two least squares standard deviations and take into account the errors in the rate constants k_{29} of: $(7.6 \pm 1.6) \times 10^{-15}$ cm^3 $molecule^{-1}$ sec^{-1} for propene; $(3.80 \pm 0.43) \times 10^{-13}$ cm^3 $molecule^{-1}$ sec^{-1} for *trans*-2-butene and $(9.9 \pm 2.2) \times 10^{-12}$ cm^3 $molecule^{-1}$ sec^{-1} for 2- methyl-2- butene (References 43 and 44).

[c] Relative to propene.

[d] Relative to *trans*-2-butene.

[e] Weighted average.

SECTION V

CONCLUSIONS

As indicated in Section I, the major purpose of the research discussed in this report was to obtain data required to develop and test computer kinetic models for atmospheric reactions of jet fuels of varying composition. Thus the final conclusions of this two-phase study will not be known until the second phase, model development and testing, is completed. However, the experimental data obtained thus far allow us to draw some conclusions concerning the relative reactivities of the various representative fuel constituents studied and the general classes of compounds they are taken to represent. In addition, preliminary conclusions can be drawn concerning the atmospheric reactions of furan, thiophene, and pyrrole. Finally, the synthetic fuel experiments, while carried out primarily for model testing purposes, also allow us to draw some qualitative conclusions concerning the effects of composition on reactivity in NO_x-air photo oxidations. These conclusions are briefly summarized below.

The results of the single compound-NO_x-air irradiations indicate that there is a wide range of reactivity among the various alkane and aromatic fuel constituents, not all of which can be attributed to differences in their OH radical rate constants. In particular, relatively little O_3 is formed in alkane-NO_x-air experiments, and in no case was O_3 maxima obtained despite the relatively high OH radical rate constants for these compounds and the high hydrocarbon/NO_x ratios employed. On the other hand, experiments employing the alkylbenzenes exhibit high reactivity, achieving O_3 maxima in relatively short periods despite much lower hydrocarbon/NO_x ratios employed. These differences are not due to differences in efficiencies in converting NO to NO_2, since the data from our experiments show that all of the compounds studied are not greatly different in this regard. Rather, the differences are due primarily to differences among the organics in their effects on radical levels, with the alkanes tending to remove radicals in their initial photo oxidation reactions, and

the alkylbenzenes tending to form products which act as photoinitiators in enhancing radical levels. Higher radical levels cause the organic to be consumed more rapidly, which in turn causes more rapid conversion of NO to NO_2, and thus more rapid formation of O_3.

While more reactive than the alkanes, benzene has been shown to be considerably less reactive than the methylbenzenes, even after its relatively low OH radical rate constant is taken into account. In particular, the results of the benzene-NO_x-air experiments indicate that the presence of benzene tends to suppress, rather than enhance, radical levels in these systems, though not to as large an extent as is the case for the alkanes. In addition, there is some indication that the suppression of radical levels decreases with time, suggesting the formation of a photoreactive product. The lower reactivity of benzene can be attributed to the fact that it cannot form methylglyoxal, which is believed to be the major radical source in NO_x-air photooxidations of toluene and the xylenes (References 12, 15-17), but it is necessary to assume that benzene forms other photoreactive products in order for model calculations to fit results of benzene-NO_x-air experiments (Reference 38).

Before this study, no data were available concerning the reactivities of compounds such as tetralin and naphthalenes in NO_x-air irradiations. Despite its similarity to o-xylene in its substitution around the aromatic ring, tetralin more closely resembles benzene in its reactivity, since it has a greater tendency to remove radicals from the system than to form photoreactive products. The naphthalenes are also much less reactive than the alkylbenzenes, and their photooxidations involves both radical removal and radical initiation processes, the former being more important early in the experiment, and the latter being more important later, presumably after the concentrations of their photoreactive product(s) have built up. Since little else is known concerning the details of the NO_x-air photo oxidation of these compounds, or concerning the identities and reactions of the products formed, any model developed to represent their photo oxidations will have to be primarily empirical in nature, but, at a minimum, the model will have to take these observations into account.

The results of the experiments with the three synthetic fuels are qualitatively consistent with the relative reactivities of the individual fuel components derived from the single component runs. As expected, increasing the total aromatic/alkane ratio increases the rate at which O_3 is formed in the fuel-NO_x-air irradiations, and this can be attributed both to the increased formation of radical initiators from the higher level of alkylbenzenes and to the reduced rates of removal of radicals from the photo oxidation of the lower level of alkanes. On the other hand, increasing the aromatics also tends to reduce the maximum O_3 yields formed in the fuel-NO_x-air irradiations. This simultaneous enhancement of reaction rates and suppression of O_3 yields caused by increased levels of aromatics has been observed previously in both experiments and computer model calculations (References 33 and 40), and is attributed to enhanced NO_x sinks in the photo oxidation of the aromatics, since the ultimate yield of O_3 formed in these systems is limited by the availability of NO_x, which is required for O_3 formation.

Increasing the alkylbenzene/bicyclic aromatic ratio in the fuel, while holding the total aromatics/alkanes ratio constant, increases both the rate of O_3 formation and the maximum O_3 yield. The increased rate of O_3 formation is expected, since the single component runs indicated that the bicyclic aromatics, whose levels are reduced, have much less of a tendency to form radical initiators in the system than do the alkylbenzenes, whose levels are increased. In view of the fact that previous experiments (References 33 and 40) indicated that increasing levels of alkylbenzenes in multicomponent-NO_x-air irradiations suppress maximum O_3 yields, the increase in O_3 yields when they are increased in this fuel is somewhat unexpected, and suggest that this increase in O_3 is due primarily to the fact that the levels of bicyclic aromatics were reduced. Thus, it can be concluded that the presence of bicyclic aromatics in these fuels tend to reduce the maximum yields of O_3 that can be formed to an even greater extent than do the alkylbenzenes, indicating that NO_x sinks in atmospheric photo-oxidations of the bicyclic aromatics are even more important than is the case for the alkylbenzenes.

This study has obtained, for the first time, data concerning the atmospheric reactions of the heterocyclic compounds furan, thiophene, and pyrrole. The O_3 and OH and NO_3 radical rate constants measured in this program, when taken with those determined previously from these laboratories for furan and thiophene (Reference 30) show that the heterocyclics, especially furan and thiophene, react relatively rapidly with these reactive atmospheric species. The rate constants for these compounds are summarized in Table 14, together with their corresponding atmospheric lifetimes under clean tropospheric conditions. [Ozone, daytime OH radical, and nighttime NO_3 radical concentrations were taken from References 50-52, and the daytime NO_3 concentrations were calculated, assuming an upper limit, moderately "clean" tropospheric NO_2 concentration of 500 ppt (Reference 53).] Table 14 shows that, as is the case with the other fuel constituents studied in this program, reaction with OH radicals is the major daytime removal process for these compounds (and is thus their major removal process in our environmental chamber experiments), but at night reaction with NO_3 can be an important, if not dominant, removal process for these heterocyclic organics.

Even after taking their relatively high OH radical rate constants into account, furan and pyrrole were found to be extremely reactive in NO_x-air irradiations, and addition of only small amounts (less than 2 percent on a mole carbon basis) to the fuels markedly enhanced the rate at which O_3 was formed in fuel-NO_x-air irradiations. This is because the presence of these compounds dramatically increases OH radical levels, even more so than do the alkylbenzenes, probably due to the formation of highly photoreactive products. If such products are formed, they must react and be removed from the system extremely rapidly, since in furan-NO_x-air and pyrrole-NO_x-air experiments, the system is essentially "dead" after the initially present heterocycle has reacted, behaving like a NO_x-air irradiation. Most other relatively reactive organics, such as aromatics or alkenes, form products which are sufficiently long-lived that their reactions will cause NO oxidation and O_3 formation to continue after the parent organic is consumed.

TABLE 14. RATE CONSTANTS AND ATMOSPHERIC LIFETIMES FOR FURAN, THIOPHENE, AND PYRROLE.

	Furan	Thiophene	Pyrrole
Rate Constant[a] (cm^3 $molecule^{-1}$ sec^{-1})			
O_3	2.4×10^{-18}	$<6 \times 10^{-20}$	1.6×10^{-17}
OH	4.0×10^{-11}	9.6×10^{-12}	1.2×10^{-10}
NO_3	1.4×10^{-12}	3.2×10^{-14}	4.9×10^{-11}
Daytime Lifetime (1/e)			
O_3 (30 ppb)[b]	6.7 days	>0.7 yr	24 hr
OH (1×10^6 cm^{-3})[c]	6.9 hr	29 hr	2.3 hr
NO_3 (0.037 ppt)[d]	9.3 days	1.1 yr	6.4 hr
Nighttime Lifetime			
NO_3 (10 ppt)[e]	50 min	36 hr	1.4 min

[a] O_3 and OH radical rate constants for furan and thiophene from Reference 30; other values from this study (Section IV).

[b] Value appropriate for clean troposphere (Reference 50).

[c] Value appropriate for clean troposphere (Reference 51).

[d] Value calculated assuming an upper limit value of 0.5 ppb of NO_2 for the moderately clean troposphere (e.g., Reference 53), using the rate constants given in Reference 14. NO_3 photolysis rates calculated for a solar zenith angle of 40^o.

[e] Representative level observed in the moderately clean troposphere (Reference 52).

The presence of furan or pyrrole in the fuels, while increasing the rate of O_3 formation, also tends to suppress the maximum amount of O_3 which can be formed. This result is analogous to the effect of increasing aromatic levels in the fuels, and indicates that, in addition to enhancing radical levels, the presence of these compounds may also enhance NO_x removal rates.

Thiophene, which is comparable in reactivity to toluene in NO_x-air irradiations, also appears to involve the formation of photoreactive product(s) in its photooxidation mechanism, as indicated by radical levels observed in thiophene-NO_x-air irradiations. It is much less reactive than furan and pyrrole, and has a much smaller effect on fuel-NO_x-air irradiations when included as 2 percent of the fuel, and this can be attributed primarily to its lower OH radical rate constant. However, it is also possible that the photoreactive product(s) formed from thiophene react more slowly than those formed from furan and pyrrole, since total radical initiation rates in thiophene-NO_x-air irradiations rise relatively slowly but continuously with time (as shown by Figure 17 in Section III-B-3). If the photoreactive product(s) reacted rapidly, one would expect a rapid initial increase in radical initiation rates, followed by a leveling off at a relatively constant level as the intermediate(s) achieve steady state. Model calculations will be useful in exploring this possibility.

The foregoing observations provide insights concerning the atmospheric chemistry of representatives of the major classes of compounds present, or anticipated to be present, in current or future turbine engine fuels and allow us to make qualitative statements concerning effects of composition on the atmospheric reactivity of these fuels. However, in order to make quantitative predictions concerning the effects of changes in composition on fuel reactivity, or to make predictions of atmospheric impacts of fuel releases under conditions more representative of the "real world" than those found in environmental chamber experiments, model calculations are required, and development of such models is the ultimate goal of this program.

We believe that the experiments carried out in this first phase of this program, when combined with results of previous laboratory and

environmental chamber studies, provide a sufficient data base to allow initiation of the development of a predictive model for the atmospheric reactivities of present and future turbine engine fuels. In particular, this program has given us data, which have not been available previously, concerning the atmospheric reactivities of representative bicyclic aromatics and heterocyclic organics. In many respects the chemistry of these compounds was found to be quite different than was expected based on results for previously studied compounds. In the case of the alkanes, where the chamber radical source has been shown to have a dominant impact on the results of the experiments, we have carried out experiments under conditions such that the radical source was directly measured for each experiment. This has not been the case in previous studies with these compounds. This will allow more comprehensive testing of models for these compounds. In the case of the alkylbenzenes, while there have been a number of studies on the atmospheric reactions of toluene and more limited studies on some of the xylenes, our experiments on the homologous series benzene, toluene, m-xylene, and mesitylene constitute the first systematic study of the effect of substitution around the aromatic ring on the atmospheric reactivity of this important class of compounds, whose photo-oxidation mechanisms are highly uncertain.

In short, although significant uncertainties remain, we now have a much broader data base concerning the atmospheric reactions of representative constituents and potential impurities of turbine engine fuels than has been the case previously. Without these data, meaningful development of predictive models for the atmospheric impacts of releases of these fuels would not be possible.

REFERENCES

1. Clewell, H.J., III, Fuel Jettisoning U. S. Air Force Aircraft, Volume 1, Summary and Analysis, ESL-TR-80-17, Engineering and Services Laboratory, Air Force Engineering and Services Center, Tyndall AFB, Florida, March 1980.

2. Conkle, J.P., Lackey, W.W., Martin, C.L., and Richardson, A., III, Organic Compounds in the Exhaust of a J85-5 Turbine Engine, Report No. SAM-TR-80-29, September 1980.

3. Churchill, A.V., Delaney, C.L., and Lander, H.R., "Future Aviation Turbine Fuels," Paper No. 78-268, presented at American Institute of Aeronautics and Astronautics 16th Aerospace Sciences Meeting, Huntsville, Alabama, 16-18 January 1978.

4. Bouble, R.W. and Martone, J.A., USAF Aircraft Engine Emission Goal: An Initial Review, ESL-TR-79-30, Engineering and Services Laboratory, Air Force Engineering and Services Center, Tyndall AFB, Florida, September 1979.

5. Scott, A.H., Jr., The Implications of Alternative Aviation Fuels on Airbase Air Quality, ESL-TR-80-38, Engineering and Services Laboratory, Air Force Engineering and Services Center, Tyndall AFB, Florida, August 1980.

6. Carter, W.P.L., Ripley, P.S., Smith, C. G., and Pitts, J.N., Jr., Atmospheric Chemistry of Hydrocarbon Fuels, ESL-TR-81-53, Engineering and Services Laboratory, Air Force Engineering and Services Center, Tyndall AFB, Florida, November 1981.

7. Winer, A.M., Atkinson, R., Carter, W.P.L., Long, W.D., Aschmann, S.M., and Pitts, J.N., Jr., High Altitude Jet Fuel Photochemistry, ESL-TR-82-38, Engineering and Services Laboratory, Air Force Engineering and Services Center, Tyndall AFB, Florida, October 1982.

8. Sickles, J.E., II, Eaton, W.C., Ripperton, L.A., and Wright, R.S., Literature Survey of Emissions Associated with Emerging Energy Technologies, EPA-600/7-77-104, 1977.

9. Falls, A.H. and Seinfeld, J.H., "Continued Development of a Kinetic Mechanism for Photochemical Smog," Environ. Sci. Technol., vol 12, pp. 1398-1406, 1978.

10. Hendry, D.G., Baldwin, A.C., Barker, J.R., and Golden, D.M., Computer Modeling of Simulated Photochemical Smog, EPA-600/3-78-059, June 1978.

11. Carter, W.P.L., Lloyd, A.C., Sprung, J.L., Pitts, J.N., Jr., "Computer Modeling of Smog Chamber Data: Progress in Validation of a Detailed Mechanism for the Photooxidation of Propene and n-Butane in Photochemical Smog," Int. J. Chem. Kinet., vol 11, pp. 45-101, 1979.

12. Atkinson, R., Carter, W.P.L., Darnall, K.R., Winer, A.M., and Pitts, J.N., Jr., "A Smog Chamber and Modeling Study of the Gas Phase NO_x-Air Photooxidation of Toluene and the Cresols," Int. J. Chem. Kinet., vol 12, pp. 779-836, 1980.

13. Whitten, G.Z., Killus, J.P., and Hogo, H., Modeling of Simulated Photochemical Smog with Kinetic Mechanisms, Volume 1, EPA-600/3-80-028A, February 1980.

14. Atkinson, R. and Lloyd, A.C., "Smog Chemistry and Urban Airshed Modeling," pp. 559-592. In Oxygen and Oxy-Radicals in Chemistry and Biology, Rodgers, M.A.J. and Powers, E.L. (Eds.), Academic Press, 1981.

15. Atkinson, R., Lloyd, A.C., and Winges, L., "An Updated Chemical Mechanism for Hydrocarbon/NO_x/SO_2 Photooxidations Suitable for Inclusion in Atmospheric Simulation Models," Atmos. Environ., vol 16, pp. 1341-1355, 1982.

16. Leone, J.A. and Seinfeld, J.H., "Updated Chemical Mechanism for Atmospheric Photooxidation of Toluene," Int. J. Chem. Kinet., 16, pp. 159-193, 1984.

17. Atkinson, R. and Lloyd, A.C., "Evaluation of Kinetic and Mechanistic Data for Modeling of Photochemical Smog," J. Phys. Chem. Ref. Data, in press, 1984.

18. Atkinson, R., Darnall, K.R., Lloyd, A.C., Winer, A.M., and Pitts, J.N., Jr., "Kinetics and Mechanisms of the Reaction of the Hydroxyl Radical with Organic Compounds in the Gas Phase," Adv. Photochem., vol 11, pp. 375-488, 1979.

19. Carter, W.P.L., Atkinson, R., Winer, A.M., and Pitts, J.N., Jr., "Experimental Investigation of Chamber-Dependent Radical Sources," Int. J. Chem. Kinet., vol 14, pp. 1071-1103, 1982.

20. Doyle, G.J., Bekowies, P.J., Winer, A.M., and Pitts, J.N., Jr., "Charcoal-Adsorption Air Purification System for Chamber Studies Investigating Atmospheric Photochemistry," Environ. Sci. Technol., vol 11, pp. 45-51, 1977.

21. Stephens, E.R., Burleson, F.R., and Cardiff, E.A., "The Production of Pure Peroxyacyl Nitrate," J. Air Pollut. Control Assoc., vol 15, pp. 87-89, 1965.

22. Stephens, E.R. and Price, M.A., "Analysis of an Important Air Pollutant: Peroxyacetyl Nitrate," J. Chem. Educ., vol 50, pp. 351-354, 1973.

23. Pitts, J.N., Jr., Darnall, K., Carter, W.P.L., Winer, A.M., and Atkinson, R., Mechanisms of Photochemical Reactions in Urban Air, EPA-600/3-79-110, November 1979.

24. Winer, A.M., Peters, J.M., Smith, J.P., Pitts, J.N., Jr., "Response of Commercial Chemiluminescent NO-NO_2 Analyzers to Other Nitrogen-Containing Compounds," Environ. Sci. Technol., vol 8, pp. 1118-1121, 1974.

25. Zafonte, L., Rieger, P.L., and Holmes, J.R., "Nitrogen Dioxide Photolysis in the Los Angeles Atmosphere," Environ. Sci. Technol., vol 11, pp. 483-487, 1977.

26. Pitts, J.N., Jr., Atkinson, R., Carter, W.P.L., Winer, A.M., and Tuazon, E.C., Chemical Consequences of Air Quality Standards and of Control Implementation Programs, Final Report to California Air Resources Board Contract No. A1-030-32, April 1983.

27. Carter, W.P.L., Dodd, M.C., Long, W.D., and Atkinson, R., Outdoor Chamber Study to Test Multi-Day Effects: Volume I: Experimental, Results, and Discussion, Draft Final Report to EPA-ESRL, Cooperative Agreement No. CR830260-01, June 1984.

28. Atkinson, R., Aschmann, S.M., and Pitts, J.N., Jr., "Kinetics of the Reactions of Naphthalene and Biphenyl with OH Radicals and O_3 at 294 ± 1 K," Environ. Sci. Technol., vol 18, pp. 110-113, 1984.

29. Atkinson, R., Carter, W.P.L., Aschmann, S.M., Winer, A.M., and Pitts, J.N., Jr., "Kinetics of the Reaction of OH Radicals with a Series of Branched Alkanes at 297 ± 2 K," Int. J. Chem. Kinet., vol 16, pp. 469-481, 1984.

30. Atkinson, R., Aschmann, S.M., and Carter, W.P.L., "Kinetics of the Reactions of O_3 and OH Radicals with Furan and Thiophene at 298 ± 2 K," Int. J. Chem. Kinet., vol 15, pp. 51-61, 1983.

31. Atkinson, R., Aschmann, S.M., Carter, W.P.L., Winer, A.M., and Pitts, J.N., Jr., "Alkyl Nitrate Formation from the NO_x-Air Photooxidations of C_2-C_8 n-Alkanes," J. Phys. Chem., vol 86, pp. 4563-4569, 1982.

32. Atkinson, R., Aschmann, S.M., Carter, W.P.L., Winer, A.M., and Pitts, J.N., Jr., "Formation of Alkyl Nitrates from the Reactions of Branched and Cyclic Peroxy Radicals with NO," Int. J. Chem. Kinet., in press, 1984.

33. Killus, J.P. and Whitten, G.Z., "A Mechanism Describing the Photochemical Oxidation of Toluene in Smog," Atmos. Environ., vol 16, pp. 1973-1988, 1982.

34. Darnall, K.R., Atkinson, R., and Pitts, J.N., Jr., "Observation of Biacetyl from the Reaction of OH Radicals with o-Xylene. Evidence for Ring Cleavage," J. Phys. Chem., vol 83, pp. 1943-1946, 1979.

35. Nojima, K., Fukaya, K., and Kanno, S., "The Formation of Glyoxals by the Photochemical Reaction of Aromatic Hydrocarbons in the Presence of Nitrogen Monoxide," Chemosphere, vol 5, pp. 247-252, 1974.

36. Bandow, H., Washida, N., and Akimoto, H., "FTIR Studies of the Photooxidation of Aromatic Hydrocarbons," Presented at the XIth International Conference on Photochemistry, College Park, Maryland, 21-26 August 1983.

37. Takagi, H., Washida, N., Akimoto, H., Nagasawa, K., Usui, Y., and Okuda, M., "Photooxidation of o-Xylene in the NO-H_2O-Air System," J. Phys. Chem., vol 84, 478-483, 1980.

38. Carter, W.P.L., Atkinson, R., Plum, C.N., Sanhueza, E., and Pitts, J.N., Jr., "Photolysis Rates of the α-Dicarbonyls: Implications for Mechanisms for the Atmospheric Photooxidations of Aromatic Hydrocarbons," Presented at the XIth International Conference on Photochemistry, College Park, Maryland, 21-26 August 1983.

39. Gitchell, A., Simonaitis, R., and Heicklen, J., "The Inhibition of Photochemical Smog. 1. Inhibition by Phenol, Benzaldehyde, and Aniline," J. Air Pollut. Control Assoc., vol 24, 357-361, 1974.

40. Atkinson, R., Carter, W.P.L., and Winer, A.M., "Evaluation of Hydrocarbon Reactivities for Use in Control Strategies," Final Report to the California Air Resources Board, Contract No. AO-105-32, May 1983.

41. Pitts, J.N., Jr., Winer, A.M., Aschmann, S.M., Carter, W.P.L., and Atkinson, R., "Experimental Protocol for Determining Hydroxyl Radical Reaction Rate Constants," EPA-600/3-82-038, October 1982.

42. Atkinson, R. and Aschmann, S.M., "Kinetics of the Reaction of OH Radicals with a Series of Alkenes at 295 ± 2 K," Int. J. Chem. Kinet., in press, 1984.

43. Atkinson, R., Aschmann, S.M., Winer, A.M., and Pitts, J.N., Jr., "Kinetics of the Gas-Phase Reactions of NO_3 Radicals with a Series of Dialkenes, Cycloalkenes, and Monoterpenes at 295 ± 1 K, Environ. Sci. Technol., vol 18, pp. 370-375, 1984.

44. Atkinson, R., Plum, C.N., Carter, W.P.L., Winer, A.M., and Pitts, J.N., Jr., "Rate Constants for the Gas Phase Reactions of NO_3 Radicals with a Series of Organics in Air at 298 ± 1 K," J. Phys. Chem., vol 88, pp. 1210-1215, 1984.

45. Atkinson, R., Carter, W.P.L., Plum, C.N., Winer, A.M., and Pitts, J.N., Jr., "Kinetics of the Gas Phase Reactions of NO_3 Radicals with a Series of Aromatics at 296 ± 2 K, Int. J. Chem. Kinet., in press, 1984.

46. Schott, G. and Davidson, N., "Shock Waves in Chemical Kinetics: The Decomposition of N_2O_5 at High Temperatures," J. Am. Chem. Soc., vol 80, pp. 1841-1853, 1958.

47. Tuazon, E.C., Sanhueza, E., Atkinson, R., Carter, W.P.L., Winer, A.M., and Pitts, J.N., Jr., "Direct Determination of the Equilibrium Constant at 298 K for the $NO_2 + NO_3 \rightleftarrows N_2O_5$ Reactions," J. Phys. Chem., in press, 1984.

48. Malko, M.W. and Troe, J., "Analysis of the Unimolecular Reaction $N_2O_5 + M \rightleftarrows NO_2 + NO_3 + M$," Int. J. Chem. Kinet., vol 14, pp. 399-416, 1982.

49. Japar, S.M. and Niki, H., "Gas Phase Reaction of the Nitrate Radical with Olefins," J. Phys. Chem., vol 79, 1629-1632, 1975.

50. Singh, H.B., Ludwig, F.L., and Johnson, W.B., "Tropospheric Ozone: Concentrations and Variabilities in Clean Remote Atmospheres," Atmos. Environ., vol 12, pp. 2185-2196, 1978.

51. Crutzen, P.J., "The Global Distribution of Hydroxyl, in Atmospheric Chemistry, E.D. Goldberg, Ed.), pp. 313-328, Springer-Verlag, Berlin, 1982.

52. Platt, U.F., Winer, A.M., Biermann, H.W., Atkinson, R., and Pitts, J.N., Jr., "Measurement of Nitrate Radical Concentrations in Continental Air," Environ. Sci. Technol., vol 18, pp. 365-369, 1984.

53. Kley, D., Drummond, J.W., McFarland, M., and Liu, S.C., "Tropospheric Profiles of NO_x," J. Geophys. Res., vol 86, 3153-3161, 1981.

(The reverse of this page is blank.)

APPENDIX A

CHRONOLOGICAL SUMMARY OF ENVIRONMENTAL CHAMBER EXPERIMENTS

APPENDIX A

CHRONOLOGICAL SUMMARY OF ENVIRONMENTAL CHAMBER EXPERIMENTS

A summary of the purpose, experimental conditions, and major results of all environmental chamber experiments in this program, listed in the order in which they were executed, is given in Table A-1. This table also indicates which chamber-flushing procedures were employed between experiments, since this was changed several times during the program. Unless indicated otherwise, all other procedures were as discussed in Section II-B. In some cases, runs for other SAPRC programs were carried out in conjunction with the runs for this program; these are also indicated in Table A-1, since they constitute part of the history of the reaction bag employed. (However, there is no evidence for any interferences or contamination as a result of those experiments.) Further details concerning the specific experimental operations, analytical instrumentation employed, and data obtained in the individual environmental chamber experiments are given in the detailed data tabulations in Volume II of this report.

TABLE A-1. CHRONOLOGICAL SUMMARY OF INDOOR TEFLON CHAMBER EXPERIMENTS.

ITC run no.	Date	Description	Purpose	Initial concentrations and experimental conditons	Major results and remarks
				New bag #101 installed. For the following runs, the chamber was filled and emptied twice before the final fill at the start of each run, and emptied and refilled at least once after each run.	
690	11/23	"Dummy" Propene-NO_x	Chamber conditioning	Initial NO = 0.21 ppm NO_2 = 0.23 ppm Propene = ~0.76 ppm. 5-hr run.	0.6 ppm ozone formed.
691	11/28	NO_2 actinometry actinometry	Determine light intensity.	Quartz tube technique - NO_2 in N_2 employed.	k_1 = 0.29 min^{-1}; same as in the previous determination.
692	11/28	NO_x-air	Monitor chamber effects.	Initial NO = 0.39 ppm NO_2 = 0.11 ppm Propene, n-butane tracers. 2-hr run.	Radical input rate = 0.15 ppm min^{-1}. NO oxidation rate = 0.12 ppb min^{-1}. In the normal to high range for this chamber.
693	11/29	Propene-NO_x	Standard control run for chamber performance.	Inital NO = 0.38 ppm NO_2 = 0.11 ppm Propene = 1.10 ppm. 6-hr run.	Final O_3 = 0.78 ppm, in reasonable agreement with model predictions.
694	11/30	Isobutene-NO_x	(Carried out for another program.)	Initial NO = 0.40 ppm NO_2 = 0.11 ppm Isobutene = 1.14 ppm. 6-hr run.	Maximum O_3 = 0.90 ppm in 5.25 hours.
695	11/31	NO_x-air	Monitor chamber effects.	Inital NO = 0.40 ppm NO_2 = 0.10 ppm Propene, n-butane tracers. 2-hr run.	Radical input rate = 0.13 ppb min^{-1}. NO oxidation rate = 0.23 ppb min^{-1}. Comparable to results of the previous NO_x-air run.

TABLE A-1. CHRONOLOGICAL SUMMARY OF INDOOR TEFLON CHAMBER EXPERIMENTS (CONTINUED).

ITC run no.	Date	Description	Purpose	Initial concentrations and experimental conditions	Major results and remarks
696	11/31	NO_2 actinometry	Determine light intensity.	Quartz tube technique employed.	k_1 = 0.29 min^{-1}, exactly the same as in the previous two determinations.
697	11/31	Ozone decay	Determine O_3 dark decay rates.	Initial O_3 = 1.14 ppm; left in chamber 15.6 hr overnight). Dark run.	Final O_3 = 0.96 ppm; O_3 decay rate = 1.1% hr^{-1}.
698	12/2	Benzene-NO_x	Derive data base required for NO_x-air reactions of alkylbenzene fuel constituents.	Initial NO = 0.40 ppm NO_2 = 0.10 ppm Benzene = 13.92 ppm. 5-hr run.	Maximum O_3 = 0.37 ppm after 4 hr, declined to 0.33 ppm after 5 hr. Final benzene = 11.7 ppm. Reasonably good repeat of similar benzene run previously carried out in this chamber.
699	12/5	Toluene-NO_x	Same as above.	Initial NO = 0.39 ppm NO_2 = 0.12 ppm Toluene = 1.50 ppm. 4.5-hr run.	Maximum O_3 = 0.49 ppm after 3.25 hr, declined to 0.43 ppm at end of run. Final toluene = 0.85 ppm.
700	12/6	NO_x-air	Monitor chamber effects.	Initial NO = 0.39 ppm NO_2 = 0.12 ppm Propene, n-butane tracers. 2-hr run.	Radical input rate = 0.26 ppb min^{-1}. NO oxidation rate = 0.39 ppb min^{-1}. Consistent with previous determinations with this bag.
701	12/6	NO_2 actinometry	Monitor light intensity.	Quartz tube technique employed.	k_1 = 0.29 min^{-1}; consistent with previous determinations.
702	12/7	m-Xylene-NO_x	Same as runs 698 and 699.	Initial NO = 0.41 ppm NO_2 = 0.11 ppm m-Xylene = 0.50 ppm. 4.5-hr run.	Maximum O_3 = 0.63 ppm after 3.25 hr, declined to 0.61 ppm at end of run. Final m-xylene = 63 ppb.
703	12/8	Mesitylene-NO_x	Same as above.	Initial NO = 0.39 ppm NO_2 = 0.11 ppm Mesitylene = 0.58 ppm. 4-hr run.	Maximum O_3 = 0.71 ppm after 2.5 hr, declined to 0.68 ppm at end of run. Final mesitylene = 18 ppb.

TABLE A-1. CHRONOLOGICAL SUMMARY OF INDOOR TEFLON CHAMBER EXPERIMENTS (CONTINUED).

ITC run no.	Date	Description	Purpose	Initial concentrations and experimental conditions	Major results and remarks
704	12/9	NO_x-air	Monitor chamber effects.	Initial NO = 0.39 ppm NO_2 = 0.13 ppm Propene, n-butane tracers. 2-hr run.	Radical input rate = 0.22 ppb min^{-1}. NO oxidation rate = 0.29 ppb min^{-1}. Consistent with previous determinations with this bag.
705	12/9	NO_2 actinometry	Monitor light intensity.	Quartz tube technique employed.	k_1 = 0.29 min^{-1}; consistent with previous determinations.
706	12/12	Mesitylene-NO_x	Same as run 703. Determine effect of varying initial mesitylene.	Initial NO = 0.39 ppm NO_2 = 0.11 ppm Mesitylene = 0.29 ppm. 6.25-hr run.	Ozone did not reach a true maximum, but its formation leveled off by end of run. Final O_3 = 0.64 ppm. All mesitylene reacted by end of run.
707	12/13	NO_x-air	Monitor chamber effects at the higher initial NO_x levels.	Initial NO = 0.80 ppm NO_2 = 0.21 ppm Propene, n-butane tracers. 2-hr run.	Radical input rate = 0.24 ppb min^{-1}. NO oxidation rate = 0.26 ppb min^{-1}. Similar to previous determinations in this bag, despite higher initial NO_x.
708	12/13	NO_2 actinometry	Monitor light intensity.	Quartz tube technique employed. Used both old and NO_2 bottle and a new one.	k_1 = 0.30 min^{-1} with old bottle, 0.31 min^{-1} with the new one. Consistent with each other and previous determinations.
709	12/14	Mesitylene-NO_x	Same as run 703. Determine effect of increasing initial NO_x.	Initial NO = 0.79 ppm NO_2 = 0.21 ppm Mesitylene = 0.52 ppm. 6-hr run.	Ozone did not reach a true maximum but leveled off by end of run. Final O_3 = 0.78 ppm. Final mesitylene = 1.5 ppb.
710	12/15	Benzene-NO_x	Repeat of run 698. Determine reproducibility following an extensive series of aromatic-NO_x runs.	Initial NO = 0.43 ppm NO_2 = 0.12 ppm Benzene = 13.93 ppm. 6-hr run.	Maximum O_3 = 0.37 ppm after 4.5 hr, declined to 0.30 ppm by end of run. Final benzene = 10.59 ppm. Good repeat of previous run.

TABLE A-1. CHRONOLOGICAL SUMMARY OF INDOOR TEFLON CHAMBER EXPERIMENTS (CONTINUED).

ITC run no.	Date	Description	Purpose	Initial concentrations and experimental conditions	Major results and remarks
711	12/16	Furan-NO_x	Derive data base required to develop model for NO_x-air reactions of furan.	Initial NO = 0.37 ppm NO_2 = 0.15 ppm Furan = 0.40 ppm. 4.75-hr run.	Maximum O_3 = 0.47 ppm after 2.75 hr, declined to 0.46 ppm by end of run. No detectable furan in 2-hr sample.
712	12/19	NO_x-air	Monitor chamber effects. Check for evidence of contamination following a furan-NO_x run.	Inital NO = 0.41 ppm NO_2 = 0.10 ppm Propene, n-butane tracers. 2-hr run.	Radical input rate = 0.22 ppb min^{-1}. NO oxidation rate = 0.43 ppb min^{-1}. Radical input rate in normal range for this bag; NO oxidation rate somewhat high and suggests some contamination.
				For the following runs the chamber was flushed for at least 1 hr prior to the first fill, but it was still filled and emptied twice prior to the final fill, and emptied and refilled after each run.	
713	12/20	Furan-NO_x	Same as run 711. Determine effect of varying initial NO_x.	Initial NO = 0.78 ppm NO_2 = 0.21 ppm Furan = 0.38 ppm. 6-hr run.	Maximum O_3 of only 45 ppb formed after 4.75 hr, declined to 37 ppb at the end of the run. Final furan = 10 ppb. Most furan consumed before 2 hr. The NO to NO_2 conversion was relatively rapid until around the time the furan was consumed, then essentially it stopped, and the run looked like a NO_x-air irradiation.
714	12/21	NO_x-air	Monitor chamber effects at the higher NO_x level.	Initial NO = 0.81 ppm NO_2 = 0.20 ppm Propene, n-butane tracers. 2-hr run.	Radical input rate = 0.18 ppb min^{-1}. NO oxidation rate = 0.43 ppb min^{-1}. Consistent with the results of the previous determinations in this bag.

TABLE A-1. CHRONOLOGICAL SUMMARY OF INDOOR TEFLON CHAMBER EXPERIMENTS (CONTINUED).

HC run no.	Date	Description	Purpose	Initial concentrations and experimental conditions	Major results and remarks
715	12/22	Furan-NO_x	Same as run 711. Determine the effect of varying initial furan.	Initial NO = 0.39 ppm NO_2 = 0.10 ppm Furan = 0.21 ppm. 6-hr run.	Final O_3 = 59 ppb, essentially constant at end. Final furan = 5 ppb. The furan consumption rate was initially slow, then it speeded up and finally slowed down again. Most furan consumed by ~2 hr, after which run looked like a NO_x-air irradiation. (Similar to results of run 713.)
716	12/23	Propene-NO_x	Standard control run for chamber performance.	Initial NO = 0.38 ppm NO_2 = 0.11 ppm Propene = 1.04 ppm 6-hr run. Chamber flushed twice and not used for 11 days.	Final O_3 = 0.71 ppm. Reasonably good repeat of run 693 (where final O_3 = 0.78 ppm), and consistent with model predictions.
717	1/4	NO_x-air	Monitor chamber effects.	Initial NO = 0.40 ppm NO_2 = 0.12 ppm Propene, n-butane tracers. 2-hr run.	Radical input rate = 0.18 ppb min^{-1}. NO oxidation rate = 0.30 ppb min^{-1}. Within normal range for this reactor.
718	1/4	NO_2 actinometry	Monitor light intensity.	Quartz tube technique employed.	k_1 = 0.31 min^{-1}, within the range previously observed.
719	1/5	Fuel injection test	Test injection and analysis procedure for the preliminary batch of shale-derived JP-4 received from the Air Force.	240 µl fuel (50 ppmC, nominal) injected into chamber.	Analytical problems were encountered which were corrected.
720	1/9	Fuel injection test	Same as above.	240 µl fuel (50 ppmC, nominal) injected into chamber. Left in chamber overnight.	Good reproducibility in analyses for selected C_6-C_{13} fuel components. Good reproducibility in injection (relative to run 719) for selected C_6-C_{12} components. Levels of all components declined by ~30% overnight.

TABLE A-1. CHRONOLOGICAL SUMMARY OF INDOOR TEFLON CHAMBER EXPERIMENTS (CONTINUED).

ITC run no.	Date	Description	Purpose	Initial concentrations and experimental conditions	Major results and remarks
721	1/11	JP-4 (shale)-NO_x	Derive data base to test models for this fuel in NO_x-air irradiations.	Initial NO = 0.41 ppm NO_2 = 0.13 ppm Fuel ≅ 100 ppmC, nominal (480 μl injected). 6-hr irradiation. For most of the following runs, the chamber was flushed for at least 2 hr prior to the run and after the runs, though for a few runs the empty-and-refill procedure used previously was employed. See data sheets.	Final O_3 = 0.68 ppm; leveling off but not yet at true maximum. Final uncorrected NO_2 = 0.20 ppm, leveling off slowly. 50 ppb PAN formed.
722	1/12	JP-4(shale)-NO_x	Same as above Initial fuel varied.	Initial NO = 0.39 ppm NO_2 = 0.15 ppm Fuel ≅ 50 ppmC, nominal (240 μl injected). 6-hr run.	Final O_3 = 0.45 ppm, still increasing. Final uncorrected NO_2 = 0.36 ppm, still declining.
723	1/13	NO_x-air	Monitor chamber effects. Check for contamination by fuel.	Initial NO = 0.41 ppm NO_2 = 0.10 ppm Propene, n-butane tracers. 2-hr irradiation.	Radical input rate = 0.29 ppb min^{-1}. NO oxidation rate = 0.62 ppb min^{-1}. Radical input slightly higher than normal for this bag. NO oxidation rate at least ~50% higher than normal. Evidence for some contamination by fuel components.
724	1/17	NO_x-air	Monitor chamber effects at lower initial NO_x levels.	For this run and the following, the pre-injection empty-and-refill procedure	Radical input rate = 0.06 ppb min^{-1}. NO oxidation rate = 0.36 ppb min^{-1}. In contrast with results of the previous

TABLE A-1. CHRONOLOGICAL SUMMARY OF INDOOR TEFLON CHAMBER EXPERIMENTS (CONTINUED).

ITC run no.	Date	Description	Purpose	Initial concentrations and experimental conditions	Major results and remarks
724 (continued)			Check for continuing contamination.	was employed. Initial NO = 0.26 ppm NO_2 = 0.06 ppm Propene, n-butane tracers. 2-hr run.	run, the radical input rate was unusually low for this bag. the NO oxidation rate was within the normal range.
725	1/18	JP-4(shale)-NO_x	Same as runs 721 and 722. Initial NO_x varied.	Initial NO = 0.18 ppm NO_2 = 0.05 ppm JP-4(shale) = 50 ppmC, nominal (240 µl fuel injected). 6-hr run.	Final O_3 = 0.45 ppm, still increasing. Final NO_2 = 0.12 ppm, still declining.
726	1/19	NO_x-air	Monitor chamber effects. Check for contamination by fuel.	Initial NO = 0.39 ppm NO_2 = 0.12 ppm Propene, n-butane tracers. 2-hr run.	Radical input rate = 0.13 ppb min^{-1}. NO oxidation rate = 0.28 ppb min^{-1}. Back to being within the normal range for this bag.
727	1/19	NO_2 actinometry	Monitor light intensity.	Quartz tube technique employed. Different NO-NO_x monitor employed than in previous actinometry experiments.	k_1 = 0.35 min^{-1}, about 20% above the previous determinations. This may be due to employing a different NO-NO_x monitor, but subsequent runs showed the two monitors gave good agreement in k_1 determinations. Reason for this shift in k_1 values unknown.
728	1/20	Propene-NO_x	Control run for chamber performance.	Initial NO = 0.37 ppm NO_2 = 0.10 ppm Propene = 1.05 ppm. 6-hr run.	Maximum O_3 = 0.63 ppm after 6 hr, about 12% lower than observed in run 716 and ~20% lower than observed in run 693.
729	1/23	Thiophene-NO_x	Derive data base to test models for the NO_x-air reactions of thiophene.	Initial NO = 0.39 ppm NO_2 = 0.10 ppm Thiophene = 0.43 ppm. 6-hr run.	Relatively unreactive run; NO slowly converted to NO_2 throughout the run. 6-hr O_3 = 70 ppb and raising. Less than half the thiophene reacted.

TABLE A-1. CHRONOLOGICAL SUMMARY OF INDOOR TEFLON CHAMBER EXPERIMENTS (CONTINUED).

ITC run no.	Date	Description	Purpose	Initial concentration and experimental conditions	Major Results and Remarks
730	1/24	Thiophene-NO_x	Same as above. Initial thiophene increased for greater reactivity.	Initial NO = 0.36 ppm NO_2 = 0.11 ppm Thiophene = 1.78 ppm. 5-hr run.	Maximum O_3 = 0.41 ppm at 3.25 hours, declined to 0.29 ppm at end of run. More than 60% of the thiophene reacted.
731	1/25	NO_x-air	Monitor chamber effects.	Initial NO = 0.40 ppm NO_2 = 0.13 ppm Propene, n-butane tracers. 2-hr run.	Radical input rate = 0.21 ppb min^{-1}. NO oxidation rate = 0.30 ppb min^{-1}. Within the normal range for this bag.
732	1/25	NO_2 actinometry	Monitor light intensity.	Quartz tube technique employed. Same NO-NO_x monitor employed as in previous NO_2 actinometry run.	k_1 = 0.34 min^{-1}, consistent with results of the previous actinometry run (ITC-727).
733	1/26	Thiophene-NO_x	Same as run 729 and 730. Initial NO_x reduced.	Initial NO = 0.21 ppm NO_2 = 0.04 ppm Thiophene = 0.43 ppm. 6.25-hr run.	Final O_3 = 0.24 ppm. O_3 essentially constant at end of run. Almost 80% of the thiophene consumed.
734	1/27	NO_x-air	Monitor chamber effects at the NO_x level of run 733.	Initial NO = 0.21 ppm NO_2 = 0.05 ppm Propene, n-butane tracers. 2-hr run.	Radical input rate = 0.17 ppb min^{-1}. NO oxidation rate 0.37 ppb min^{-1}. Within the normal range for this bag.
-	1/31	Pyrrole analysis test	Test procedures for the analyses of pyrrole.	16 µl (1 ppm nominal) pyrrole injected into chamber, and numerous samples taken. Then lights turned on for 65 min.	After initial problems, a satisfactory procedure for analyses of pyrrole found. When lights turned on, ~1/3 of the pyrrole was consumed in 65 min.

TABLE A-1. CHRONOLOGICAL SUMMARY OF INDOOR TEFLON CHAMBER EXPERIMENTS (CONTINUED).

ITC run no.	Date	Description	Purpose	Initial concentrations and experimental conditions	Major results and remarks
735	2/1	Pyrrole-NO_x	Derive data base to test models for the NO_x-air reactions of pyrrole.	Initial NO = 0.42 ppm NO_2 = 0.07 ppm Pyrrole = 0.53 ppm. 2-hr irradiation. O_3 and NO_x monitored in the dark for ~2.5 hr after end of irradiation.	Pyrrole was found to be extremely reactive. Maximum O_3 = 0.32 ppm within only ~30 min; declined gradually after that. 95% of pyrrole consumed in 30 min. Significant levels of NO_2 apparently remained at end of run, since both NO_2 and O_3 declined in the dark after the lights were turned off. Small induction period for NO → NO_2 conversion seen.
				New bag #102 installed. Flushed for 1.3 hr.	
736	2/3	Propene-NO_x	Bag conditioning and check for normal O_3 formation.	Initial NO = 0.36 ppm NO_2 = 0.09 ppm Propene = 0.51 ppm. 7.25-hr run.	O_3 maximum not obtained. Final O_3 = 0.28 ppm. Consistent with model predictions.
737	2/6	NO_x-Air	Monitor chamber effects in new bag.	Initial NO = 0.39 ppm NO_2 = 0.10 ppm Propene, n-butane tracers. 2-hr run.	Radical input rate = 0.06 ppb-min^{-1} NO oxidation rate = 0.27 ppb min^{-1} Radical input rate extremely low, but NO oxidation rate within normal range.
738	2/6	NO_2 actinometry	Monitor light intensity.	Quartz tube technique employed.	k_1 = 0.33 min^{-1}, within the range observed in the previous two determinations.
739	2/7	Tetralin-NO_x	Derive data base to test models for the NO_x-air reactions of tetralin.	Initial NO = 0.40 ppm NO_2 = 0.11 ppm Tetralin = 0.24 ppm. 6-hr run.	No O_3 formed. Less than half the NO converted. Less than 40% of the tetralin reacted. Tetralin quite unreactive compared to other aromatics.

TABLE A-1. CHRONOLOGICAL SUMMARY OF INDOOR TEFLON CHAMBER EXPERIMENTS (CONTINUED).

ITC run no.	Date	Description	Purpose	Initial concentrations and experimental conditions	Major results and remarks
740	2/8	NO_x-Air	Monitor chamber effects in chamber exposed to tetralin.	Initial NO = 0.40 ppm NO_2 = 0.11 ppm Propene, n-butane tracers. 2-hr run.	Radical input rate = 0.08 ppb min^{-1}. NO oxidation rate = 0.15 ppb min^{-1}. Similar to the results of the previous NO_x-air run.
741	2/8	NO_2 actinometry	Monitor light intensity.	Quartz tube technique employed.	k_1 = 0.33 min^{-1}, same as previous determination.
742	2/9	Mesitylene-NO_x	Repeat mesitylene run in a different reactor.	Initial NO = 0.35 ppm NO_2 = 0.13 ppm Mesitylene = 0.52 ppm. 4.5-hr run.	Final O_3 = 0.77 ppm; leveled off at end. 0.46 ppm PAN formed. Final mesitylene = 15 ppb. Similar to results of previous runs.
743	2/10	Furan-NO_x	Repeat furan run in a different reactor.	Initial NO = 0.38 ppm NO_2 = 0.11 ppm Furan = 0.37 ppm. 6.25-hr run.	O_3 rose rapidly to ~0.5 ppm in the first 2.5 hr, then more slowly to a maximum of 0.6 ppm at 5.5 hr. All furan consumed within the first 2 hr. Qualitatively similar to results of previous furan runs.
744	2/13	Thiophene-NO_x	Repeat thiophene run in a different reactor.	Initial NO = 0.43 ppm NO_2 = 0.09 ppm Thiophene = 1.64 ppm. 4.5-hr run.	Maximum O_3 = 0.48 ppm at 3.25 hr. Approximately half the thiophene consumed. Similar to results of previous thiophene run ITC-733.
745	./14	NO_x-Air	Monitor chamber effects.	Initial NO = 0.41 ppm NO_2 = 0.11 ppm Propene, n-butane tracers. 2-hr run.	Radical input rate = 0.13 ppb min^{-1} NO oxidation rate = 0.13 ppb min^{-1} The radical input rate is higher than observed previously for this bag, but is within the range seen in the previous bag. The NO oxidation rate is relatively low.
746	2/14	NO_2 actinometry	Monitor light intensity.	Quartz tube technique employed.	k_1 = 0.33 min^{-1}, same as observed in the previous two determinations.

TABLE A-1. CHRONOLOGICAL SUMMARY OF INDOOR TEFLON CHAMBER EXPERIMENTS (CONTINUED).

ITC run no.	Date	Description	Purpose	Initial concentrations and experimental conditions	Major results and remarks
747	2/15	Tetralin-NO_x	Continue series of tetralin runs started with run 739. Higher initial tetralin employed for greater reactivity.	Initial NO = 0.40 ppm NO_2 = 0.09 ppm Tetralin = 9.3 ppm. 6.5-hr run.	Maximum O_3 = 0.48 ppm at 6 hr.
748	2/16	Tetralin-NO_x	Same as above Lower initial NO_x employed.	Initial NO = 0.18 ppm NO_2 = 0.04 ppm Tetralin = 8.4 ppm. 5.75-hr run.	Maximum O_3 = 0.35 ppm at 4.25 hr.
749	2/17	NO_x-Air	Monitor chamber effects at the lower NO_x levels.	Initial NO = 0.19 ppm NO_2 = 0.04 ppm Propene, n-butane tracers. 2-hr run.	Radical input rate = 0.10 ppb min^{-1}. NO oxidation rate = 0.25 ppb min^{-1}. Similar to the results of the previous determination.
750	2/22	Tetralin-NO_x	Continue tetralin series with lower tetralin levels. Tracers included to monitor radical levels.	Initial NO = 0.41 ppm NO_2 = 0.12 ppm Tetralin = 4.4 ppm Propene, n-butane tracers. 6-hr run.	Final O_3 = 0.46 ppm, still rising. OH levels measured by tracers in first 2 hr ~5 times lower than in NO_x-air irradiations at similar NO_x levels.
751	2/23	Naphthalene-NO_x	Derive data base to test models for the NO_x-air reactions of naphthalene.	Initial NO = 0.41 ppm NO_2 = 0.12 ppm Napthalene = 0.75 ppm. 7-hr run.	Final O_3 = 0.11 ppm and still raising. Less than half the naphthalene consumed in 6 hr. Naphthalene, like tetralin, is much less reactive than the alkylbenzenes.

TABLE A-1. CHRONOLOGICAL SUMMARY OF INDOOR TEFLON CHAMBER EXPERIMENTS (CONTINUED).

ITC run no.	Date	Description	Purpose	Initial concentrations and experimental conditions	Major results and remarks
752	2/24	NO_x-Air	Monitor chamber effects.	Initial NO = 0.44 ppm NO_2 = 0.11 ppm Propene, n-butane tracers. 2-hr run.	Radical input rate = 0.20 ppb min^{-1}. NO oxidation rate = 0.28 ppb min^{-1}. Both radical input and NO oxidation rates higher than observed previously for this bag, but is within the range observed for the previous bag.
753	2/24	NO_2 actinometry	Monitor light intensity.	Quartz tube technique employed.	k_1 = 0.32 min^{-1}, similar to results of the previous determinations.
754	2/27	Propene-NO_x	Monitor chamber effects; specifically determine whether exposure to naphthalene or tetralin suppresses O_3 yields in propene-NO_x irradiations.	Initial NO = 0.43 ppm NO_2 = 0.13 ppm Propene = 0.98 ppm. 6-hr run.	Final O_3 = 0.81 ppm, leveling off. O_3 yield within normal range.
755	2/28	Naphthalene-NO_x	Continue naphthalene series with lower NO_x and more naphthalene for greater reactivity and with tracers to monitor radical levels.	Initial NO = 0.19 ppm NO_2 = 0.05 ppm Naphthalene = 1.40 ppm Propene, n-butane tracers. 6-hr run.	Maximum O_3 = 0.26 ppm at 5 hr Radical levels in first 1.5 hr ~4-8 times lower than in NO_x-air runs with similar NO_x levels
756	2/29	Naphthalene-NO_x	Same as above. Initial naphthalene increased.	Initial NO = 0.21 ppm NO_2 = 0.05 ppm Naphthalene = 2.74 ppm Propene, n-butane tracers. 5.25-hr run.	Maximum O_3 = 0.24 ppm at 4 hr. Radical levels in first 45 minutes too low to measure; at least 4 times lower than initial radical levels in previous run.

TABLE A-1. CHRONOLOGICAL SUMMARY OF INDOOR TEFLON CHAMBER EXPERIMENTS (CONTINUED).

ITC run no.	Date	Description	Purpose	Initial concentrations and experimental conditions	Major results and remarks
757	3/1	NO_x-air	Monitor chamber effects.	Initial NO = 0.20 ppm NO_2 = 0.05 ppm Propene, n-butane tracers. 2-hr run.	Radical input rate = 0.28 ppb min^{-1}. NO oxidation rate = 0.49 ppb min^{-1}. Both somewhat higher than observed previously, and suggest contamination.
758	3/1	NO_2 actinometry	Monitor light intensity.	Quartz tube technique employed. Before the following run, the chamber was flushed for 3.5 hr with the lights on and then flushed with the lights off to reduce contamination indicated by run ITC-757.	k_1 = 0.32 min^{-1}, within the range previously observed.
759	3/2	Propene-NO_x	Control run to check for chamber performance. Also, condition chamber.	Initial NO = 0.41 ppm NO_2 = 0.15 ppm Propene = 1.02 ppm. 6-hr run.	Final O_3 = 0.80 ppm, leveling off. Within the normal range.
760	3/5	NO_x-air	Determine if extended flush and propene-NO_x run returned chamber effects to normal.	Initial NO = 0.42 ppm NO_2 = 0.13 ppm Propene, n-butane tracers.	Radical input rate = 0.17 ppb min^{-1}. NO oxidation rate = 0.29 ppb min^{-1}. Radical input rate within normal range. NO oxidation rate still high, but lower than in previous NO_x-air run.
761	3/6	NO_x-air + n-octane	Obtain data to test models for atmospheric reactions of n-octane.	Initial NO = 0.42 ppm NO_2 = 0.11 ppm Propene, n-butane tracers. 9.4 ppm n-octane added after 2 hr. Run ended	Prior to n-octane addition: Radical input rate = 0.14 ppb min^{-1} NO oxidation rate = 0.27 ppb min^{-1}. Within the normal range for NO_x-air irradiations. Addition of n-octane caused the NO oxidation

TABLE A-1. CHRONOLOGICAL SUMMARY OF INDOOR TEFLON CHAMBER EXPERIMENTS (CONTINUED).

ITC run no.	Date	Description	Purpose	Initial concentrations and experimental conditions	Major results and remarks
761 (continued)				5 hr later.	rate to increase to 1.2 ppb min^{-1} (for first 2 hr after addition), but suppressed the OH radical levels by at least a factor of 20. No O_3 formed.
762	3/7	NO_x-air + n-octane	Same as above. Initial NO_x reduced.	Initial NO = 0.22 ppm NO_2 = 0.06 ppm Propene, n-butane tracers 9.4 ppm n-octane added after 2 hr. Run ended 5 hr later.	Prior to n-octane addition: Radical input rate = 0.12 ppb min^{-1}. NO oxidation rate = 0.24 ppb min^{-1}. Addition of n-octane caused the NO oxidation rate (for the first 2 hr after addition) to increase to 0.7 ppb min^{-1}, and the OH radical level to be suppressed by at least a factor of 10. O_3 = 0.11 ppm at the end of run.
763	3/8	NO_x-air + n-octane	Same as above. Amount of n-octane reduced by factor of 10.	Initial NO = 0.22 ppm NO_2 = 0.05 ppm Propene, n-butane tracers. 0.96 ppm n-octane added after 2 hr. Irradiation continued 5.25 hr after that.	Prior to n-octane addition: Radical input rate = 0.11 ppb min^{-1}. NO oxidation rate = 0.20 ppb min^{-1}. After n-octane addition: NO oxidation rate (for the first 2 hr after addition) increased to 0.5 ppb min^{-1}, while the OH radical level was suppressed by a factor of ~5.
764	3/9	NO_2 actinometry	Monitor light intensity.	Quartz tube technique employed.	k_1 = 0.32 min^{-1}, same as previous determination.
765	3/12	NO_x-air + methylcyclohexane	Obtain data to test models for atmospheric reactions of methylcyclohexane.	Initial NO = 0.36 ppm NO_2 = 0.15 ppm Propene, n-butane tracers. 0.92 ppm methylcyclohexane added 2 hr after start of run. Run ended 5 hr later.	Prior to methycyclohexane addition: Radical input rate = 0.16 ppm min^{-1}. NO oxidation rate = 0.37 ppb min^{-1}. After addition: NO oxidation rate increased to to 0.9 ppb min^{-1}, OH radical levels suppressed by factor of ~4. No O_3 formation occurred.

TABLE A-1. CHRONOLOGICAL SUMMARY OF INDOOR TEFLON CHAMBER EXPERIMENTS (CONTINUED).

ITC run no.	Date	Description	Purpose	Initial concentrations and experimental conditions	Major results and remarks
766	3/13	NO_x-air + methylcyclo-hexane	Same as above. Methylcyclohexane increased by factor of ~10. NO_x decreased.	Initial NO = 0.21 ppm NO_2 = 0.06 ppm Propene, n-butane tracers. 8.7 ppm methylcyclohexane added 2 hr after start of of run. Run ended 5 hr later.	Prior to methycyclohexane addition: Radical input rate = 0.10 ppb min^{-1}. NO oxidation rate = 0.18 ppb min^{-1}. After addition: NO oxidation rate increased to 0.8 ppb min^{-1}. OH radical levels suppressed by at least a factor of 40. 0.12 ppm O_3 formed.
767	3/14	NO_x-air + methycyclohexane	Same as above. Initial NO_x increased.	Initial NO = 0.43 ppm NO_2 = 0.13 ppm Propene, n-butane tracers. 8.8 ppm methylcyclohexane added after 2.25 hr. Run ended 5 hr later.	Prior to methylcyclohexane addition: Radical input rate = 0.09 ppb min^{-1} NO oxidation rate = 0.13 ppb min^{-1} After addition: NO oxidation rate increased to 1.1 ppb min^{-1}. OH radical levels suppressed at least a factor of 5.
768	3/15	JP-4 (shale)-NO_x	Derive data base to test models for this fuel in NO_x-air irradiations. Repeat of run ITC-721 with a different bag.	Initial NO = 0.43 ppm NO_2 = 0.10 ppm Fuel = 100 ppmC (nominal). 7-hr run. Between runs, chamber flushed for 3 hr at 100% lights, then for 2 hr with lights off.	6-hr O_3 = 0.71 ppm, in good agreement with results of ITC-721 (where 6 hr O_3 = 0.68 ppm). Final O_3 = 0.82 ppm, still raising. 6-hr PAN = 37 ppb.
769	3/16	NO_2 actinometry	Monitor light intensity.	Quartz tube technique employed.	k_1 = 0.31 ppm, within normal range.
770	3/19	NO_x-air + n-butane	Control run for purpose of comparing with	Initial NO = 0.41 ppm NO_2 = 0.14 ppm Propene, propane tracers.	Before n-butane injection: Radical input rate = 0.10 ppb min^{-1}. NO oxidation rate = 0.20 ppb min^{-1}.

TABLE A-1. CHRONOLOGICAL SUMMARY OF INDOOR TEFLON CHAMBER EXPERIMENTS (CONTINUED).

ITC run no.	Date	Description	Purpose	Initial concentrations and experimental conditions	Major results and remarks
770 (continued)			results of NO_x-air + n-octane and NO_x-air + methylcyclohexane runs. Also, monitor chamber effects.	9.4 ppm n-butane added after 2 hr. Run continued for 4.25 hr after that.	After n-butane addition: NO oxidation rate increased to 1.4 ppb min^{-1} and OH radical levels suppressed by a factor of 2. Negligible O_3 formation.
771	3/20	2,3-dimethylnaphthalene-NO_x	Obtain data to test models for atmospheric reactions of 2,3-dimethylnaphthalene (2,3-DMN).	2,3-DMN flushed into chamber by passing N_2 at 2 ℓ min^{-1} through a tube packed with 2,3-DMN for 14.7 hr. Initial NO = 0.21 ppm, NO_2 = 0.06 ppm, 2,3-DMN = 0.40 ppm. 5.25-hr run. Chamber flushed between runs for 3 hr at 100% lights, then for 2 hr dark.	Maximum O_3 = 0.33 ppm at 4.75 hr. 56 ppb PAN formed. 2,3-DMN much more reactive than expected based on results of naphthalene runs.
772	3/21	NO_x-air	Monitor chamber effects. Check for contamination by 2,3-DMN.	Initial NO = 0.34 ppm, NO_2 = 0.11 ppm. Propene, n-butane tracers. 2-hr run.	Radical input rate = 0.30 ppb min^{-1}. NO oxidation rate = 0.58 ppb min^{-1}. Both roughly a factor of 2 higher than previous runs. Suggests some contamination.
773	3/21	NO_2 actinometry	Monitor light intensity.	Quartz tube technique employed.	k_1 = 0.32 min^{-1}. Both Columbia and Teco NO-NO_x monitors used, and gave good agreement. k_1 value within the expected range.
774	3/22	2,3-dimethylnaphthalene-NO_x	Same as 771. Initial NO_x increased.	2,3-DMN flushed into chamber starting on the previous day as described for run ITC-771.	Final O_3 = 0.34 ppm, near maximum. 69 ppb PAN formed. OH radical levels in second hour of the run

TABLE A-1. CHRONOLOGICAL SUMMARY OF INDOOR TEFLON CHAMBER EXPERIMENTS (CONTINUED).

ITC run no.	Date	Description	Purpose	Initial concentrations and experimental conditions	Major results and remarks
774 (continued)			Tracers added to monitor radical levels.	Initial NO = 0.45 ppm NO_2 = 0.12 ppm 2,3-DMN = 0.33 ppm Propene, n-butane tracers. 6-hr run	roughly half what was observed in NO_x-air runs *ITC-772* and *ITC-776*.
775	3/23	2,3-dimethyl-naphthalene-NO_x	Same as above. Initial 2,3-DMN and NO_x reduced.	2,3-DMN flushed into chamber starting on previous day. Initial NO = 0.22 ppm NO_2 = 0.07 ppm 2,3-DMN = 0.14 ppm Propene, n-butane tracers. 6-hr run. Chamber flushed between runs for 3 hr at 100% lights, then for 2 hr dark.	Final O_3 = 0.289 ppm, still raising. Final PAN = 31 ppb.
776	3/20	NO_x-air	Monitor chamber effects.	Initial NO = 0.44 ppm NO_2 = 0.12 ppm Propene, n-butane tracers. 2-hr run.	Radical input rate = 0.22 ppb min^{-1}. NO oxidation rate = 0.39 ppb min^{-1}. Within the normal range.
777	3/26	NO_2 actinometry	Monitor light intensity.	Quartz tube technique employed.	k_1 = 0.32 min^{-1}, same as observed previously.
778	3/29	Pyrrole-NO_x	Obtain data to test models for atmospheric reactions of pyrrole.	Initial NO = 0.38 ppm NO_2 = 0.11 ppm Pyrrole = 0.97 ppm. 1-hr run.	All pyrrole consumed in 30 min, at which time O_3 = 0.51 ppm. O_3 rose by only 9 ppb in the following 30 min. Poor agreements between Teco and Columbia on NO and NO_2 data, with Teco values considered more reasonable.

TABLE A-1. CHRONOLOGICAL SUMMARY OF INDOOR TEFLON CHAMBER EXPERIMENTS (CONTINUED).

ITC run no.	Date	Description	Purpose	Initial concentratioins and experimental conditions	Major results and remarks
779	3/30	Pyrrole-NO_x	Same as above. Initial pyrrole reduced.	Initial NO = 0.39 ppm NO_2 = 0.10 ppm Pyrrole = 0.27 ppm. 90-min run.	Over 90% of pyrrole consumed in first hour, during which time 0.4 ppm of NO was converted to NO_2. Final O_3 = 69 ppb. Still poor agreement on NO and NO_2 data.
780	4/2	NO_x-air + pyrrole	Same as above. Determine effect of pyrrole addition on radical levels. Also monitor chamber effects.	Initial NO = 0.37 ppm NO_2 = 0.12 ppm Propene, n-butane tracers. 0.1 ppm pyrrole added 2 and 4 hr after beginning of irradiation. 5-hr run (total).	Before pyrrole addition: Radical input rate = 0.20 ppb min^{-1}. NO oxidation rate = 0.23 ppb min^{-1} . Within normal range. After first pyrrole addition: 0.16 ppm NO oxidized. No O_3 formed. Average OH radical levels for first hour after the pyrrole addition was ~50% higher than for hour before. After second pyrrole addition: 0.10 ppm NO oxidized in 1 hr. Negligible O_3 formation. OH radical levels ~20% higher than before the first pyrrole addition. Better agreement between Teco and Columbia on NO and NO_2 data.
				For the following runs, the standard procedure between runs was to flush for 3 hr with lights on followed by 2 hr in the dark.	
781	4/5	Standard synthetic fuel-NO_x	Derive data to test models for atmospheric reactions of fuels whose exact composition is known.	Initial NO = 0.42 ppm NO_2 = 0.10 ppm Fuel = 43 ppmC. 6-hr run.	Final O_3 = 0.75 ppm, near maximum. Formed more O_3 than corresponding run with shale-derived JP-4 (run ITC-722).

TABLE A-1. CHRONOLOGICAL SUMMARY OF INDOOR TEFLON CHAMBER EXPERIMENTS (CONTINUED).

ITC run no.	Date	Description	Purpose	Initial concentrations and experimental conditions	Major results and remarks
782	4/6	NO_x-air irradiation	Monitor background reactivity.	Initial NO = 0.36 ppm NO_2 = 0.12 ppm Propene, n-butane tracers. 2-hr run.	Radical input rate = 0.21 ppb min^{-1} NO oxidation rate = 0.23 ppb min^{-1} Within the normal range.
783	4/6	NO_2 actinometry	Monitor light intensity.	Quartz tube technique employed.	k_1 = 0.32 min^{-1}, within the normal range.
784	4/9	Synthetic fuel-NO_x	Same as ITC-781. Initial fuel increased.	Initial NO = 0.43 ppm NO_2 = 0.06 ppm Fuel = 88 ppmC. 6-hr run.	Maximum O_3 = 0.75 ppm at 5.5 hr.
785	4/10	Synthetic fuel-NO_x	Same as above. Initial NO_x reduced.	Initial NO = 0.21 ppm NO_2 = 0.05 ppm Fuel = 45 ppmC. 6-hr run.	Maximum O_3 = 0.60 ppm at 5.5-6 hr.
786	4/11	Synthetic fuel + furan-NO_x	Test effect of furan as a fuel impurity on its reactivity in NO_x-air irradiations.	Initial NO = 0.43 ppm NO_2 = 0.06 ppm Fuel = 72 ppmC Furan = 0.37 ppm. 4.5-hr run.	Maximum O_3 = 0.64 ppm at 2.25 hr. 2% (as C) furan in fuel significantly reduces time to O_3 maximum, but may also slightly reduce amount of O_3 formed. (Compare with run ITC-784.)
787	4/12	NO_x-air	Monitor background reactivity.	Initial NO = 0.21 ppm NO_2 = 0.05 ppm Propene, n-butane tracers. 2-hr run.	Radical input rate = 0.19 ppb min^{-1}. NO oxidation rate = 0.48 ppb min^{-1}. NO oxidation rate somewhat high, but both within normal range.
788	4/13	Synthetic fuel + thiophene-NO_x	Test effect of thiophene as a fuel impurity on	Initial NO = 0.44 ppm NO_2 = 0.05 ppm Fuel = 89 ppmC.	Maximum O_3 = 0.72 ppm at 5 hr. Similar to results of run ITC-784. Thiophene at the 2% (as C) level has little effect on O_3.

TABLE A-1. CHRONOLOGICAL SUMMARY OF INDOOR TEFLON CHAMBER EXPERIMENTS (CONTINUED).

ITC run no.	Date	Description	Purpose	Initial concentrations and experimental conditions	Major results and remarks
788 (continued)			its reactivity in NO_x-air irradiations.	Thiophene = 0.37 ppm. 6-hr run.	
789	4/16	NO_x-air	Monitor background reactivity.	Initial NO = 0.38 ppm NO_2 = 0.11 ppm Propene, n-butane tracers. 2-hr run.	Radical input rate = 0.21 ppb min^{-1}. NO oxidation rate = 0.38 ppb min^{-1}. Within the normal range for this bag.
790	4/16	NO_2 actinometry	Monitor light intensity.	Quartz tube technique employed.	k_1 = 0.30 min^{-1}, within the normal range.
791	4/17	Propene-NO_x	Control run for chamber performance.	Initial NO = 0.42 ppm NO_2 = 0.11 ppm Propene = 0.95 ppm. 7-hr run.	Final O_3 = 0.77 ppm, essentially constant at end. Similar to results of previous such runs.
				New bag #103 installed. Blacklights washed.	
792	4/19	Propene-NO_x	Condition new bag reactor.	Initial NO = 0.34 ppm NO_2 = 0.13 ppm Propene = 0.98 ppm. 6.25 hr run.	Final O_3 = 0.75 ppm, leveling off. Essentially same result as previous run in old bag.
793	4/20	NO_x-air	Monitor background reactivity for new bag.	Initial NO = 0.36 ppm NO_2 = 0.12 ppm Propene, n-butane tracers. 2-hr run.	Radical input rate = 0.13 ppb min^{-1} NO oxidation rate ~0. Normal result for new bag.
794	4/20	NO_2 actinometry	Monitor light intensity.	Quartz tube technique employed.	k_1 = 0.35 min^{-1}. Somewhat higher value than before. May be due to washing of lamps.

TABLE A-1. CHRONOLOGICAL SUMMARY OF INDOOR TEFLON CHAMBER EXPERIMENTS (CONTINUED).

ITC run no.	Date	Description	Purpose	Initial concentrations and experimental conditions	Major results and remarks
795	4/23	Synthetic fuel #2 - NO_x	Fuel #2 has higher aromatics than standard synthetic fuel. Test effects of this on reactivity.	Initial NO = 0.39 ppm NO_2 = 0.11 ppm Fuel = 45 ppmC. 6-hr run.	Final O_3 = 0.76 ppm, near maximum. Initiation time for O_3 formation ~30 min less than ITC-781, which used the standard fuel at similar fuel and NO_x levels.
796	4/24	Synthetic fuel #2 - NO_x	Same as above - initial fuel increased.	Initial NO = 0.41 ppm NO_2 = 0.12 ppm Fuel = 97 ppmC. 6.25-hr run.	Maximum O_3 = 0.60 ppm at 4.25 hr. More O_3 formed and shorter initiation times observed than in run ITC-784, the comparable run with the standard fuel.
797	4/25	NO_x-air + n-octane	Derive data to test models for reactions of n-octane. Also monitor background reactivity of chamber.	Initial NO = 0.44 ppm NO_2 = 0.11 ppm Propene, n-butane tracers 0.91 ppm n-octane added after 2 hr. Irradiation continued for 4.5 hr after that.	Before n-octane addition: Radical input rate = 0.13 ppb min^{-1}. NO oxidation rate $\approx$ 0. Same as previous NO_x-air run. After n-octane addition: NO oxidation rate = 0.67 ppb min^{-1}. OH radical levels suppressed by a factor of ~4.
798	4/26	Naphthalene-NO_x	Derive data to test models for reactions of naphthalene.	Initial NO = 0.43 ppm NO_2 = 0.12 ppm Naphthalene = 1.93 ppm Propene, n-butane tracers. 6.25-hr run.	Final O_3 = 0.20 ppm, still raising. ~40% naphthalene reacted. OH radical levels 5-10 times lower than in corresponding NO_x-air runs.
799	4/26	Synthetic fuel #3 - NO_x	Synthetic fuel #3 has same alkane/aromatic ratio as the standard fuel, but has	Initial NO = 0.43 ppm NO_2 = 0.12 ppm Fuel = 94 ppmC. 6-hr run.	Maximum O_3 = 0.84 ppm at 5-5.25 hr. Increasing alkylbenzene/bicyclic aromatic ratio decreases initiation time and increases reactivity of fuel, based on results of this run and comparable standard

TABLE A-1. CHRONOLOGICAL SUMMARY OF INDOOR TEFLON CHAMBER EXPERIMENTS (CONTINUED).

ITC run no.	Date	Description	Purpose	Initial concentrations and experimental conditions	Major results and remarks
799 (continued)			more alkylbenzenes and less bicyclic aromatics. Test effect of this on reactivity.		fuel run ITC-784.
800	4/30	NO_x-air + methylcyclohexane	Derive data to test models for reactions of methylcyclohexane. Also, monitor background reactivity of chamber.	Initial NO = 0.40 ppm NO_2 = 0.14 ppm Propene, n-butane tracers. 1.10 ppm methylcyclohexane added after 2 hr. Run ended 4 hr later.	Before methylcyclohexane addition: Radical input rate = 0.16 ppb min^{-1}. NO oxidation rate = 0.13 ppb min^{-1}. Within normal range. After methylcyclohexane addition: NO oxidation rate = 0.89 ppb min^{-1}. OH radical levels suppressed by a factor of 3.
801	5/1	Synthetic fuel #3 - NO_x	Same as ITC-799. Initial fuel reduced.	Initial NO = 0.42 ppm NO_2 = 0.13 ppm Fuel = 41 ppmC. 7-hr run.	Final O_3 = 0.88 ppm, still raising. Formed more O_3, and had shorter initiation times than the corresponding standard fuel run (ITC-781).
802	5/2	Naphthalene-NO_x	Same as ITC-798.	Initial NO = 0.42 ppm NO_2 = 0.11 ppm Naphthalene = 0.84 ppm Propene, n-butane tracers. 6-hr run.	Final O_3 = 0.12 ppm, still raising. OH radical levels a factor of 2-3 lower than in corresponding NO_x-air irradiations.
803	5/3	NO_x-air	Monitor chamber effects.	Initial NO = 0.22 ppm NO_2 = 0.07 ppm Propene, n-butane tracers. 2-hr run.	Radical input rate = 0.19 ppb min^{-1}. NO oxidation rate = 0.25 ppb min^{-1}. Within the normal range.
804	5/3	NO_2 actinometry	Monitor light intensity.	Quartz tube technique employed.	k_1 = 0.32 min^{-1}, within the normal range.

TABLE A-1. CHRONOLOGICAL SUMMARY OF INDOOR TEFLON CHAMBER EXPERIMENTS (CONTINUED).

ITC run no.	Date	Description	Purpose	Initial concentrations and experimental conditions	Major results and remarks
805	5/4	Standard synthetic fuel-NO_x	Repeat standard run ITC-784.	Initial NO = 0.40 ppm NO_2 = 0.18 ppm Fuel = 98 ppmC. 6-hr run.	Maximum O_3 = 0.79 ppm at 5.75 hr. Good repeat of ITC-784.
806	5/7	2,3-Dimethyl-naphthalene-NO_x	Derive data to test models for reactions of 2,3-DMN.	2,3-DMN flushed into chamber at 2 ℓ min^{-1} for 14.5 hr. Initial NO = 0.24 ppm NO_2 = 0.09 ppm 2,3-DMN = 0.49 ppm. 6-hr run.	Final O_3 = 0.35 ppm, still raising. ~98% of the initial 2,3-DMN reacted.
807	5/9	Synthetic fuel + pyrrole-NO_x	Test effect of pyrrole as a fuel impurity in NO_x-air irradiations.	Initial NO = 0.35 ppm NO_2 = 0.14 ppm Fuel = 77 ppmC Pyrrole = 0.19 ppm. 5.25-hr run.	Maximum O_3 = 0.64 ppm at 3 hr. Pyrrole at the 1% level (as C) significantly increased rates of O_3 formation, but seems to slightly suppress O_3 yields.
808	5/10	NO_x-air	Monitor chamber effects.	Initial NO = 0.33 ppm NO_2 = 0.13 ppm Propene, n-butane tracers. 2-hr run.	Radical input rate = 0.15 ppb min^{-1}. NO oxidation rate = 0.22 ppb min^{-1}, within the normal range.
809	5/10	NO_2 actinometry	Monitor light intensity.	Quartz tube technique employed.	k_1 = 0.34 min^{-1}, consistent with previous determinations.
810	5/11	Propene-NO_x	Control run for chamber performance.	Initial NO = 0.40 ppm NO_2 = 0.12 ppm Propene = 0.93 ppm. 6.25-hr run.	Final O_3 = 0.78 ppm, consistent with previous such runs.

TABLE A-1. CHRONOLOGICAL SUMMARY OF INDOOR TEFLON CHAMBER EXPERIMENTS (CONTINUED).

ITC run no.	Date	Description	Purpose	Initial concentrations and experimental conditions	Major results and remarks
				Two isoprene-NO_x-air runs carried out for another program. The normal chamber flush procedure was employed between runs.	
813	5/21	NO_2 actinometry	Monitor light intensity.	Quartz tube technique employed.	k_1 = 0.34 min^{-1}. Within the normal range.
814	5/21	NO_x-air	Monitor chamber effects.	Initial NO + 0.43 ppm NO_2 = 0.10 ppm Propene, n-butane tracers. 2-hr run.	Radical input rate = 0.10 ppb min^{-1}. NO oxidation rate = 0.12 ppb min^{-1}. Consistent with previous determinations in this bag.
				Eight runs involving methyl-vinyl ketone, methacrolein, cyclohexane and biacetyl were carried out for another program. Normal chamber flush procedure employed.	
822	5/30	Ozone decay	Determine O_3 dark decay rates.	Ozone flushed into the chamber for 28 min using a pen-ray O_3 source. Ozone in chamber for 13-14 hr, but O_3 data available only for 9.75 hr.	O_3 dark decay rate = 0.43 ± 0.03% hr^{-1}, within the normal rate for this chamber.
				One methacrolein-NO_x-air run was carried out for another program. Normal flush procedure employed.	

TABLE A-1. CHRONOLOGICAL SUMMARY OF INDOOR TEFLON CHAMBER EXPERIMENTS (CONTINUED).

ITC run no.	Date	Description	Purpose	Initial concentrations and experimental conditions	Major results and remarks
824	6/1	NO_x-air	Monitor chamber effects.	Initial NO = 0.33 ppb NO_2 = 0.07 ppm Propene, n-butane tracers. 2-hr run.	Radical input rate = 0.08 ppb min^{-1}. NO oxidation rate = 0.06 ppb min^{-1}. Both somewhat lower than observed previously in this bag.
825	6/1	Acetaldehyde	Monitor NO_x offgassing rate.	Initial acetaldehyde = 0.4 ppm. 3-hr irradiation.	PAN formed at a rate of 1.7 ± 0.1 ppb hr^{-1}, which is within the normal range for this chamber.
826	6/4	NO_x-air + mesitylene	Determine reactivity of alkylbenzenes and tetralin at high NO_x/hydrocarbon ratios and measure the effect of the presence of these compounds on OH radical levels.	Initial NO = 0.72 ppm NO_2 = 0.17 ppm Propene, n-butane tracers. 0.09 ppm mesitylene added after 2 hr. Run ended 4 hr later.	Before mesitylene addition: NO oxidation rate = 0.03 ppb min^{-1}. Radical input rate = 0.08 ppb min^{-1}. After mesitylene addition: NO oxidation rate (first hr) = 1.3 ppb min^{-1}. OH radical levels only slightly increased in first hour, but increased by a factor of 2-3 for second-fourth hr. No O_3 formed.
827	6/6	NO_x-air + m-xylene	Same as above.	Initial NO = 0.88 ppm NO_2 = 0.17 ppm Propene, n-butane tracers. 0.14 ppm m-xylene added after 2 hr. Run ended 4 hr later.	Before m-xylene addition: NO oxidation rate = 0.09 ppb min^{-1}. Radical input rate = 0.11 ppb min^{-1}. After m-xylene addition: NO oxidation rate (first hr) = 0.79 ppb min^{-1}. OH radical levels not greatly affected in first hr, but increased by a factor of ~3 subsequently. No O_3 formed.

TABLE A-1. CHRONOLOGICAL SUMMARY OF INDOOR TEFLON CHAMBER EXPERIMENTS (CONTINUED).

ITC run no.	Date	Description	Purpose	Initial concentrations and experimental conditions	Major results and remarks
828	6/7	NO_x-air + toluene	Same as above.	Initial NO = 0.83 ppm NO_2 = 0.18 ppm Propene, n-butane tracers. 0.43 ppm toluene added after 2 hr. Run ended 4 hr later.	Before toluene addition: NO oxidation rate = 0.07 ppb min^{-1}. Radical input rate = 0.07 ppb min^{-1}. After toluene addition: NO oxidation rate (first hour) = 0.36 ppb min^{-1}. OH radical levels increased each hr, with the final level ~3 times higher than initially. No O_3 formed.
829	6/8	NO_x-air irradiation	Monitor chamber effects.	Initial NO = 0.21 ppm NO_2 = 0.05 ppm Propene, n-butane tracers. 2-hr run.	Radical input rate = 0.06 ppb min^{-1}. NO oxidation rate = 0.08 ppb min^{-1}. Within the normal range.
830	6/8	NO_2 actinometry	Monitor light intensity.	Quartz tube technique employed.	k_1 = 0.34 min^{-1}, within the normal range.
831	6/11	NO_x-air + benzene	Same as runs 826-828.	Initial NO = 0.84 ppm NO_2 = 0.17 ppm Propene, n-butane tracers. 2.0 ppm benzene added after 2 hr. Run ended 4 hr later.	Before benzene addition: NO oxidation rate = 0.14 ppb min^{-1}. Radical input rate = 0.16 ppb min^{-1}. After benzene addition: NO oxidation rate (first hour) = 0.35 ppb min^{-1}. OH radical levels suppressed by a factor of ~2 after benzene addition, increased subsequently, but did not reach initial levels. No O_3 formed.
832	6/12	NO_x-air + tetralin	Same as above.	Initial NO = 0.84 ppm NO_2 = 0.16 ppm Propene, n-butane tracers. 3.9 ppm tetralin added after 2 hr. Run ended 4 hr later.	Before tetralin addition: NO oxidation rate = 0.11 ppb min^{-1}. Radical input rate = 0.11 ppb min^{-1}. After tetralin addition: NO oxidation rate (first hr) = 2.07 ppb min^{-1}. OH radical levels suppressed by a factor of ~4.

TABLE A-1. CHRONOLOGICAL SUMMARY OF INDOOR TEFLON CHAMBER EXPERIMENTS (CONCLUDED).

ITC run no	Date	Description	Purpose	Initial concentrations and experimental conditions	Major results and remarks
833	6/13	NO_2 actinometry	Monitor light intensity.	Quartz tube technique employed.	$k_1 = 0.33\ min^{-1}$, within the normal range.

END

FILMED

1-85

DTIC